PHASE TRANSITIONS IN ASYMPTOTICALLY ADS BLACK HOLES AND GAUGE THEORY DUALS

By

TANAY KUMAR DEY

INSTITUTE OF PHYSICS, BHUBANESWAR

A THESIS SUBMITTED TO THE
BOARD OF STUDIES IN PHYSICAL SCIENCE DISCIPLINE

IN PARTIAL FULFILLMENT OF REQUIREMENTS
FOR THE DEGREE OF

DOCTOR OF PHILOSOPHY

OF

HOMI BHABHA NATIONAL INSTITUTE

November, 2007

Contents

Synopsis

According to the AdS/CFT correspondence, type IIB string theory on $AdS_5 \times S^5$ is dual to the four-dimensional $\mathcal{N} = 4, SU(N)$ gauge theory on the boundary. In the weak coupling limit and large curvature, the string theory can be approximated by the supergravity description. However, because of the dual nature of the AdS/CFT correspondence, this corresponds to strongly coupled regime of gauge theory. The study of gauge theory in this regime is very difficult due to lack of systematic formulation. In this thesis, we systematically exploit this correspondence in order to gain understanding about the strongly coupled regime of gauge theory by studing the weakly coupled gravity theory. In particular, we have obtained a phenomenological description of the thermodynamic behaviour which can be encoded in a matrix model. Such a construction is by no means unique but our main interests are restricted to the behaviour near the critical point where qualitative behaviours are believed to be universal in the sense that, it does not depend on precise details of the theory. Therefore, the effective model presented here belongs to the same universality class that of the gauge theory. In addition, wherever possible we have pushed the correspondence furthere to make semi-quantitative analysis and obtain the behaviour of effective action under variation of different thermodynamic quantities.

We begin with a discussion of the thermodynamics of five dimensional bulk theory in the supergravity limit and review the formalism to construct an effective Lagrangian for the strongly coupled dual. The bulk has two configurations with same asymptotic

geometry. One of them is the thermal AdS and the other is the black hole. Though thermal AdS can exist for arbitrary temperature, the black hole nucleates only above a particular temperature T_{min}. Above this temperature T_{min}, there are two black hole solutions. Depending on their horizon sizes, we call them big and small. Bigger one is the stable one, and has a positive specific heat. From the free energy calculation one can see even in the presence of the black holes, thermal AdS remains the preferred phase for $T < T_c$. While for $T > T_c$, it is the big black hole phase that takes over. This phase transition at $T = T_c$ is a first order transition and known as Hawking-Page (HP) transition [1]. The small black hole remains unstable at all temperature due to its negative specific heat and acts as a bounce for the decay of big black hole at $T > T_c$. Witten [2] identified this phase transition with the large N confinement/deconfinement transition of the boundary gauge theory in the strong coupling regime. In the boundary theory which is a gauge theory on an S^3 one can show all the degrees of freedom got massive except a Wilson loop operator. One can integrate out the rest and write down a effective Lagrangian which has the Wilson loop operator as its degree of freedom. For low enough temperature it can be approximated by a simple matrix model known as (a, b) matrix model [3] as it has two parameters a and b[1]. For certain ranges of these two parameters, the matrix model captures complete thermodynamic behaviour of the bulk theory. These parameters depend on the 't Hooft coupling λ and the temperature T. Both turn out to be monotonically increasing functions of temperature for fixed λ.

We incorporate Gauss-Bonnet (GB) correction to the gravity action and study various phases of the bulk geometry with AdS asymptotics [4]. These phase structures depend crucially on GB coupling $\alpha^{'}$. Except within a certain range of this coupling, there is only one black hole phase, otherwise there exist three black hole phases. We call them small, intermediate or unstable, and big black hole phases. It turns out

[1]This is done by assuming that the weak coupling results are to be valid in the strong coupling regime mainly for 't Hooft coupling $\lambda \to \infty$

that there are two first order phase transitions. One of them is from small black hole to the big one at a temperature much lower than that of inverse AdS curvature scale. The other one is similar to that of the usual HP transition where a crossover occurs from thermal AdS to the big black hole phase. We then study the dual gauge theory at the boundary by the same two-parameter matrix model. We find the λ dependence of these parameters. By introducing higher derivative terms in the bulk, we study corrections of order $1/\lambda$ in the gauge theory. This essentially allows us to find the λ dependence of (a, b) for large but finite λ. We find that a is an increasing function of λ while b decreases with λ.

Furthermore, we find that the simple (a, b) model fails to capture all the phases (small, intermidiate and large black hole phases) in the bulk. To incorporate all the bulk phases, we constructed a toy model which requires introduction of higher dimensional operators in the matrix model. This model has four parameters which depend on the temperature as well as the gauge coupling. Besides reproducing all the qualitative features of the bulk, this model also gives an extra saddle point. We interpret this saddle point as a phase in string theory which has no analogue in the supergravity. This stringy phase arises at the Gross-Witten transition point [5]. This Gross-Witten transition may be identified as a crossover from supergravity black hole solution to string state in the bulk side [6]. In the bulk side, this stringy phase may also serve as a bounce for the decay of the small black hole to the thermal AdS.

Finally, we include the effects of electric charge with the above theory [7]. On the gravity side these charges come from the rotation of the internal S^5. We first focus our attention on the phase structures of this bulk theory in both canonical and grand canonical ensembles. In the grand canonical ensemble, the phase structure crucially depends on $\alpha^{'}$ as well as chemical potential Φ. For a certain range of the chemical potential Φ and $\alpha^{'}$, there exist three black hole phase and have two HP transitions.

Outside this range, only one black hole phase survives and unlike simple GB theory, we get a HP transition. For the canonical ensemble the number of black hole phases are similar to the GB theory but here thermal AdS is not an allowed geometry. Therefore, there exist only one first order phase transition between small and big black hole (in the certain range of $\alpha^{'}$ and fixed charge q). We then construct a matrix model for the gauge theory dual. This model is similar to the one discussed in the previous paragraph. However the four coefficients are now not only function of λ, and T, but also depend on the chemical potential. In the grand canonical ensemble, like GB theory, matrix model has an extra saddle point that has no analogue in the gravity side and we interpret this as a bounce. In the canonical ensemble, since chemical potential can take any value, one has to sum over all the values. To do that it is necessary to know the exact dependence of parameters on potential. This is very hard to determine in the strong coupling limit. For simplicity, we write down the model where only two parameters are explicitly dependent on chemical potential and other two are constant. This is consistent with one of the possible scenarios of the grand canonical case. Amusingly we find that the model correctly reproduces the corresponding bulk behaviour.

References:

[1] S. W. Hawking and D. N. Page, *Thermodynamics Of Black Holes In Anti-De Sitter Space*, Commun. Math. Phys. **87**, 577 (1983).

[2] E. Witten, *Anti-de Sitter space, thermal phase transition, and confinement in gauge theories*, Adv. Theor. Math. Phys. **2**, 505 (1998) [arXiv:hep-th/9803131].

[3] L. Alvarez-Gaume, C. Gomez, H. Liu and S. Wadia, *Finite temperature effective action, AdS_5 black holes, and 1/N expansion*, Phys. Rev. D **71**, 124023 (2005) [arXiv:hep-th/0502227].

[4] T. K. Dey, S. Mukherji, S. Mukhopadhyay and S. Sarkar, *Phase Transitions in Higher Derivative Gravity*, JHEP **0704**, 014 (2007) [arXiv:hep-th/0609038].

[5] D. J. Gross and E. Witten, *Possible Third Order Phase Transition In The Large N Lattice Gauge Theory*, Phys. Rev. D **21**, 446 (1980).

[6] G. T. Horowitz and J. Polchinski, *A correspondence principle for black holes and strings*, Phys. Rev. D **55**, 6189 (1997) [arXiv:hep-th/9612146].

[7] T. K. Dey, S. Mukherji, S. Mukhopadhyay and S. Sarkar, *Phase transitions in higher derivative gravity and gauge theory: R-charged black holes*, JHEP **0709**, 026 (2007) [arXiv:0706.3996 [hep-th]].

List of Figures

List of Figures

List of Publications

[**1**] *"BORN-INFELD BLACK HOLES IN THE PRESENCE OF A COSMOLOGICAL CONSTANAT"*,
Tanay K. Dey,
Phys.Lett. **B595**, (2004) 484.

[**2**] *"R-CHARGED ADS BUBBLE"*,
Anindya Biswas, Tanay K. Dey and Sudipta Mukherji,
Phys.Lett. **B613** (2005) 208.

***[3]** *"PHASE TRANSITIONS IN HIGHER DERIVATIVE GRAVITY"*,
Tanay K. Dey, Sudipta Mukherji, Subir Mukhopadhyay, Swarnendu Sarkar,
JHEP 04 (2007) 014.

***[4]** *"PHASE TRANSITIONS IN HIGHER DERIVATIVE GRAVITY AND GAUGE THEORY: R-CHARGED BLACK HOLES"*,
Tanay K. Dey, Sudipta Mukherji, Subir Mukhopadhyay, Swarnendu Sarkar,
JHEP 09 (2007) 026.

A (*) indicates papers on which this thesis is based.

Chapter 1

Introduction

1.1 An overview

One of the most exciting developments in theoretical physics in the past decade is perhaps the AdS/CFT correspondence [1]. This correspondence provides us with an equivalence between superstring theory on certain ten dimensional backgrounds involving Anti de-Sitter space-time and four dimensional supersymmetric Yang-Mills theories. This conjecture, if true, has indeed a far reaching consequence. First of all, it relates a gravitational theory, such as string theory, to a theory which does not involve gravity. Therefore, many puzzling issues in gravitational physics, including black hole information loss paradox, may, in principle, be addressed within the frame work of a non-gravitational theory. Alternatively, this conjecture relates highly non-perturbative problems in Yang-Mills theory to problems in classical superstring or supergravity theory. For example, the correspondence suggests that the type IIB string theory on $AdS_5 \times S^5$ is dual to a four dimensional $\mathcal{N} = 4$, $SU(N)$ gauge theory. In the weak coupling and large radius of curvature limit, the string theory can be approximated by a supergravity description. However, because of the dual nature of the correspondence, the gauge theory is strongly coupled. One therefore hopes to understand features of strongly coupled $SU(N)$ gauge theory by studying the

supergravity limit of type IIB string theory on $AdS_5 \times S^5$. Indeed many insights into strongly coupled gauge theories have emerged by exploiting this avenue [1, 2, 3, 4]. At the same time, due to this very dual nature of the correspondence and an absence of a systematic formulation of strongly coupled gauge theory, quantitative checks of this conjecture have been difficult.

This thesis serves as an attempt to understand some features of these strongly coupled gauge theories. By assuming AdS/CFT correspondence, in this thesis, we try to construct a phenomenological Lagrangian of strongly coupled $\mathcal{N} = 4$, $SU(N)$ gauge theory which qualitatively reproduces various phases of supergravity theory on $AdS_5 \times S^5$. By no means we expect this Lagrangian to be unique, except perhaps near the critical points where the qualitative behaviours are believed to be universal. Wherever possible, we try to push the correspondence further to make a semi-quantitative analysis and obtain the behaviour of the effective action under the variation of different thermodynamic quantities. Before we go on to discuss this construction, in the next section of this chapter, we start with a general description of D-branes [5]. This chapter serves as a brief introduction to AdS/CFT conjecture and also helps us to set our notations and conventions.

1.2 D-brane

There are five different superstring theories in ten dimensions, namely- type I, IIA, IIB, $E_8 \times E_8$ heterotic, and $SO(32)$ heterotic [6, 7, 8, 9, 10, 11, 12, 13, 14]. The type II theories have two supersymmetries ($\mathcal{N} = 2$), while the other three have only one supersymmetry ($\mathcal{N} = 1$). Based on the periodic and anti-periodic condition on the left and right moving worldsheet fermions, there are four sectors namely $(R - R)$, $(R - NS)$, $(NS - R)$, and $(NS - NS)$, where R stands for Ramond and NS for Neveu-Schwarz. While same boundary conditions for both the left and right moving strings give the spacetime bosons, opposite boundary conditions give us fermions.

Consequently, $(R-R)$ and $(NS-NS)$ sectors represent space time bosons and $(R-NS)$ and $(NS-R)$ are fermions. The $(NS-NS)$ sector contains graviton, two form or antisymmetric tensor $B_{\mu\nu}$ and dilaton ϕ as massless fields. The $(R-R)$ sector contains antisymmetric massless tensor fields of various ranks. In this thesis these $p+1$ form potentials will be denoted by A_{p+1}. Depending on p being even or odd, theory is type IIA or IIB respectively . In order to carry the charge of $p+1$ form, one needs to introduce extended p dimensional objects. In string theory, such objects are also the ones on which open string end-points, obeying Neumann boundary condition along $p+1$ space time direction and Dirichlet boundary conditions in $(10-p-1)$ spatial directions, can attach; they are known as Dirichlet-p branes or in short Dp branes. In this thesis we briefly describe Dp brane, and for more details we reffer to the existing literature [5, 15, 16, 17, 18, 19, 11, 12]. As we have mentioned before, these branes are charged under the $p+1$ form where the minimal coupling is given by

$$\mu_p \int_{M_{p+1}} A_{p+1}, \tag{1.1}$$

where μ_p is the charge of the brane and is related to the tension T_p of the brane as

$$\mu_p = T_p (2\pi)^{7/2} l_s^4 g_s, \tag{1.2}$$

where

$$T_p = \frac{1}{(2\pi)^3 l_s^4 g_s}. \tag{1.3}$$

Here l_s and g_s are the string length and the string coupling respectively. The value of the tension T_p is determined from the string amplitude [11, 12], through a process of a closed string exchange between two D-branes. The dynamics of the D-branes are encoded in the fluctuation of the open strings which end on them. In the low energy limit, this is given by a gauge theory with gauge group $U(1)$ that lives on the $p+1$ dimensional world volume of a single D-brane [20]. D-branes preserve $1/2$ of the 32 supersymmetries in the bulk. The gauge theory thus has 16 super charges which for $p=3$ gives $\mathcal{N}=4$.

1.3 D-brane in Type II String Theory

In closed string description, Dp-brane can be regarded as p dimensional solutions of the effective low energy string action of type II string theory (see for example [21, 22, 23, 24, 25, 26]). The action has massless fields the metric $g^{\mu\nu}$, a scalar ϕ (vacuum expectation value (vev) of which gives string coupling), $p+2$ form field strengths F_{p+2} from the $(R-R)$ sector, $(NS-NS)$ 3-form fields and their supersymmetric partners. More specifically, the action in the Einstein frame is [26]

$$I_E = \frac{1}{16\pi G_{10}} \int d^{10}x\sqrt{|g|}\left(R - \frac{1}{2}g^{\mu\nu}\partial_\mu\phi\partial_\nu\phi - \frac{1}{2}\sum_p \frac{1}{(p+2)!}e^{a_p\phi}F^2_{p+2} + ...\right), \quad (1.4)$$

with $$a_p = -\tfrac{1}{2}(p-3),$$

where dots represent the $(NS-NS)$ 3-form fields and the fermionic terms. a_p is commonly called the dilaton coupling. The closed string coupling is determined as the vev of dilaton and is given by $g_s^2 = e^{2\phi}$ in our normalisation. The open string coupling on the other hand is given by g_s and is identified as the Yang-Mills (YM) gauge coupling via the relation $g^2_{YM} = 4\pi g_s(2\pi l_s)^{p-3}$ (see [12]). G_{10} is the ten dimensional gravitational constant and related with the coupling g_s and string length l_s via $G_{10} = 8\pi^6 g_s^2 l_s^8$.

The equations of motion for graviton, dilaton and field strength are respectively

$$\begin{aligned}
R^\mu_\nu &= \frac{1}{2}\partial^\mu\phi\partial_\nu\phi + \frac{1}{2(p+2)!}e^{a_p\phi}\left((p+2)F^{\mu\xi_2\ldots\xi_{p+2}}F_{\nu\xi_2\ldots\xi_{p+2}} - \frac{p+1}{8}\delta^\mu_\nu F^2_{p+2}\right),\\
\bigtriangledown^2\phi &= \frac{1}{\sqrt{g}}\partial_\mu\left(\sqrt{g}\partial_\nu\phi g^{\mu\nu}\right) = \frac{a_p}{2(p+2)!}F^2_{p+2},\\
\partial_\mu\left(\sqrt{g}e^{a_p\phi}F^{\mu\nu_2\ldots\nu_{p+2}}\right) &= 0.
\end{aligned} \quad (1.5)$$

The solution of these equations of motion are [26]

$$ds^2 = H^{-2\frac{d-2}{\Delta}}\left(-fdt^2 + \sum_{i=1}^{p}(dx^i)^2\right) + H^{2\frac{p+1}{\Delta}}\left(f^{-1}dr^2 + r^2(d\Omega_{d-1})^2\right), \quad (1.6)$$

$$\text{where} \qquad H = 1 + \left(\frac{h}{r}\right)^{d-2}, \quad f = 1 - \left(\frac{r_0}{r}\right)^{d-2},$$

$$\begin{aligned} \Delta &= (p+1)(d-2) + 4a_p^2, \\ h^{2(d-2)} + r_0^{d-2} h^{d-2} &= \frac{\Delta Q^2}{16(d-2)^2} \qquad \text{and} \quad d = 10 - (p+1). \end{aligned} \tag{1.7}$$

Here r_0 and Q are integration constants. Q turns out to be related to the charge μ_p of the p-brane via the relation [26]

$$\mu_p = \Omega_{d-1} Q / ((2\pi)^{7/2} l_s^4 g_s), \tag{1.8}$$

where Ω_{d-1} is the metric on the round $(d-1)$ sphere. The metric has a singularity at $r = 0$ due to the presence of the source. In general, for generic values of r_0 and Q, the solutions break all the supersymmetries. However, for specific r_0 and Q, solution preserves a fraction of space-time supersymmetry. The metric has a horizon at $r = r_0$ where $f(r)$ vanishes. When we take $r_0 \to 0$, horizon sits on top of the singularity and the solution becomes extremal preserving $1/2$ of the space-time supersymmetry.

In the subsequent part of this thesis, we will specialise to $p = 3$ or $a_p = 0$, that is, we will be focusing on $D3$-brane. In this case the dilaton is a constant. Thus from (1.7) we have $d = 6$ and $\Delta = 16$.

1.3.1 Near horizon limit of extremal brane

The extremal solution is obtained by considering $r_0 = 0$. It follows from (1.7) that $h^4 = Q/4$. In this case the solution reduces to,

$$\begin{aligned} f(r) &= 1, \\ H &= 1 + \frac{Q}{4r^4}, \\ ds^2 &= H^{-\frac{1}{2}} \left(-dt^2 + dx_1^2 + dx_2^2 + dx_3^2 \right) + H^{\frac{1}{2}} \left(dr^2 + r^2 d\Omega_5^2 \right). \end{aligned} \tag{1.9}$$

We know from equation (1.2), a single Dp-brane charge μ_p is related with the tension T_p of the brane. Thus if we consider N number of coincident Dp-branes, we have to

choose integration constant Q such that

$$\frac{\mu_p}{T_p(2\pi)^{7/2}l_s^4 g_s} = N. \tag{1.10}$$

Then by using equation (1.8), one can write Q in terms of N, g_s and l_s. We get

$$Q = 16\pi g_s l_s^4 N. \tag{1.11}$$

Thus the final metric solution for the extremal N $D3$-brane is

$$\begin{aligned} ds^2 &= H^{-\frac{1}{2}}\left(-dt^2 + dx_1^2 + dx_2^2 + dx_3^2\right) + H^{\frac{1}{2}}\left(dr^2 + r^2 d\Omega_5^2\right), \\ \text{where} \quad H &= 1 + \frac{4\pi g_s l_s^4 N}{r^4} = 1 + \frac{l^4}{r^4}, \quad \text{and} \quad \frac{l^4}{l_s^4} = 4\pi g_s N. \end{aligned} \tag{1.12}$$

In the asymptotic region, this metric approaches Minkowski space, i.e, $H \sim 1$. However in the near horizon limit, $r << l$, we can neglect the factor 1 in H of (1.12) and the metric reduces to

$$ds^2 = \frac{r^2}{l^2}\left(-dt^2 + dx_1^2 + dx_2^2 + dx_3^2\right) + \frac{l^2}{r^2}dr^2 + l^2 d\Omega_5^2. \tag{1.13}$$

This is an *Anti de Sitter* $(AdS) \times S^5$ geometry, where both the radii of the two spaces are given by l. This five dimensional AdS space can also be obtained from the universal covering space of a surface obeying [1]

$$-X_0^2 + X_1^2 + X_2^2 + X_3^2 + X_4^2 - X_5^2 = -l^2, \tag{1.14}$$

By construction, the space has $SO(2,4)$ isometry, and it is homogeneous and isotropic. To get the form of the AdS space of (1.13), we make the coordinates transformation as

$$\begin{aligned} r &= (X_5 + X_4) \\ \tau &= -\frac{iX_0 l}{r} \quad \text{and} \quad x_\alpha = \frac{X_\alpha l}{r} \quad \text{where} \quad \alpha = 1, 2, 3. \end{aligned} \tag{1.15}$$

Then the metric (1.14) reduces to

$$ds^2 = \frac{r^2}{l^2}\left(-d\tau^2 + dx_1^2 + dx_2^2 + dx_3^2\right) + \frac{l^2}{r^2}dr^2 \tag{1.16}$$

We note here the isometry group of $AdS_5 \times S^5$ is $SO(2,4) \times SO(6)$, the two factors are coming from AdS_5 and S^5 respectively. Having discussed the near horizon limit of extremal $D3$-brane, we now focus our attention to the non-extremal one and its near horizon limit.

1.3.2 Near horizon limit of non-extremal brane

The non-extremal solution is obtain by considering r_0 finite. The solution is

$$ds^2 = H^{-\frac{1}{2}}\left(-fdt^2 + dx_1^2 + dx_2^2 + dx_3^2\right) + H^{\frac{1}{2}}\left(f^{-1}dr^2 + r^2 d\Omega_5^2\right), \tag{1.17}$$

where

$$\begin{aligned} H &= 1 + \frac{\sqrt{r_0^8 + Q^2/4} - r_0^4}{2r^4}, \\ f &= 1 - \left(\frac{r_0}{r}\right)^4. \end{aligned} \tag{1.18}$$

Note that the metric approaches Minkowski space in the asymptotic limit. In the near horizon limit, we get

$$ds^2 = \frac{r^2}{l'^2}\left(-fdt^2 + dx_1^2 + dx_2^2 + dx_3^2\right) + \frac{l'^2}{fr^2}dr^2 + l'^2 d\Omega_5^2, \tag{1.19}$$

which is $AdS_{bh} \times S^5$, with same radii for the two spaces. Here $\{bh\}$ means that it is a black hole in five dimensional AdS space. In (1.19) we have defined l' as $l'^4 = \left(\sqrt{r_0^8 + Q^2/4} - r_0^4\right)/2$. Notice that at $r_0 = 0$, the metric reduces to the extremal one. We can associate thermodynamic quantities like entropy, temperature and free energy with this non-extremal black hole. All these quantities can explicitly be computed from the metric and the action. Here we briefly discuss all these quantities. For details we refer the reader to the next chapter and reference [24]. The Hawking temperature can be calculated from the metric solution by using the standard relation [27]

$$T_H = -\frac{1}{4\pi}\frac{dg_{tt}}{dr}\Big|_{r=r_0}. \tag{1.20}$$

From which it follows that

$$T_H = \frac{\sqrt{2}}{\pi} r_0 \left(r_0^4 + \sqrt{r_0^8 + Q^2/4} \right)^{-\frac{1}{2}}. \tag{1.21}$$

Note that because of this nonzero temperature, $AdS_{bh} \times S^5$ breaks all the space-time supersymmetries.

The entropy follows from the Bekenstein area law [28] as,

$$S_{bh} = \frac{A_h}{4G_{10}} = \frac{2\pi A_h}{\kappa^2}. \tag{1.22}$$

Here we have defined $\kappa^2 = 8\pi G_{10}$ and A_h is the horizon area of the black hole which is

$$A_h = L^3 \pi^3 r_0^3 \left(\frac{r_0^4}{2} + \frac{1}{2} \sqrt{r_0^8 + Q^2/4} \right)^{\frac{1}{2}}. \tag{1.23}$$

Here L^3 is the volume of the x_i space. The ADM mass, which is also equal to internal energy of the black hole, can be written from the action as [24],

$$M = \frac{L^3 \pi^3}{\kappa^2} \left[\frac{3\, r_0^4}{2} + \sqrt{r_0^8 + Q^2/4} \right]. \tag{1.24}$$

Note that in the extremal limit, temperature and entropy are zero and the ADM mass reduces to the extremal mass, which is

$$M_0 = \frac{L^3 \pi^3}{2\kappa^2} Q. \tag{1.25}$$

One can easily verify that these thermodynamic quantities satisfy the first law of thermodynamics $dM = T_H dS$. We now define a quantity

$$\frac{\delta M}{M_0} = \frac{M - M_0}{M_0} = \frac{\left[\frac{3\, r_0^4}{2} + \sqrt{r_0^8 + Q^2/4} - \frac{Q}{2} \right]}{Q/2}. \tag{1.26}$$

If we consider the radius r_0^4 to be very small, then it means that we slightly perturb the solution away from its extremality. Then the equation (1.26), written in the lowest power of r_0^4, turns out to be

$$\frac{\delta M}{M_0} = 3 \frac{r_0^4}{Q}. \tag{1.27}$$

Similarly entropy may be recast as

$$S_{bh} = \frac{L^3\pi^4 Q^{5/4}}{\kappa^2}\left(\frac{r_0^4}{Q}\right)^{\frac{3}{4}}. \tag{1.28}$$

In terms of $\frac{\delta M}{M_0}$, entropy can be rewritten as

$$S_{bh} = \frac{L^3\pi^3 Q^{5/4}}{\kappa^2 3^{3/4}}\left(\frac{\delta M}{M_0}\right)^{\frac{3}{4}}. \tag{1.29}$$

Finally the free energy with respect to AdS becomes

$$F_{bh} = E - T_H S_{bh} = \frac{L^3\pi^3}{\kappa^2}\left[-\frac{r_0^4}{2} + \sqrt{r_0^8 + Q^2/4}\right] \tag{1.30}$$

and the perturbative form is

$$F_{bh} = \frac{L^3\pi^3}{2\,\kappa^2}Q\left[1 - \frac{r_0^4}{Q}\right] = \frac{L^3\pi^3}{2\,\kappa^2}Q\left[1 - \frac{1}{3}\left(\frac{\delta M}{M_0}\right)\right]. \tag{1.31}$$

Then using (1.25), we see that the free energy of this black hole with respect to the extremal one is

$$F_{bh} = -\frac{L^3\pi^3}{6\,\kappa^2}Q\left(\frac{\delta M}{M_0}\right). \tag{1.32}$$

This relation will be useful in later discussion.

Having discussed the brane geometry and thermodynamics, in the next section we consider gauge theory that resides on the brane world volume.

1.4 Gauge Theory on the Brane

In D-brane picture, to describe the near horizon solitonic solution of the previous section, we consider a set of N parallel $D3$-branes. These are stuck together or very close to each other in ten dimensions [29]. The end points of open strings live on the (3+1) dimensional plane of the brane, while the closed strings live in the bulk. Due to the presence of the brane space-time will be curved. The total action of the whole configuration is described by $S = S_{brane} + S_{bulk} + S_{int}$. In the brane action there are

gauge fields and massive fields, and in the bulk action there are graviton, dilaton, higher form fields and massive fields. S_{int} describes the interaction between the brane and the bulk.

In the low energy limit, that is $\alpha^{'} \to 0$, $\kappa \sim g_s \alpha^{'2} \to 0$ (where $\alpha^{'} = l_s^2$), the bulk and brane are fully decoupled and they do not contain any massive mode. Furthermore, since we are dealing with N coincident $D3$-branes, the end point of open strings can attach branes in $U(N)$ number of different ways. Therefore, the gauge group must be $U(N)$ with 16 super charges. This ten dimensional theory reduces to four dimensional $\mathcal{N} = 4$ super Yang Mills theory, when we compactify all the transverse coordinates. So we conclude from here that the effective quantum theory on N coincident $D3$-branes is $\mathcal{N} = 4$ super Yang Mills with gauge group $U(N)$. In passing, we also note that isometry group of the theory is $SO(2,4) \times SO(6)$. The first factor represents super conformal symmetry and the other one is due to the R-symmetry which comes from the dimensional reduction. In this case, half of the super charges of IIB theory is preserved and it gives unbroken $U(N)$ gauge theory.

1.5 Statistical Mechanics of Non-extremal 3-brane

In the D-brane picture the excitations are described by a gas of massless open string states moving along the brane in arbitrary directions. The mass of the excited 3-brane is [15, 30]

$$M = M_0 + \delta M = \frac{\sqrt{\pi}}{\kappa} L^3 + \sum_{i=1}^{k} \frac{2\pi}{L} |n_i| + \mathcal{O}(g). \tag{1.33}$$

Here k is the number of open strings and n is the excitation label. The term $\mathcal{O}(g)$ takes care of the interaction among the strings.

Following [30], we may alternatively consider the statistical mechanics of massless open string states in the grand canonical ensemble. Consider a system with N_1

massless bosons and fermions degrees of freedom. The partition function is

$$Z = \prod_n \left(\frac{1+q^n}{1-q^n}\right)^{N_1}, \tag{1.34}$$

where we have defined $q = e^{-2\pi/LT}$. Here T is the temperature of the system. Now the thermodynamic quantities like free energy F and internal energy E (with respect to extremal brane) and entropy S of the system can easily be calculated from the partition function and these are

$$\begin{aligned} F_0 &= -\frac{\pi^2}{48} N_1 L^3 T^4, \\ E &= \frac{\pi^2}{16} N_1 L^3 T^4, \\ S_0 &= \frac{\pi^2}{12} N_1 L^3 T^3. \end{aligned} \tag{1.35}$$

Using this method it is easy to calculate these quantities for N number of $D3$-branes stacked on top of one another. The massless open string can now be attached to any two of the branes. Thus there are N^2 states for each state we had before. Therefore, in the partition function Z of equation (1.34), we have power $N_1\, N^2$ instead of N_1. So, the thermodynamic quantities take the form

$$\begin{aligned} F_0 &= -\frac{\pi^2}{48} N_1 N^2 L^3 T^4, \\ E &= \frac{\pi^2}{16} N_1 N^2 L^3 T^4, \\ S_0 &= \frac{\pi^2}{12} N_1 N^2 L^3 T^3. \end{aligned} \tag{1.36}$$

The last two equations give the entropy as

$$S_0 = \frac{2}{3} N_1^{1/4} \sqrt{\pi N} L^{3/4} E^{3/4}. \tag{1.37}$$

Setting $E = \delta M$ in equation (1.37), one can obtain the entropy of N number of non-extremal 3-branes in terms of $\frac{\delta M}{M_0}$ as

$$S_0 = \frac{2}{3} N_1^{1/4} \pi^{7/8} N^{5/4} \kappa^{-3/4} L^3 (\delta M/M_0)^{3/4}, \tag{1.38}$$

where

$$M_0 = \frac{\sqrt{\pi}}{\kappa} N L^3, \tag{1.39}$$

is the mass of N number of extremal $D3$-branes [15]. If we include all eight bosonic and fermionic modes in the statistical treatment i.e for $N_1 = 8$, we get the entropy as

$$S_0 = \frac{2^{7/4}}{3} \pi^{7/8} N^{5/4} \kappa^{-3/4} L^3 (\delta M/M_0)^{3/4}. \tag{1.40}$$

Now we would like to compare this entropy formula with the entropy formula of non-extremal black hole in equation (1.29). By comparing the mass of the extremal black hole of equation (1.25) with the extremal brane of equation (1.39), one can write down Q in terms of N as

$$Q = 2\kappa\pi^{-5/2} N. \tag{1.41}$$

Then the black hole entropy in terms of $\frac{\delta M}{M_0}$ is

$$S_{bh} = \frac{2^{5/4}}{3^{3/4}} \pi^{7/8} N^{5/4} \kappa^{-3/4} L^3 (\delta M/M_0)^{3/4}. \tag{1.42}$$

Hence the two entropies are related as

$$S_0 = \left(\frac{4}{3}\right)^{1/4} S_{bh}. \tag{1.43}$$

Next we consider the temperature of the two theories. In the statistical method we know that $dE = TdS$ and $dE = dM$. Also using $dM = T_H dS_{bh}$ for black holes we immediately get

$$T_H = \left(\frac{4}{3}\right)^{1/4} T. \tag{1.44}$$

Now coming back to the free energy of the statistical system and it can similarly be written as

$$F_0 = -\frac{\sqrt{\pi}}{3\,\kappa} N L^3 \left(\frac{\delta M}{M_0}\right) \tag{1.45}$$

and black hole free energy of equation (1.32) with respect to extremal black hole can be rewritten by using equation (1.41)

$$F_{bh} = -\frac{\sqrt{\pi}}{3\,\kappa} N L^3 \left(\frac{\delta M}{M_0}\right). \tag{1.46}$$

Thus the relation between these two free energies is

$$F_0 = F_{bh}. \tag{1.47}$$

Notice that here we have calculated the entropy and the free energy for both sides in the weak coupling limit at different temperatures. The gauge theory is on $S^1 \times S^3$ which is the boundary of thermal AdS where the thermal circle is denoted as S^1. We should, therefore, calculate these two quantities at the same temperature [31]. Let us call this temperature T_H. Then we replace T of (1.36) in terms of T_H by using equation (1.44). Now if we do the similar computation as earlier to get relations analogous to (1.43) and (1.47), these would be changed as

$$S_0 = \frac{4}{3} S_{bh} \qquad \text{and} \qquad F_0 = \frac{4}{3} F_{bh}. \tag{1.48}$$

Thus except numerical factor there is a matching of thermodynamic quantities between the theory of AdS space and the boundary gauge theory in the weak coupling limit. It is argued in [31], that if we compute these quantities in the strong coupling limit of boundary gauge theory, this discrepancy may not appear. In fact, in the 't Hooft large N limit, the entropy and free energy of the boundary theory are given respectively [27, 31] as

$$S = S_0 f(g^2_{YM} N) \qquad \text{and} \qquad F = F_0 f(g^2_{YM} N). \tag{1.49}$$

The function f is not a constant, rather it has a perturbative expansion in weak [32, 29, 31] and strong coupling limits [27, 29] respectively as

$$\begin{aligned} f(g^2_{YM} N) &= 1 - \frac{3}{2\pi^2} g^2_{YM} N + \frac{3+\sqrt{2}}{\pi^3} \left(g^2_{YM} N\right)^{3/2} + .. \quad \text{for small} \quad g^2_{YM} N \\ &= \frac{3}{4} + \frac{45}{32} \frac{\zeta(3)}{(g^2_{YM} N)^{3/2}} + ... \qquad\qquad\qquad\qquad \text{for large} \quad g^2_{YM} N. \end{aligned} \tag{1.50}$$

So, at the strong coupling limit, entropy and free energy of both side exactly match.

1.6 AdS/CFT Correspondence and Implications

In the previous sections we have shown that there are precise matchings of thermodynamic quantities between the weak coupling theory of AdS bulk space and the strong coupling boundary gauge theory of AdS bulk. We also noticed that the isometry group of $AdS_5 \times S^5$ was $SO(2,4) \times SO(6)$, the two factors are coming from AdS_5 and S^5 respectively. These symmetries are exactly the conformal group and R-symmetry group of $\mathcal{N} = 4$ Super Yang-Mills theory on the $D3$-brane as we mentioned in section 1.4.

Following these observations, Maldacena conjectured an equivalence between these two different theories. This is known as AdS/CFT correspondence. According to this conjecture [1], type IIB superstring theory on asymptotically $AdS_5 \times S^5$ is dual to $U(N)$, $\mathcal{N} = 4$ SYM (CFT) on the boundary 3+1 dimensional Minkowski space. More generally a $p+1$ dimensional quantum theory of gravity is dual (which we explain at the end of this section) to p dimensional quantum gauge theory. In the large N limit, this duality is between the weakly coupled gravity theory and strongly coupled gauge theory.

Due to the absence of a formulation of string theory on AdS space and lack of adequate techniques to study strong coupling regimes of gauge theories, quantitative check of this conjecture is difficult. Nevertheless, encouraging agreements of the qualitative features between the bulk and the boundary theories have accumulated over the last few years [1, 2, 3, 4, 29, 26]. One of the remarkable checks [4] in this direction is the identification of the crossover from the thermal AdS phase to black hole phase, (known as Hawking-Page transition [33]), with the large N deconfinement transition of the gauge theory on the boundary. In the next chapter we discuss this identification in more detail. We end this section by noticing that the supergravity description of the bulk is only valid at $\alpha' \to 0$ limit. Now recall from (1.12), that we

have

$$\frac{l^4}{l_s^4} = 4\pi g_s N = g_{YM}^2 N = \lambda, \tag{1.51}$$

where l is AdS length scale, $l_s = \sqrt{\alpha'}$ and λ is 't Hooft coupling. In the limit $l_s \to 0$, for fixed g_s, $N \to \infty$. Consequently, the gauge coupling λ is very large in this limit.

In order to study the supergravity limit, it will be useful for us to analyse IIB supergravity under S^5 compactification. We review this compactification in the next section. The results of this section will be used in the next chapter.

1.7 Type IIB Supergravity Action

The ten dimensional type IIB action in (1.4) in supergravity limit ($\alpha' \to 0$), reduces to

$$I_{10} = \frac{1}{16\pi G_{10}} \int d^{10}x \sqrt{|g^{(10)}|} \left[R^{(10)} - \frac{1}{2}\frac{1}{5!} F_5^{(10)2} \right]. \tag{1.52}$$

Since we will be focusing on $D3$-brane only, the dilaton will be constant. Hence action in (1.52) does not carry any explicit dilaton dependence. To get the five dimensional action in $AdS_5 \times S^5$ geometry we consider the spontaneous compactification of the ten dimensional action on S^5 [34, 35]. Separating the metric as

$$ds^2 = g_{\mu\nu}^{(5)} dx^\mu dx^\nu + l^2 d\Omega_5^2. \tag{1.53}$$

Here $g_{\mu\nu}^{(5)}$ is the metric of AdS_5 and $d\Omega_5^2$ is the metric on S^5, which can be represented by five angular coordinates $\theta_1, \theta_2, \theta_3, \theta_4, \theta_5$. Since the metric is diagonal, ten dimensional Ricci scalar will be totally decoupled in two components, one coming from AdS_5 part and another from S^5 part respectively. We denote them by $R^{(5)}$ and $R^{(S)}$. Since we are interested to get five dimensional action in AdS_5, we keep first component as it is and evaluate the second one from S^5 metric. Then the value of $R^{(S)}$ is $20/l^2$. Similarly the five form field strength $F^{(10)}$ has nonvanishing components $F^{(10)}_{\mu_1\mu_2\mu_3\mu_4\mu_5} = F^{(5)}_{\mu_1\mu_2\mu_3\mu_4\mu_5}$ and $F^{(10)}_{\theta_1\theta_2\theta_3\theta_4\theta_5} = F_1^{(5)} \epsilon_{\theta_1\theta_2\theta_3\theta_4\theta_5}$, where $F_1^{(5)}$ is a zero-form field strength on the AdS_5. To write down the both components of the form field in

terms of zero-form field in the action, we use the Hodge dual transformation for the first component which is $F^{(5)}_{\mu_1\mu_2\mu_3\mu_4\mu_5} = \frac{1}{l^5} F_2^{(5)} \epsilon_{\mu_1\mu_2\mu_3\mu_4\mu_5}$. Here $F_2^{(5)}$ is also a zero-form field strength on the AdS_5. After rearranging the all fields and integrating over the S^5 the ten dimensional action reduces to the five dimensional form as

$$I_5 = \frac{1}{16\pi G_5} \int d^5x \sqrt{|g^{(5)}|} \left[R^{(5)} + \frac{20}{l^2} - \frac{1}{2}\frac{1}{l^5} \left(F_1^{(5)2} + F_2^{(5)2} \right) \right], \tag{1.54}$$

where G_5 is the five-dimensional gravitational constant related to G_{10} as $G_5 = G_{10}/\pi^3 l^5$. The Bianchi identities for the zero-form field imply that they are constant and the self-duality of the five form field demands that they are same. The equation of motion of form field gives the value of the zero-form field. Thus the value of the last term of the above integral can easily be calculated. This comes to $(8/l^2)$ (see [34] for more detail). Therefore, the final form of the five dimensional action is

$$I_5 = \frac{1}{16\pi G_5} \int d^5x \sqrt{|g^{(5)}|} \left[R^{(5)} + \frac{12}{l^2} \right]. \tag{1.55}$$

With this brief introduction, in the next section we discuss the structure of the thesis. This section also serves as a summary of the work done in this thesis.

1.8 Plan of the Thesis

Assuming AdS/CFT conjecture, in the subsequent chapters we study different types of bulk theories as well as their corresponding boundary gauge theories.

In *chapter 2*, we consider bulk space consisting of AdS-Schwarzschild black hole. In particular, we discuss the thermodynamic features of AdS-Schwarzschild black hole. We then study the Hawking-Page (HP) transition and identify that with the deconfinement transition of the boundary theory. Finally, following [36] we construct a phenomenological effective Lagrangian for the strongly coupled boundary theory which reproduces the qualitative features of the bulk theory. As we will discuss in detail, this Lagrangian consists of two terms in power of eigen values of the Wilson

loop operators. The coefficients of these terms depend on the temperature and the 't Hooft coupling λ. We numerically analyse the dependence of these two coefficients on T for fixed λ.

In the next chapter, we study the behaviour of this phenomenological Lagrangian as we perturbatively decrease λ. This is done by adding higher derivative terms in the bulk action. Adding higher derivative terms imply that we are increasing the bulk coupling constant. Consequently, the dual nature of the correspondence suggests that the boundary theory becomes weaker. In this chapter, we introduce Gauss-Bonnet term in the bulk supergravity Lagrangian. As before we study thermodynamics of the bulk theory and their corresponding boundary duals. We compute how two parameters of the above model behave as a function of λ at fixed temperature. This is done by comparing the bulk and boundary theory near the HP point. Furthermore, we notice that in order to reproduce the complete phase diagram of the bulk, we need to introduce suitable higher order operators in gauge theory. This involves introduction of more parameters which also depend on λ and T.

In *chapter 4*, we study the bulk phases of R-charged black hole in the presence of higher derivative terms. These charges appear due to rotation of internal S^5. In gauge theory, it corresponds to introducing chemical potential μ. We study how our previous model captures qualitative phase structures of the bulk. Here we study the theory in both canonical and grand canonical ensembles.

In *chapter 5*, we end with a summary of our results.

Bibliography

[1] J. M. Maldacena, *The large N limit of superconformal field theories and supergravity*, Adv. Theor. Math. Phys. **2**, 231 (1998) [Int. J. Theor. Phys. **38**, 1113 (1999)] [arXiv:hep-th/9711200].

[2] S. S. Gubser, I. R. Klebanov and A. M. Polyakov, *Gauge theory correlators from non-critical string theory*, Phys. Lett. B **428**, 105 (1998) [arXiv:hep-th/9802109].

[3] E. Witten, *Anti-de Sitter space and holography*, Adv. Theor. Math. Phys. **2**, 253 (1998) [arXiv:hep-th/9802150].

[4] E. Witten, *Anti-de Sitter space, thermal phase transition, and confinement in gauge theories*, Adv. Theor. Math. Phys. **2**, 505 (1998) [arXiv:hep-th/9803131].

[5] J. Polchinski, *Dirichlet-Branes and Ramond-Ramond Charges*, Phys. Rev. Lett. **75**, 4724 (1995) [arXiv:hep-th/9510017].

[6] J. H. Schwarz, Phys. Rep. **89**, 223 (1982), M. B. Green, Surv. High Energy Phys. **3**, 127 (1983)

[7] D. J. Gross, J. A. Harvey, E. Martinec, and R. Rohm, Phys. Rev. Lett. **54**, 502 (1985), Nucl. Phys. **B256**, 253 (1985)

[8] M. B. Green, J. H. Schwarz and E. Witten, *Superstring theory.* vol1. (Cambridge Univ. Press, 1987).

[9] M. B. Green, J. H. Schwarz and E. Witten, *Superstring theory.* vol2 (Cambridge Univ. Press, 1987).

[10] D. Lust, S. Theisen, *Lectures on string theory*, (Springer-Verlag, 1989).

[11] Joseph Polchinski, *String theory.*vol1. (Cambridge Univ. Press, 1998).

[12] Joseph Polchinski, *String theory.*vol2. (Cambridge Univ. Press, 2001).

[13] Barton Zwiebach, *A first course in string theory.* (Cambridge Univ. Press, 2004).

[14] K. Becker, M. Becker and J. H. Schwarz, *String theory and M-theory, A modern introduction*, (Cambridge Univ. Press, 2006).

[15] J. Polchinski, S. Chaudhuri and C. V. Johnson, *Notes on D-Branes*, arXiv:hep-th/9602052.

[16] J. Polchinski, *Tasi lectures on D-branes*, arXiv:hep-th/9611050.

[17] C. P. Bachas, *Lectures on D-branes*, arXiv:hep-th/9806199.

[18] A. Giveon and D. Kutasov, *Brane dynamics and gauge theory*, Rev. Mod. Phys. **71**, 983 (1999) [arXiv:hep-th/9802067].

[19] C. V. Johnson, *D-Brane Primer*, hep-th/0007170.

[20] E. Witten, *Bound states of strings and p-branes*, Nucl. Phys. B **460**, 335 (1996) [arXiv:hep-th/9510135].

[21] M. J. Duff, R. R. Khuri and J. X. Lu, *String solitons*, Phys. Rept. **259**, 213 (1995) [arXiv:hep-th/9412184].

[22] S. P. de Alwis, *A note on brane tension and M-theory*, Phys. Lett. B **388**, 291 (1996) [arXiv:hep-th/9607011].

[23] K. S. Stelle, *BPS branes in supergravity*, arXiv:hep-th/9803116.

[24] R. Argurio, *Brane physics in M-theory*, arXiv:hep-th/9807171.

[25] R. D'Auria and P. Fre, *BPS black holes in supergravity: Duality groups, p-branes, central charges and the entropy*, arXiv:hep-th/9812160.

[26] J. L. Petersen, *Introduction to the Maldacena conjecture on AdS/CFT*, Int. J. Mod. Phys. A **14**, 3597 (1999) [arXiv:hep-th/9902131].

[27] S. S. Gubser, I. R. Klebanov and A. A. Tseytlin, *Coupling constant dependence in the thermodynamics of N = 4 supersymmetric Yang-Mills theory*, Nucl. Phys. B **534**, 202 (1998) [arXiv:hep-th/9805156].

[28] J. D. Bekenstein, *Extraction of energy and charge from a black hole*, Phys. Rev. D **7** (1973) 949.

[29] O. Aharony, S. S. Gubser, J. M. Maldacena, H. Ooguri and Y. Oz, *Large N field theories, string theory and gravity*, Phys. Rept. **323**, 183 (2000) [arXiv:hep-th/9905111].

[30] S. S. Gubser, I. R. Klebanov and A. W. Peet, *Entropy and Temperature of Black 3-Branes*, Phys. Rev. D **54**, 3915 (1996) [arXiv:hep-th/9602135].

[31] I. R. Klebanov, *TASI lectures: Introduction to the AdS/CFT correspondence*, arXiv:hep-th/0009139.

[32] A. Fotopoulos and T. R. Taylor, *Comment on two-loop free energy in N = 4 supersymmetric Yang-Mills theory at finite temperature*, Phys. Rev. D **59** (1999) 061701 [arXiv:hep-th/9811224].

[33] S. W. Hawking and D. N. Page, *Thermodynamics of black holes in anti-de Sitter space*, Commun. Math. Phys. **87**, 577 (1983).

[34] H. J. Kim, L. J. Romans and P. van Nieuwenhuizen, *The Mass Spectrum Of Chiral* $N = 2$ $D = 10$ *Supergravity On* S^5, Phys. Rev. D **32**, 389 (1985).

[35] Y. Kiem and D. Park, *A non-perturbative evidence toward the positive energy conjecture for asymptotically locally AdS_5 IIB supergravity on S^5*, Phys. Rev. D **59**, 044010 (1999) [arXiv:hep-th/9809174].

[36] L. Alvarez-Gaume, C. Gomez, H. Liu and S. Wadia, *Finite temperature effective action, AdS_5 black holes, and $1/N$ expansion*, Phys. Rev. D71 (2005) 124023 [arXiv:hep-th/0502227].

Chapter 2

AdS-Schwarzschild Black Holes and Boundary Gauge Theory

2.1 Introduction

In the previous chapter, we briefly discussed the AdS/CFT correspondence. Due to the dual nature of the correspondence, any quantitative check of this conjecture becomes difficult. When the bulk is in the weak coupling phase, it is well described by supergravity. However the dual boundary gauge theory is then strongly coupled. At this moment, lattice gauge theory is perhaps the only way to analyse these theories. On the other hand, when the gauge theory is weak, we can reliably do perturbative computations. Unfortunately then the gravity becomes strongly coupled. Supergravity approximation is no longer valid and one needs a string theoretic description. However, string theory in AdS space is not yet well understood. Consequently, most of the features supporting the conjecture are qualitative in nature. In this chapter we first discuss supergravity/gauge theory correspondence from a somewhat different perspective. We will assume the validity of AdS/CFT conjecture. Using this correspondence we will try to construct a phenomenological Lagrangian which may describe the strongly coupled gauge theory. As we will discuss, we do not expect this

Lagrangian to be unique unless perhaps when we are sufficiently close to the critical points. The Lagrangian was first proposed in [1] and in this chapter we will briefly review this work.

In the next section, we start by focusing on the bulk supergravity. More specifically, we analyse the AdS-Schwarzschild black hole. In section 2.3, we review thermodynamic quantities associated with AdS-Schwarzschild black hole [2, 3, 4, 5, 6, 7, 8]. We then take a fresh look at the HP transition. In section 2.5, as in thermodynamics of first order phase transition, we construct the Landau function by identifying black hole horizon as an order parameter. On shell, this function reproduces the free energy of the black hole. In section 2.6, we turn our attention to the boundary gauge theory. Here we review the work of [9, 10, 11, 1]. In these works effective strong coupling gauge theory action was phenomenologically constructed. This action is constructed in terms of Wilson loop operators. The coefficient of various terms are expected to depend explicitly on the coupling λ and the temperature T. We end the section by discussing the variation of these coefficients as a function of temperature T (at $\lambda \to \infty$) near the HP point.

2.2 AdS-Schwarzschild Black Holes

We start by considering five dimensional gravitational action in the presence of a negative cosmological constant Λ

$$I = \int d^5x\sqrt{-g_5}\Big[\frac{R}{\kappa_5} - 2\Lambda\Big], \tag{2.1}$$

where R is Ricci scalar and κ_5 is related with gravitational constant G_5 as $\kappa_5 = 16\pi G_5$. As we noted in section 1.7, this action arises when we compactify IIB supergravity on S^5. By varying the action with respect to metric $g_{\mu\nu}$, the equations of motion are

$$\kappa_5^{-1}(R_{\mu\nu} - \frac{1}{2}g_{\mu\nu}R) + \Lambda g_{\mu\nu} = 0, \tag{2.2}$$

where $R_{\mu\nu}$ is the Riemann tensor. We solve these equations by considering a metric ansatz

$$ds^2 = -Udt^2 + Vdr^2 + r^2 d\Omega_3^2, \tag{2.3}$$

where $d\Omega_3$ is the metric on 3-sphere and U and V are unknown functions of r. By comparing components of $R_{\mu\nu}$ from metric ansatz and substituting in the equations of motion, one can easily show that

$$U = \frac{1}{V} \quad \text{and} \quad U(r) = 1 - \frac{m}{r^2} + \frac{r^2}{l^2}. \tag{2.4}$$

Thus the metric is

$$ds^2 = -\left(1 - \frac{m}{r^2} + \frac{r^2}{l^2}\right) dt^2 + \left(1 - \frac{m}{r^2} + \frac{r^2}{l^2}\right)^{-1} dr^2 + r^2 d\Omega_3^2, \tag{2.5}$$

where l is related to the cosmological constant as $l^2 = -6/\kappa_5\Lambda$ and m is the integration constant, related with the ADM mass of the black hole, M via the relation

$$M = \frac{3\,\omega_3\, m}{\kappa_5}, \tag{2.6}$$

where ω_3 is the volume of the unit 3-sphere. In the asymptotic limit, $r \to \infty$, the metric reduces to the AdS metric

$$ds^2 = -\left(1 + \frac{r^2}{l^2}\right) dt^2 + \left(1 + \frac{r^2}{l^2}\right)^{-1} dr^2 + r^2 d\Omega_3^2. \tag{2.7}$$

The metric has a curvature singularity at $r = 0$ and the horizon is located at r_+, where r_+ is a real positive root of the equation

$$1 - \frac{m}{r^2} + \frac{r^2}{l^2} = 0. \tag{2.8}$$

If we expand the Euclidean version of metric (2.5) around r_+ the metric behaves as

$$ds^2 \sim \frac{dr^2}{A(r - r_+)} + A(r - r_+)d\tau^2 + r^2 d\Omega_3^2, \tag{2.9}$$

where $A = \frac{2l^2+4r_+^2}{r_+l^2}$. It has a removable coordinate singularity if the Euclidean time τ has a particular period β. To see this, let us consider 2-dimensional space with polar coordinates ρ and θ. Metric is given by

$$ds_p^2 = d\rho^2 + \rho^2 d\theta^2. \tag{2.10}$$

To get a regular geometry, polar angle θ has to be periodic with period 2π. Otherwise at $\rho = 0$, there will be a conical singularity. Defining ρ as $r = \frac{A\rho^2}{4} + r_+$, we see that the metric (2.9) reduces to

$$ds^2 = d\rho^2 + \left(\frac{\rho A}{2}\right)^2 d\tau^2 + ... \tag{2.11}$$

Therefore to remove the conical singularity at the horizon, τ has to be periodic with periodicity

$$\beta = \frac{4\pi}{A} = \frac{2\pi r_+ l^2}{2r_+^2 + l^2}. \tag{2.12}$$

Now we identify this period with the inverse temperature. In statistical mechanics of a quantum system in the state $|q\rangle$, the canonical partition function for inverse temperature β_{st} is

$$Z = \sum_q \langle q| \, e^{-\beta_{st} H} \, |q\rangle \,, \tag{2.13}$$

where H is the Hamiltonian of the system. In the path integral approach, one may derive this quantity by considering system is in a state $|q^i\rangle$ at time t_i. The probability that the system will be found in the state $\left|q^f\right\rangle$ at a final time t_f

$$\left\langle q^f_{t_f} \middle| q^i_{t_i} \right\rangle = \left\langle q^f \middle| \, e^{-i(t_f - t_i)H} \, \middle| q^i \right\rangle. \tag{2.14}$$

By identifying this probability with the partition function, one may write

$$Z = \left\langle q^f \middle| \, e^{-i(t_f - t_i)H} \, \middle| q^i \right\rangle = \int \mathcal{D}q(t) \, e^{iS[q(t)]}. \tag{2.15}$$

The two formulas (2.13) and (2.15) are identical, provided the following changes are made in the last formula:

- set $i(t_f - t_i) = \beta = \beta_{st}$ or $t_i = 0$, and $it_f = \beta = \beta_{st}$, since the origin of time can be arbitrary.

- set $q^i = q^f = q$, so that the initial and the final states are the same; the fact that the two states differ by an Euclidean time β, requires that the configurations be periodic so that

$$q(\beta) = q(0), \tag{2.16}$$

in the functional integrations. Thus periodicity of the Euclidean time of the space-time is identified with the inverse temperature of the system and equilibrium condition demands that the temperature of black hole should be same with the inverse of β.

We would now like to calculate the Euclidean action. This will be used to compute various thermodynamic quantities. Following Witten's approach [4], we note that from the equation of motion that the Ricci scalar R can be written in terms of AdS length scale l as

$$R = -\frac{20}{l^2}. \tag{2.17}$$

Then the action is

$$I = -\frac{8}{\kappa_5 l^2}\int d^5x\sqrt{-g_5} = -\frac{8i}{\kappa_5 l^2}\int d^5x\, r^3\,\sqrt{\gamma} = \frac{8}{\kappa_5 l^2}\int_0^\beta d\tau\int_{r_+}^R dr\, r^3\,\omega_3. \tag{2.18}$$

Here γ is the determinant of the metric on the 3-sphere. In the large volume limit ($r \to \infty$), the action diverges. However this divergence can be removed if we calculate this action by considering thermal AdS as[1] the reference background. This requires the two geometries to be identical at asymptotic boundary. In particular periodicities in Euclidean time directions of these two geometries must be the same. Thus from equations (2.5) and (2.7) it follows

$$\sqrt{1+\frac{r^2}{l^2}}\beta_{ads} = \sqrt{1+\frac{r^2}{l^2}-\frac{m}{r^2}}\beta, \tag{2.19}$$

[1]Thermal AdS is given by the Euclidean version of AdS metric 3.5 with any periodicity along Euclidean time.

where β_{ads} is the period of the thermal AdS back ground. Now the action is

$$\begin{aligned}\Delta I &= I_{\text{blackhole}} - I_{\text{AdS}},\\ &= \frac{8\,\omega_3}{\kappa_5\,l^2}\left[\int_0^{\beta} d\tau \int_{r_+}^{R} r^3 dr - \int_0^{\beta_{ads}} d\tau \int_0^{R} r^3 dr\right],\\ &= \frac{\omega_3\,\beta\,r_+^2}{\kappa_5}\left(1-\frac{r_+^2}{l^2}\right). \qquad (2.20)\end{aligned}$$

In getting the last expression we have used the boundary condition (2.19).

2.3 Thermodynamics

Thermodynamic properties follow from ΔI in (2.20). Before we do so, let us first define some dimensionless quantities as

$$\bar{r} = \frac{r_+}{l} \text{ and } \bar{m} = \frac{m}{l^2}. \qquad (2.21)$$

In terms of these quantities, the Euclidean time period β, or the inverse temperature, can be written as

$$\beta = \frac{2\pi\,\bar{r}\,l}{2\bar{r}^2+1}. \qquad (2.22)$$

Figure 2.1 shows the nature of inverse temperature β vs. horizon radius $\bar{r}$. It starts with zero at $\bar{r}=0$ and reaches maximum value (or minimum temperature $T_{min}=\frac{\sqrt{2}}{\pi l}$) at $\bar{r}=\frac{l}{\sqrt{2}}$, and finally goes to zero for large $\bar{r}$. Therefore, unlike Schwarzschild black hole in flat space, in AdS space black hole exists only beyond a critical temperature T_{min}. At this critical temperature black holes start to nucleate and above this value, for a given temperature, there are always two black hole solutions. Depending on their sizes, we call them small and big black holes. As we will see later in this section, the small hole has negative specific heat, while the large hole has positive specific heat. Since in thermodynamics, system with negative specific heat is unstable, we call the small black hole unstable.

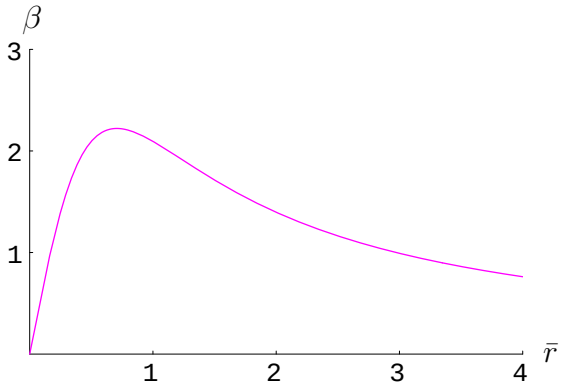

Figure 2.1: Inverse temperature β vs horizon radius $\bar{r}$.

The mass of the black hole be calculated by interpreting $e^{-\Delta I}$ as a statistical average $e^{-\beta E}$. We know $I = \frac{\omega_3 \beta \bar{r}^2 l^2}{\kappa_5}(1-\bar{r}^2)$. So

$$\begin{aligned} E &= \frac{\partial \Delta I}{\partial \beta} = \frac{\partial \Delta I}{\partial \bar{r}} \frac{\partial \bar{r}}{\partial \beta}, \\ &= \frac{3\,\omega_3\, l^2\, \bar{r}^2}{\kappa_5}\left(1+\bar{r}^2\right) = \frac{3\,\omega_3\, \bar{m}\, l^2}{\kappa_5} = M. \end{aligned} \tag{2.23}$$

The specific heat can be calculated via the relation

$$C_p = \frac{\partial E}{\partial T} = \frac{\partial M}{\partial \bar{r}} \frac{\partial \bar{r}}{\partial T} = \frac{6\,\omega_3 l^3(\bar{r}+2\bar{r}^3)}{\kappa_5(\frac{2}{\pi} - \frac{1+2\bar{r}^2}{2\,\pi\bar{r}^2})}. \tag{2.24}$$

Notice that, specific heat is positive if $\bar{r} > \frac{l}{\sqrt{2}}$ which is the solution of the denominator $(\frac{2}{\pi} - \frac{1+2\bar{r}^2}{2\,\pi\bar{r}^2}) = 0$. Otherwise it is negative.

The entropy S of the black hole can be calculated from the Euclidean action by identifying βF as I where F is the free energy. Then the entropy is

$$S = \beta\, E - \Delta I = \frac{4\,\pi\,\omega_3\, l^3\, \bar{r}^3}{\kappa_5}, \tag{2.25}$$

and

$$F = \frac{\Delta I}{\beta} = \frac{2\pi^2 \bar{r}^2 l^2}{\kappa_5}\left(1-\bar{r}^2\right). \tag{2.26}$$

Note that the free energy is computed by subtracting the thermal AdS. So we expect that, when free energy is positive, the black hole is unstable and will decay to AdS by loosing its entropy via radiation of massless matter. This happens when $\bar{r} < 1$. However, the free energy becomes negative for the black hole size greater than 1 in dimensionless unit and it becomes stable. From equation (2.22), we see that for $\bar{r} = 1$, $T = T_c = \frac{3}{2\pi l}$. Thus a transition occurs from the thermal AdS phase to the black hole phase as we increase the temperature beyond T_c. Notice that for the thermal AdS $\bar{r} = 0$. If we identify $\bar{r}$ as an order parameter, around $T = T_c$ there is jump in the order parameter from $\bar{r} = 0$ to $\bar{r} = 1$. This can therefore be identified as a first order phase transition. In literature, this is known as Hawking-Page transition [2]. A plot of free energy vs. horizon radius for the AdS-Schwarzschild black hole is shown in figure 2.2. In figure 2.3, we have plotted the free energy as a function

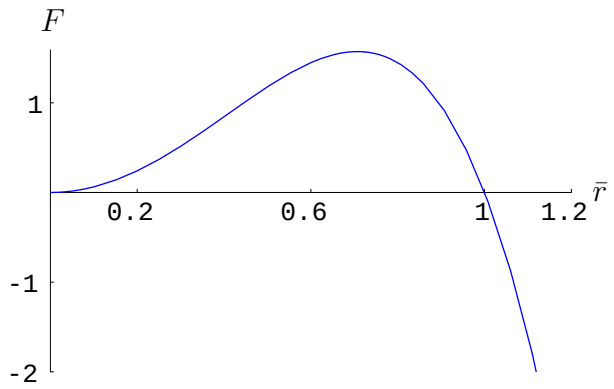

Figure 2.2: Free energy F vs. horizon radius $\bar{r}$.

of temperature T. To summarize, we therefore have the following scenario. At low temperature there is no black hole phase. If we increase the temperature, at T_{min}, two black hole solutions appear. Both of them have positive free energies with respect to the thermal AdS. Hence they are both metastable phases. However above T_c one has always positive free energy for the small black hole while the other has a negative

free energy. The later is the stable big black hole phase. There is a crossover from thermal AdS to the large black hole phase at T_c.

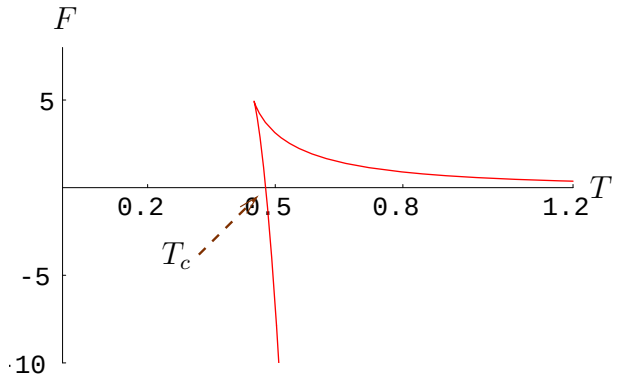

Figure 2.3: Free energy F vs. temperature T.

To understand the behaviour of the dual gauge theory, in the next section, we briefly review the Wilson loop computation of [12, 13, 14, 15, 16, 17].

2.4 Wilson Loop Computation

We consider a $SU(N)$, $\mathcal{N} = 4$ SYM gauge theory on the boundary in the limit of $N \to \infty$. Note that the boundary has the geometry of $S^1 \times S^3$, S^1 being the compactified Euclidean time. It is believed that low temperature phase is in a confined phase of mesons and glueballs. On the other hand, at the high temperature phase, because of asymptotic freedom, the gauge theory is in the deconfined phase [18, 19]. In general, to study this phase transitions we need to look for a proper order parameter. The order parameter here is the Wilson loop operator, the one which wraps the Euclidean time circle S^1. It is defined by [12]

$$W(\mathcal{C}) = \frac{1}{N}\mathrm{Tr}Pexp\left[i\int_{\mathcal{C}} dx^{\mu}A_{\mu}(x)\right] \tag{2.27}$$

where $\int_{\mathcal{C}}$ denotes the line integral along the closed Euclidean time circle S^1 and P denotes path ordering. A_μ is the gauge field on S^3. To evaluate the expectation value of this Wilson loop, we consider a rectangular loop (RT) in the Euclidean space. Here R is along one of the spatial directions x^1 and T is along the Euclidean time direction. A pair of infinitely heavy quark and anti-quark are at the end points of R. Then the expectation value of this Wilson loop for large value of time T will behave as [20]

$$\langle W(\mathcal{C}_{RT})\rangle \,|_{T\to\infty} \sim e^{-KRT}. \tag{2.28}$$

We can interpate the exponent as $-E(R)T$, where $E(R)$ is the potential between a pair of heavy quark and antiquark. The coefficient K is the force between the pair and this is independent of the separation between them. In the confining regime, pair of quark antiquark behaves as if they are connected by a string of tension K. In the confined phase $E(R) \to \infty$. This is because to bring a single quark inside the confined phase, one has to do infinite amount of work. However, in the deconfined phase $E(R)$ is finite. Thus in confined phase expectation value of the Wilson loop operator is zero and in deconfined phase this has a finite value. Therefore, there is a discreate change in the order parameter between these two phases. This is a requirement of the first order phase transition.

One can calculate the expectation value of this Wilson loop for the bulk side. For that the value of the Wilson loop is calculated from the area of the worldsheet ending on the boundary Euclidean time circle S^1 [13, 14, 15, 16, 17]. This area is the action of the worldsheet in the corresponding background. Thus the expectation value of the Willson loop is $\sim e^{-I}$. In the thermal AdS geometry, there is no contractible circle wrapping in the thermal circle S^1. So the area of this worldsheet is infinite and expectation value is zero. On the other hand, for the black hole geometry, at $r = r_+$, the thermal circle contracts to zero size at the horizon and consequently there is a finite expectation value of the Wilson loop. This leads to the identification of the thermal AdS and black hole phases of the bulk with the confined and deconfined phases of the boundary gauge theory respectively. HP transition in bulk is then the

confinement/deconfinement transition in the boundary.

2.5 Landau-Ginsburg Potential

Keeping our future analysis in mind, in this section, we try to understand the HP transition from a slightly different perspective. We know, from standard thermodynamics, that near the critical point of a phase transition, the system can be represented by a Landau function. Construction of this function goes as follows. Let us consider a function G which depends on order parameter η and temperature T in the following way [21],

$$G(T,\eta) = \alpha_0\eta^0 + \alpha_1\eta^1 + \alpha_2\eta^2 + \alpha_3\eta^3 + \alpha_4\eta^4 + ... \tag{2.29}$$

Here α_i, in general, are functions of T. We urge the function G to satisfy following criterions:

- At $\eta = 0$, G should be zero. Consequently α_0 must be zero.
- At low temperature, G has only one minimum at $\eta = 0$. This gives a condition $\frac{\partial G}{\partial \eta}\Big|_{\eta=0} = 0$. This will not allow first power of the order parameter in the expression of G. Thus α_1 has to be zero.
- Above a certain temperature T_{min}, one more minimum appears at $\eta > 0$. Minima at $\eta = 0$ and $\eta > 0$ must be separated by a maximum. For a global stability of the second minimum at high temperature, we need at least a quartic power of order parameter. Higher powers can be neglected if we are sufficiently close to the critical point. This leads to the following form of the Landau function

$$G(T,\eta) = \alpha_2\eta^2 + \alpha_3\eta^3 + \alpha_4\eta^4 + ... \tag{2.30}$$

- Furthermore, at the extrema of this function, that is at $\frac{\partial G}{\partial \eta} = 0$, we should get back the expression of the temperature. If we then plug in the expression of temperature in the Landau function, it should reduce to the free energy of

the system. From these three conditions, remaining constants $(\alpha_2, \alpha_3, \alpha_4)$ can easily be calculated and the final expression for the Landau function can also be written in terms of order parameter and temperature of the system.

If we apply this method for AdS-Schwarzschild black hole, we get the Landau function as

$$G(T, \bar{r}) = \frac{\omega_3 l^2}{\kappa_5} \left(3\bar{r}^4 - 4\pi l T \bar{r}^3 + 3\bar{r}^2\right). \tag{2.31}$$

Here we have identified horizon radius $\bar{r}$ as the order parameter. Note that $\frac{\partial G}{\partial \bar{r}} = 0$ gives back the expression of temperature of equation (2.22) and then if we substitute back the expression of temperature in (3.17), $G(T, \bar{r})$ reduces to free energy of equation (2.26). A plot of this Landau function G vs $\bar{r}$ has been given in figure 2.4. It shows

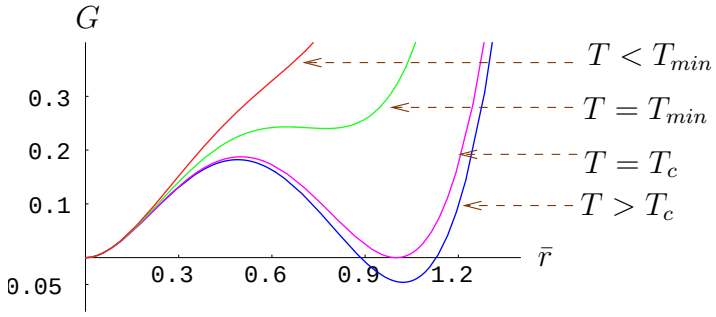

Figure 2.4: Landau free energy G vs. order parameter $\bar{r}$.

that at a very low temperature, there is only one minimum at $\bar{r} = 0$, representing the thermal AdS. If we increase the temperature, at T_{min}, two more extrema appear. Black hole nucleation starts here. However, below critical temperature T_c, the new minimum has always higher energy than that of thermal AdS. At temperature T_c, the two minima are degenerate suggesting a coexistence of both the black hole and the AdS phases. Finally, above T_c only the black hole phase becomes stable. We note that the discrete change of the order parameter at T_c represents a first order

transition.

Witten, in [4], identified this transition with the confinement/deconfinement transition on the boundary. In the next section we elaborate this by constructing a phenomenological matrix model. Here we follow [9, 10, 1].

2.6 Dual Matrix Model

It is a very hard problem to study various phases of gauge theory at strong coupling. However, if we assume AdS/CFT correspondence, it is possible to construct a phenomenologically motivated matrix model. Such a model is constructed in [1]. This model qualitatively reproduces the bulk behaviour expected from AdS/CFT. Though uniqueness of such model is always questionable (except perhaps near the critical points), it is encouraging to find atleast one simple model of strongly coupled gauge theory near criticality. In this section we discuss this model. We will call this as (a, b) model for the reasons that will be obvious later.

Since the asymptotic boundary is S^3, (a, b) matrix model represents gauge theory on $S^3 \times S^1$. At zero temperature, it is $\mathcal{N} = 4$ supersymmetric $SU(N)$ gauge theory. Supersymmetry is broken when we consider the system at finite temperature.

In the next subsection, we first discuss the boundary theory at weak coupling. Next, we review the proposal [1] of phenomenological (a, b) model for strongly coupled gauge theory. This model has two parameters namely a, and b. On generic grounds, one expect them to depend on the temperature T and the coupling λ. We end this section with a discussion on temperature dependence of a, and b at fixed large λ. Though the results are obtained in [1], we follow an approach which is suitable for our purpose.

2.6.1 Weak coupling

$\mathcal{N} = 4$, $SU(N)$ gauge theory at weak coupling has been analyzed by various authors (see for example [9, 10]). For large N, when the 't Hooft coupling $\lambda = g_{YM}^2 N$ is small or zero, some of the results are explicitly known. Specifically, when $\lambda = 0$, it was shown that the boundary gauge theory at finite temperature on $S^3 \times S^1$ undergoes a phase transition that can be identified as the"deconfinement" transition. $S^3 \times S^1$ is a compact manifold and thus allows only colour singlet states by the Gauss law constraint. Though non singlet states are never possible, there are various indications that this transition mimics the deconfinement transition in gauge theories. One of the indications comes from the fact that there is a jump of the free energy from order N^0 to order N^2 [18] while the other is a discrete change in expectation value of the Wilson loop.

We now start by considering the partition function of $\mathcal{N} = 4$ free ($\lambda \to 0$) super Yang-Mills theory on $S^1 \times S^3$ at a finite temperature T.

$$Z(\lambda, T) = \int_{S^1 \times S^3} \mathcal{D}A e^{-S_{YM}(A)}. \tag{2.32}$$

Kaluza-Klein reduction of the $\mathcal{N} = 4$ theory on $S^3 \times S^1$ leaves only one massless mode, namely, the zero mode of A_0. Here A_0 is the time component of the gauge field. One can thus write down an effective action by integrating out all the massive modes. The resulting model with the gauge fixing conditions, $\partial_i A_i = 0$ and $\partial_t \alpha(t) = 0$, is a zero dimensional matrix model given by,

$$\begin{aligned} Z(\lambda, T) &= \int [DU] e^{S_{eff}(U)}, \\ \text{where,} \qquad U &= e^{i\beta\alpha} \ , \ \alpha = \frac{1}{\omega_3} \int_{S^3} A_0, \end{aligned} \tag{2.33}$$

U is a unitary matrix and $[DU]$ is the measure. Gauge invariance requires that the effective action has to be a polynomial of $\mathrm{Tr}U^n$. Here n is an integer, allowed by the Z_n symmetry. The explicit form of the partition function is then given by [10],

$$Z = \int [DU] \exp\left[\sum_{n=1}^{\infty} \frac{1}{n} z(x^n) \left(\mathrm{Tr}(U^n)\mathrm{Tr}(U^{-n})\right)\right], \tag{2.34}$$

where, $z(x^n) = z_V(x^n) + z_S(x^n) + (-1)^{n+1} z_F(x^n)$; $x = e^{-\beta}$,

and $z_V(x^n), z_S(x^n)$ and $z_F(x^n)$ are the partition functions of vector, scalar and fermion respectively. This model can be rewritten in terms of the eigen values of the unitary matrix by diagonalizing the matrix. Consider these eigen values as $\{e^{i\,\theta_i}\}$ where θ_i runs from $(-\pi$ to $\pi)$ and lie on a unit circle. One can write down the partition function in terms of eigen values by replacing [10]

$$\int [DU] \to \prod_i \int [d\theta_i] \prod_{i<j} \sin^2\left(\frac{\theta_i - \theta_j}{2}\right); \qquad \mathrm{Tr}(U^n) \to \sum_j e^{in\theta_j} \tag{2.35}$$

Introducing the density of eigenvalues for U in the large N limit as

$$\varrho(\theta) = \frac{1}{N}\sum_{i=1}^{N} \delta(\theta - \theta_i), \qquad -\pi \le \theta < \pi, \tag{2.36}$$

and defining Wilson loop as

$$\frac{1}{N}\mathrm{Tr}(U) = \rho_n = \int_{-\pi}^{\pi} d\theta \varrho(\theta) e^{i\,n\,\theta}, \tag{2.37}$$

partition function can be written as (see [10] for details)

$$Z = \int [d\rho] e^{-N^2 V[\varrho]}, \tag{2.38}$$

where $V[\varrho]$ to leading order in $\frac{1}{N}$ has the form

$$V[\varrho] = -P \int d\theta\, d\phi\, \rho(\theta)\, \rho(\phi) \log\left(2\sin\frac{\theta-\phi}{2}\right) - S(\rho_1^2). \tag{2.39}$$

Here P denotes the principle part. Assuming that $z(x^n)$ contains only positive powers of n, we have neglected all higher powers except $n = 1$ [1]. In the following analysis, to simplify the notation, we will write $\rho_1 = \rho$. The saddle point equation of motion of the above equation is

$$P \int d\phi\, \varrho(\phi) \cot\frac{\theta-\phi}{2} = 2S'(\rho^2)\rho\sin\theta. \tag{2.40}$$

To get this equation we have used $U^\dagger = U$. In (2.40), prime represents the derivative with respect to ρ^2. The solution of the saddle point equation can easily be written

down with the help of the results in [22, 23]. In the following, we discuss that and then come back to (2.40).

Consider the partition function [22, 23]

$$Z = \int [dU] e^{S(U)} \qquad \text{with} \qquad S(U) = \frac{1}{g^2}\mathrm{Tr}(U + U^\dagger). \tag{2.41}$$

The equation of motion is

$$P \int d\phi\, \varrho(\phi) \cot\frac{\theta - \phi}{2} = \frac{2}{\lambda}\sin\theta. \tag{2.42}$$

The solution of this equation of motion is given by

$$\begin{aligned} \varrho(\theta) &= \frac{2}{\pi\lambda}\cos\frac{\theta}{2}\left[\frac{\lambda}{2} - \sin^2\frac{\theta}{2}\right]^{1/2} \qquad \lambda \le 2 \qquad |\theta| \le 2\sin^{-1}\left(\frac{\lambda}{2}\right)^{1/2}, \\ &= \frac{1}{2\pi}\left[1 + \frac{2}{\lambda}\cos\theta\right] \qquad \lambda \ge 2 \qquad |\theta| \le \pi. \end{aligned} \tag{2.43}$$

Then the corresponding Wilson loop turns out to be

$$\begin{aligned} \int_{-\pi}^{\pi} d\theta \varrho(\theta) e^{i\theta} &= \frac{1}{\lambda} \qquad \lambda \ge 2, \\ &= 1 - \frac{\lambda}{4} \qquad \lambda \le 2, \end{aligned} \tag{2.44}$$

and the free energy is

$$\begin{aligned} F &= \frac{1}{\lambda^2} \qquad \lambda \ge 2, \\ &= \frac{2}{\lambda} + \frac{1}{2}\log\frac{\lambda}{2} \qquad \lambda \le 2. \end{aligned} \tag{2.45}$$

We see a third order phase transition from gapped phase to ungapped phase at $\lambda = 2$. This is known as Gross-Witten phase transition.

Now we go back to our original equation (2.40). Equation (2.40) and (2.42) are same if we replace $\frac{1}{\lambda} = S^{'}(\rho^2)\rho$. Then one can find out the solution of saddle point equation of (2.40) from (2.44). This is

$$\begin{aligned} S^{'}(\rho^2)\rho = a\,\rho &= \rho \qquad \text{for} \quad 0 \le \rho \le \frac{1}{2}, \\ &= \frac{1}{4(1-\rho)} \qquad \text{for} \quad \frac{1}{2} \le \rho \le 1. \end{aligned} \tag{2.46}$$

In terms of the density of eigenvalues, the above transition is reflected by a jump of ρ from zero to a nonzero value below and above T_h respectively, where T_h is given by $a = z(x) = 1$. A plot of an effective potential of equation (2.46) is shown in figure 2.5.

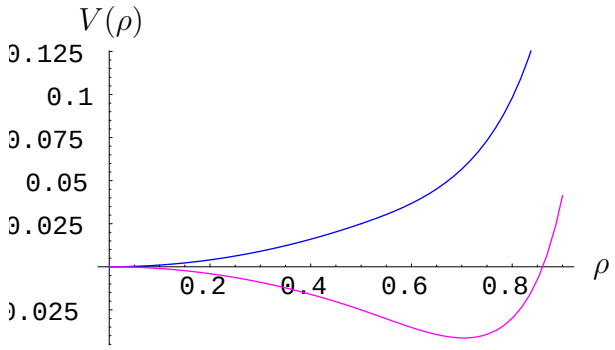

Figure 2.5: Effective potential $V(\rho)$ vs. ρ. Blue and pink lines are for $a = .8$ and $a = 1.2$ respectively.

These features are somewhat modified when a small value of the coupling λ is turned on. It is possible to write S_{eff} only in terms of powers of $\mathrm{Tr}(U)$ by using the saddle point equations. An effective action containing only the quartic interactions may be written as [2],

$$Z(\lambda, T) = \int [DU \exp\left[a(\lambda, T)\mathrm{Tr}(U)\mathrm{Tr}(U^\dagger) + \frac{b}{N^2}(\lambda, T)\Big(\mathrm{Tr}(U)\mathrm{Tr}(U^\dagger)\Big)^2\right]. \quad (2.47)$$

The equations of motion resulting from (2.47) are,

$$\begin{aligned} a\rho + 2b\rho^3 &= \rho \qquad 0 \le \rho \le \frac{1}{2}, \\ &= \frac{1}{4(1-\rho)} \qquad \frac{1}{2} \le \rho \le 1. \end{aligned} \quad (2.48)$$

[2]This model is obtained by keeping terms upto $\mathcal{O}(\lambda^2)$ in the effective action. In the large N limit such terms come from three loop computations. It also determines the sign of b. In [10] the phases for both the signs of b have been studied. An explicit computation for pure Yang Mills theory on a three sphere at finite temperature shows that b is positive, implying that the transition is of first order at weak coupling [6].

The matrix model (2.47) undergoes two different phase transitions as a function of temperature. One is a first order transition similar to the zero coupling case, when $b > 0$. The other is a third order transition for which the eigenvalue distribution goes from the gapless phase for $0 \leq \rho \leq \frac{1}{2}$, to a phase with a gap for $\frac{1}{2} \leq \rho \leq 1$.

2.6.2 Strong coupling and comparison to gravity

If we assume the validity of (2.47) in the strong coupling regime (where a and b are some complicated functions of λ and temperature), we surprisingly find that the model replicates, almost completely, the phases of gravity obtained in the supergravity approximation. To check that we first construct the effective potential that follows from (2.47). It is given by,

$$\begin{aligned} V(\rho) &= \frac{1-a}{2}\rho^2 - \frac{b}{2}\rho^4, & 0 \leq \rho \leq \frac{1}{2} \\ &= -\frac{a}{2}\rho^2 - \frac{b}{2}\rho^4 - \frac{1}{4}\log[2(1-\rho)] + \frac{1}{8} & \frac{1}{2} \leq \rho \leq 1. \end{aligned} \tag{2.49}$$

The constant $\frac{1}{8}$ is added to make the potential continuous at $\rho = 1/2$.

Before getting into the comparison betwen theories of the bulk and the boundary, we would like to recall some thermodynamic behaviour of the bulk which has been studied in the previous section. At low temperature thermal AdS phase is stable. However if we increase temperature gradually, above temperature T_{min}, two more black hole solutions appear. Smaller one is unstable and big one is stable. Finally, at temperature T_c there is a crossover from thermal AdS to the big black hole phase. Witten identified this transition with the confinement/deconfinement transition in the boundary gauge theory. A natural order parameter that characterizes phases of the boundary theory is Wilson loop operator, which is the density of eigen values in matrix model.

Now, to compare bulk and dual gauge theory, we plot equations of motion (2.48) and effective potential (2.49) in figure 2.6. The main figure is the plot of the left (dashed lines) and the right hand side (solid line) of the saddle point equations for

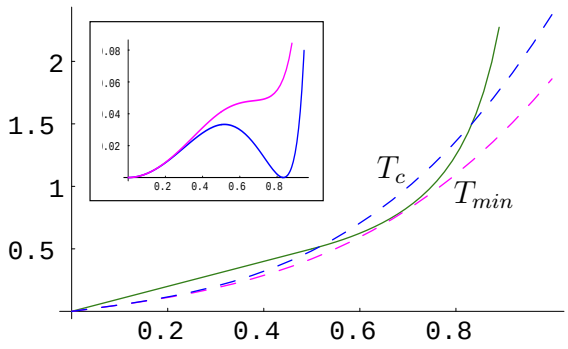

Figure 2.6: The main figure is the plot of left (dashed lines) and the right hand side (solid line) of the saddle point equations. T_{min} is the point where the two roots of (2.48) merge. T_c is the curve corresponding to the Hawking-Page transition temperature. The insert is the potential corresponding to these temperatures

the parameters $a < 1$ and $b > 0$. The insert figure is of the effective potentials for the corresponding values of the parameters of the equations of motion (2.48). The main figure shows that $\rho = 0$ is always a solution that represents the thermal AdS. For particular values of the parameters, two more roots appear at $\rho > 0$, those can be identified with stable and unstable black holes and the values of the parameters may be related to the black hole nucleation temperature T_{min}. Then, if we increase the values of parameters in the same direction, there is a phase transition between $\rho = 0$ phase and $\rho > 0$ phase. This can again be compared with the Hawking-Page transition of the bulk. Thus, this simplified model indeed qualitatively reproduces the thermodynamic behaviour of the gravity when $a < 1$ and $b > 0$ [1]. It is indeed surprising that this simple model falls in the same universality class as that of the gauge theory at strong coupling. A new feature that is not visible in the supergravity approximation is the appearance of a third order transition that was mentioned in the earlier paragraph. It was conjectured that this should correspond to black hole/string transition [24]. It should however be noted that the matching is only qualitative and the validity of the effective action (2.47) in the strong coupling regime is perhaps only limited to the regions around the critical points.

2.6.3 Temperature dependence of the parameters

The following part of this section is devoted to the study of the (a, b) model numerically. In this analysis we take $N \to \infty$ and the limit $\lambda \to \infty$. The main aim is to compute a and b as functions of T for fixed λ. This will be done by comparing the matrix model potential with the action on the gravity side.

The comparison between matrix model potential and the action of the bulk theory is valid as long as we can neglect the string loop corrections. The corresponding temperature at which the supergravity description breaks down is identified as the Gross-Witten transition point on the matrix model side [25]. Let T_{min} be the tem-

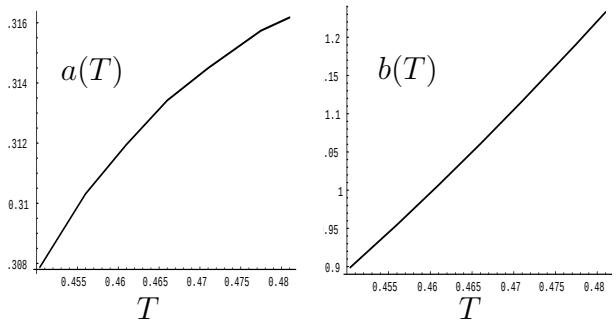

Figure 2.7: Plots of $a(T, 0)$ and $b(T, 0)$

perature at which the black hole nucleation starts. For $T > T_{min}$, it is well known that for the gravity theory, one gets two solutions for the black hole.

Consider $T > T_{min}$, for which we have[3]

$$2a\rho_{1,2}^2 + 2b\rho_{1,2}^4 + \log(1 - \rho_{1,2}) + \log(2) - \frac{1}{2} = -I_{1,2}, \tag{2.50}$$

where the $I_{1,2}$ are the actions for the large and small black-holes respectively and $\rho_{1,2}$ are the corresponding solutions in the matrix model. Since the values of $\rho_{1,2}$ are those

[3]We set l, ω_3, κ_5 to 1 in the numerical computations.

at the extremum of the left hand side of (2.50), we have two more equations that are given by (2.48).

For a given temperature, T, $I_{1,2}$ are known from the gravity side, so the problem now is to solve the above equations for $a(T)$, $b(T)$ and $\rho_{1,2}$. We do this numerically. The solutions are plotted in figure 2.7. Note that $a(T)$ and $b(T)$ increases monotonically with temperature.

2.7 Discussion

In this chapter we have reviewed five dimensional bulk theory in the supergravity limit. The bulk has two configurations with same asymptotic geometry. One of them is a black hole and the other is the thermal AdS. Black holes exist above a critical temperature but AdS exists at any temperature. At this critical temperature, two black holes nucleate. The big one has positive specific heat and small one is unstable with negative specific heat. At any temperature free energy of the small black hole is always positive. But only below Hawking temperature T_c free energy of the big black hole is greater than AdS. Thus AdS is the stable configuration up to T_c. However, above T_c free energy of the large black hole is less than that of AdS. Therefore beyond this temperature, the big black hole is globally stable. At T_c, the two phases coexist with same free energy and a first order phase transition takes place with an expected discrete change in the order parameter. This phase transition is known as Hawking-Page transition in literature. We studied this transition by constructing a Landau function. Witten identified this phase transition with the confinement/deconfinement transion in the strongly coupled boundary theory.

Finally, we have reviewed the phenomenological (a, b) matrix model on $S^1 \times S^3$ to study strong coupling gauge theory. For certain range of parameters, this model qualitatively reproduces all the features of the bulk theory. This matrix model however shows one more phase transition, where eigen value distribution goes from gapless

phase to a gapped phase, similar to the Gross-Witten third order transition. This has no analog in the bulk theory. Parameters of this model are expected to depend on temperature and gauge coupling. We have analysed their dependence on the temperature for fixed λ. We found that they are always increasing function of temperature for fixed gauge coupling $\lambda \to \infty$. However, to get their behaviour for different values of λ, one has to increase the gravitation coupling in the bulk. This can be effectively done by adding higher derivative term (we will call this as $\alpha^{'}$ corrections in the thesis). In the next chapter we include such terms and discuss the phenomenological Lagrangian of dual theory.

Bibliography

[1] L. Alvarez-Gaume, C. Gomez, H. Liu and S. Wadia, *Finite temperature effective action, AdS_5 black holes, and $1/N$ expansion*, Phys. Rev. D71 (2005) 124023 [arXiv:hep-th/0502227].

[2] S. W. Hawking and D. N. Page, *Thermodynamics of black holes in anti-de Sitter space*, Commun. Math. Phys. **87**, 577 (1983).

[3] J. D. Brown, J. Creighton and R. B. Mann, *Temperature, energy and heat capacity of asymptotically anti-de Sitter black holes*, Phys. Rev. D **50**, 6394 (1994) [arXiv:gr-qc/9405007].

[4] E. Witten, *Anti-de Sitter space, thermal phase transition, and confinement in gauge theories*, Adv. Theor. Math. Phys. **2**, 505 (1998) [arXiv:hep-th/9803131].

[5] R. G. Cai, *The Cardy-Verlinde formula and AdS black holes*, Phys. Rev. D **63**, 124018 (2001) [arXiv:hep-th/0102113].

[6] D. Youm, *The Cardy-Verlinde formula and topological AdS-Schwarzschild black holes*, Phys. Lett. B **515**, 170 (2001) [arXiv:hep-th/0105093].

[7] L. Cappiello and W. Muck, *On the phase transition of conformal field theories with holographic duals*, Phys. Lett. B **522**, 139 (2001) [arXiv:hep-th/0107238].

[8] A. Biswas and S. Mukherji, *On the Hawking-Page transition and the Cardy-Verlinde formula*, Phys. Lett. B **578**, 425 (2004) [arXiv:hep-th/0310238].

[9] B. Sundborg, *The Hagedorn transition, deconfinement and N = 4 SYM theory,* Nucl. Phys. B **573**, 349 (2000) [arXiv:hep-th/9908001].

[10] O. Aharony, J. Marsano, S. Minwalla, K. Papadodimas and M. Van Raamsdonk, *The Hagedorn/Deconfinement Phase Transition in Weakly Coupled Large N Gauge Theories*, Adv. Theor. Math. Phys. 8 (2004) 603 [arXiv:hep-th/0310285].

[11] S. Kalyana Rama and B. Sathiapalan, '*The Hagedorn transition, deconfinement and the AdS/CFT correspondence,* Mod. Phys. Lett. A **13**, 3137 (1998) [arXiv:hep-th/9810069].

[12] K. G. Wilson, *Confinement of quarks*, Phys. Rev. D **10**, 2445 (1974).

[13] S. J. Rey and J. T. Yee, *Macroscopic strings as heavy quarks in large N gauge theory and anti-de Sitter supergravity*, Eur. Phys. J. C **22**, 379 (2001) [arXiv:hep-th/9803001].

[14] J. M. Maldacena, *Wilson loops in large N field theories*, Phys. Rev. Lett. **80**, 4859 (1998) [arXiv:hep-th/9803002].

[15] S. J. Rey, S. Theisen and J. T. Yee, *Wilson-Polyakov loop at finite temperature in large N gauge theory and anti-de Sitter supergravity*, Nucl. Phys. B **527**, 171 (1998) [arXiv:hep-th/9803135].

[16] A. Brandhuber, N. Itzhaki, J. Sonnenschein and S. Yankielowicz, *Wilson loops in the large N limit at finite temperature*, Phys. Lett. B **434**, 36 (1998) [arXiv:hep-th/9803137].

[17] Y. Kinar, E. Schreiber and J. Sonnenschein, *Q anti-Q potential from strings in curved spacetime: Classical results*, Nucl. Phys. B **566**, 103 (2000) [arXiv:hep-th/9811192].

[18] J. C. Collins and M. J. Perry, *Superdense matter: neutrons or asymptotically free quarks?*, Phys. Rev. Lett. **34**, 1353 (1975).

[19] A. M. Polyakov, *Thermal properties of gauge fields and quark liberation*, Phys. Lett. B **72** (1978) 477.

[20] Kerson Huang, *Quarks, leptons and gauge fields*, (World Scientific publication, 1992).

[21] L. E. Reichl, *A Modern course in statistical physics*, (Wiley-Interscience publication, 1997).

[22] D. J. Gross and E. Witten, *Possible Third Order Phase Transition In The Large N Lattice Gauge Theory,* Phys. Rev. D **21**, 446 (1980).

[23] E. Brezin, C. Itzykson, G. Parisi and J. B. Zuber, *Planar Diagrams*, Commun. Math. Phys. **59**, 35 (1978).

[24] G. T. Horowitz and J. Polchinski, *A correspondence principle for black holes and strings,* Phys. Rev. D **55**, 6189 (1997) [arXiv:hep-th/9612146].

[25] L. Alvarez-Gaume, P. Basu, M. Marino and S. R. Wadia, *Blackhole / string transition for the small Schwarzschild blackhole of $AdS_5 \times S^5$ and critical unitary matrix models,* Eur. Phys. J. C **48**, 647 (2006) [arXiv:hep-th/0605041].

Chapter 3

Higher Derivative Gravity and Dual Matrix Model

3.1 Introduction

In this chapter, we analyse the response of the Hawking-Page transition [1] and the corresponding matrix model as we perturbatively increase the gravitational strength. Our study is partly motivated by the recent works in [2, 3, 4, 5, 6, 7]. In these papers, authors have argued in different ways that a version of HP transition occurs even at weak coupling gauge theory. By AdS/CFT dictionary [8, 9, 10, 11, 12, 13], this would show up as a transition in strongly coupled gravity theory in the bulk. Noting the fact that string theory in AdS space is as yet poorly understood, we study a much simpler system in this chapter. We add higher derivative terms in the supergravity action and study their effects on HP transition. We note here that higher derivative terms would arise in gravity action due to α' corrections in underlying string theory. While a study with a general class of higher derivative terms would be desirable, in this thesis, we consider only the effects due to Gauss-Bonnet(GB) terms. One advantage of working with GB correction to the gravity action is that the black holes can be constructed explicitly. It is known that GB corrections arise in Heterotic or K3 compactification

of type IIA theory (see for example [14]) but not in type II theories with maximally supersymmetric compactification. The lowest correction in type IIB theory on AdS_5 is of order α'^3. The thermodynamic phases of the perturbative supergravity solutions as well as their boundary duals have been studied by various authors [15, 16, 17, 18]. However the qualitative phase structures in this case is quite similar to that of gravity with GB (α') correction. In the case with Gauss Bonnet terms we do not expect the boundary theory on $S^3 \times S^1$ to be $\mathcal{N} = 4$ Yang Mills theory. However in the limit $\alpha' \to 0$ the boundary theory should reduce to the strongly coupled SYM theory. With the R^2 corrections turned on, the gravity theory should correspond to some deformation of $\mathcal{N} = 4$ SYM.

In section 3.3, we analyse the black holes in GB theory with a particular focus on their phase structures in five space-time dimensions. The phase structure depends crucially on the GB coupling. For certain range of coupling, there exists three black hole phases. We call them small, intermediate or unstable and big black hole phase. It turns out that there are two first order phase transitions. One of them is from small black hole to the big one at a temperature scale much lower than that of inverse AdS curvature. The other one is similar to that of usual HP transition where a crossover occurs from thermal AdS to the big black hole phase. We compute the change in HP temperature in powers of the GB coupling at the crossover.

In Section 3.4, we study this effective theory by using phenomenological matrix model which has been discussed in the earlier chapter. Just to recall, this model is characterised by two parameters which we call, following [19, 20], a and b. Generally, (a, b) depend on the gauge theory temperature and the 't Hooft coupling λ. Following AdS/CFT, the effect of adding higher derivative terms in the bulk translates to λ corrections to the boundary gauge theory. *Assuming* a universal nature of the (a, b) model around the critical points, we analyse the λ dependence of parameters (a, b) around the HP points. We do this numerically.

Finally, in section 3.5, we construct a toy model which captures the whole phase

diagram of the bulk. However, this requires introduction of four parameters in the matrix model potential. These four parameters again depend on the temperature as well as the gauge coupling. We then study the qualitative behaviour of this model. This chapter ends with a discussion of our results.

3.2 Gauss-Bonnet black holes

We start by considering $(n+1)$ dimensional gravitational action in the presence of a negative cosmological constant Λ along with a GB term.

$$I = \int d^{n+1}x\sqrt{-g_{n+1}}\Big[\frac{R}{\kappa_{n+1}} - 2\Lambda + \alpha(R^2 - 4R_{ab}R^{ab} + R_{abcd}R^{abcd})\Big]. \tag{3.1}$$

This action possesses black hole solutions which we call GB black holes [14, 21, 22, 23, 24, 25, 26] . In the above action, α is the GB coupling. As the higher derivative corrections are expected to appear from the α' corrections in underlying string theory, we will often refer to such corrections as α' corrections in this thesis. The metric of these holes can be expressed as

$$ds^2 = -V(r)dt^2 + \frac{dr^2}{V(r)} + r^2 d\Omega^2_{n-1}, \tag{3.2}$$

where $V(r)$ is given by

$$V(r) = 1 + \frac{r^2}{2\hat{\alpha}} - \frac{r^2}{2\hat{\alpha}}\Big[1 - \frac{4\hat{\alpha}}{l^2} + \frac{4\hat{\alpha}m}{r^n}\Big]^{\frac{1}{2}}. \tag{3.3}$$

We first define various parameters that appear in the above equation. $d\Omega^2_{n-1}$ is the metric of an $n-1$ dimensional sphere. l^2 is related to the cosmological constant as $l^2 = -n(n-1)/(2\kappa_{n+1}\Lambda)$.

Furthermore, we have defined $\hat{\alpha} = (n-2)(n-3)\alpha\kappa_{n+1}$, where κ_{n+1} is the $n+1$ dimensional gravitational constant. The parameter m in (3.3) is related to the energy of the configuration as

$$M = \frac{(n-1)\omega_{n-1}m}{\kappa_{n+1}}, \tag{3.4}$$

where ω_{n-1} is the volume of the $n-1$ dimensional unit sphere. Asymptotically, the metric (3.3) goes to AdS space, since in this limit

$$V(r) = 1 + \Big[\frac{1}{2\hat{\alpha}} - \frac{1}{2\hat{\alpha}}\Big(1 - \frac{4\hat{\alpha}}{l^2}\Big)^{\frac{1}{2}}\Big]r^2. \tag{3.5}$$

We see from here that the metric is real if and only if

$$\hat{\alpha} \leq l^2/4. \tag{3.6}$$

In our discussion, we will always consider $\hat{\alpha}$ satisfying the above bound. The metric (3.2) has a central singularity at $r = 0$. The zeros of $V(r)$ correspond to the locations of the horizons.

In five dimension, for which $n = 4$, there is a single horizon at

$$r^2 = r_+^2 = \frac{l^2}{2}\Big[-1 + \sqrt{1 + \frac{4(m-\hat{\alpha})}{l^2}}\Big]. \tag{3.7}$$

We note here that for a black hole to exist $m > \hat{\alpha}$.

3.3 Phases of GB Black holes

Thermodynamics of these black holes can be obtained via standard Euclidean action calculation which is already discussed in the previous chapter. Following these computations, the free energy and temperature can be written down as

$$\begin{aligned} F = \quad & \frac{\omega_{n-1} r_+^{n-4}}{\kappa_{n+1}(n-3)(r_+^2 + 2\hat{\alpha})}\Big[(n-3)r_+^4(1 - \frac{r_+^2}{l^2}) - \frac{6(n-1)\hat{\alpha}r_+^4}{l^2} \\ & + (n-7)\hat{\alpha}r_+^2 + 2(n-1)\hat{\alpha}^2\Big], \end{aligned}$$

$$T = \quad \frac{(n-2)}{4\pi r_+(r_+^2 + 2\hat{\alpha})}\Big[r_+^2 + \frac{n-4}{n-2}\hat{\alpha} + \frac{n}{n-2}\frac{r_+^4}{l^2}\Big]. \tag{3.8}$$

The black hole entropy is given by

$$S = \int T^{-1}\Big(\frac{\partial M}{\partial r_+}\Big)dr_+ = \frac{4\pi\omega_{n-1}r_+^{n-1}}{\kappa_{n+1}}\Big[1 + \frac{n-1}{n-3}\frac{2\hat{\alpha}}{r_+^2}\Big], \tag{3.9}$$

and the specific heat is

$$C = \frac{\partial M}{\partial T}$$

$$= \frac{4\pi(n-1)\omega_{n-1}r^{n-3}(r^2+2\hat{\alpha})^2[\hat{\alpha}l^2(n-4)+r^2(l^2(n-2)+nr^2)]}{\kappa_{n+1}[\hat{\alpha}r^2(6nr^2-l^2(n-8))+r^4(nr^2-(n-2)l^2)-2(n-4)\hat{\alpha}^2l^2]}. \quad (3.10)$$

Many interesting features of the GB black holes, related to local and global stabilities, can be inferred from a detailed study of the thermodynamic quantities. In the rest of the section, we proceed to do so by considering the holes in five dimensions ($n = 4$). Let us first introduce two dimensionless quantities

$$\bar{\alpha} = \frac{\hat{\alpha}}{l^2}, \text{and} \;\; \bar{r} = \frac{r_+}{l}. \quad (3.11)$$

We would like to express various thermodynamic quantities in terms of these dimensionless constants. The free energy given in (3.8) can be written as

$$F = -\frac{\omega_3 l^2}{\kappa_5(\bar{r}^2+2\bar{\alpha})}\Big[\bar{r}^6+(18\bar{\alpha}-1)\bar{r}^4+3\bar{\alpha}\bar{r}^2-6\bar{\alpha}^2\Big]. \quad (3.12)$$

It then follows from (3.12), that within the range of allowed value of the coupling $\bar{\alpha}$ (see (3.6)), F starts being positive at $\bar{r} = 0$ and changes sign only once as we increase $\bar{r}$. The number of extrema of the free energy, however, crucially depends on $\bar{\alpha}$. In particular, when $\bar{\alpha}$ is in the region

$$0 < \bar{\alpha} \leq \frac{1}{36}, \quad (3.13)$$

F has three extrema. At these points, F takes non-zero positive values. However, for

$$\frac{1}{36} \leq \bar{\alpha} \leq \frac{1}{4}, \quad (3.14)$$

F has no extremum for any non-zero $\bar{r}$. It starts with a nonzero value at $\bar{r} = 0$, then decreases monotonically and becomes negative at large $\bar{r}$. Typical behaviour of the free energy as a function of $\bar{r}$ is shown figure 3.1. We will refer back to this plot when we analyse the stability of these holes.

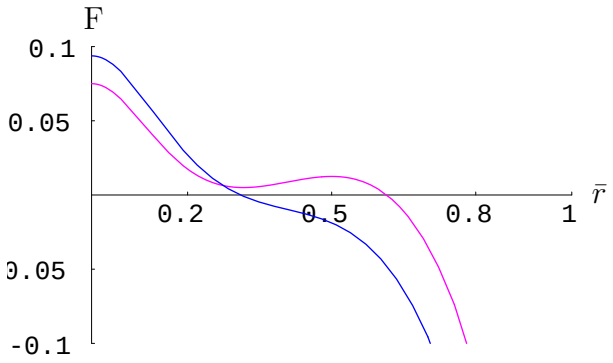

Figure 3.1: Free energy as a function of $\bar{r}$ for different values of $\bar{\alpha}$. The pink line is for $\bar{\alpha} = 1/40$ and the other one $\bar{\alpha} = 1/32$.

For now, we turn our attention to the temperature of the black holes. It follows from (3.8) that the temperature is given by [1]

$$T = \frac{\bar{r} + 2\bar{r}^3}{2\pi l(\bar{r}^2 + 2\bar{\alpha})}. \tag{3.16}$$

At $\bar{r} = 0$, temperature starts out from zero and, regardless of the value of $\bar{\alpha}$, it increases for small $\bar{r}$. However, at larger $\bar{r}$, the number of extrema depends on $\bar{\alpha}$. In the region given in (3.13), there are two of these extrema. Both of these disappear as we increase $\bar{\alpha}$ to region (3.14). A plot of the temperature as a function of $\bar{r}$ is shown in figure 3.2.

To examine the phase structure of these black holes, it is instructive to consider the behaviour of the free energy as a function of temperature (for different values of $\bar{\alpha}$).

[1] In the limit $l \to \infty$ ($\Lambda = 0$) this solution reduces to the asymptotically flat Gauss Bonnet black hole. The temperature is then given by

$$T = \frac{r_+}{2\pi(r_+^2 + 2\hat{\alpha})} \tag{3.15}$$

For finite value of $\hat{\alpha}$, temperature begins with zero value at $r_+ = 0$ and gradually increases for small r_+. Finally it reaches a maximum value at $r_+ = \sqrt{2\alpha}$ and then again goes towards zero at large r_+. Since the temperature has a maximum, above this critical value there is no black hole solution. At any temperature below there are two black hole solutions, small and large. The small black hole has positive specific heat and is locally stable. The larger one is unstable due to its negative specific heat. This is to be contrasted with the Schwarzschild black hole solution without R^2 correction, where we have only one unstable solution existing at all temperatures.

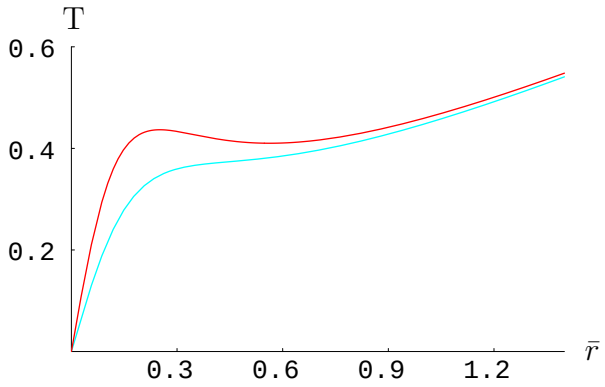

Figure 3.2: Temperature as a function of $\bar{r}$ for different values of $\bar{\alpha}$. The red line is for $\bar{\alpha} = 1/50$ and the other one $\bar{\alpha} = 1/30$.

From (3.12) and (3.16), it is possible to construct the temperature dependence of the free energy. However, the analytical expression is not very illuminating. Therefore, we plot the nature of the free energy as a function of temperature in figure 3.3. This plot is for two different values of $\bar{\alpha}$ belonging to the two different regions given in (3.13) and (3.14). Note that, as we increase $\bar{\alpha}$ from region (3.13) to region (3.14), nature of F changes at a critical value $\bar{\alpha} = \bar{\alpha}_c = 1/36$. We therefore study these two regions separately.

3.3.1 Phase structure for $\bar{\alpha} \leq \bar{\alpha}_c$:

When $\bar{\alpha} \leq \bar{\alpha}_c$, the free energy is shown by the red line in figure 3.3. At low temperature, it has only one branch (shown as branch I in the figure). However, when the temperature is increased beyond a certain value (which we call T_1), two new branches appear (II and III). One of these two branches (II) meets branch I at a temperature beyond, say T_3, and they both disappear. On the other hand, branch III continues to decrease rapidly, cuts branch I at temperature, say T_2, and becomes negative at a temperature which we will call T_c in the future. While computing specific heat using (3.10), we find that it is positive for branch I, and III. Therefore, these phases

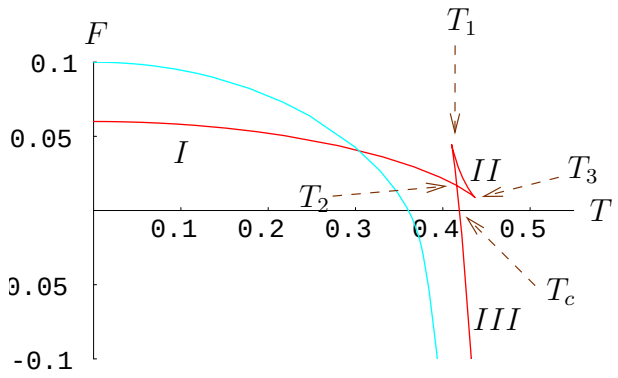

Figure 3.3: Free energy as a function of temperature. The red one is for $\bar{\alpha} = 1/50$ while the other one is for $\bar{\alpha} = 1/30$.

correspond to stable black holes. They, however, differ in their sizes; branch I represents smaller sized black holes than that of branch III. Going back now to branch II, we find that the specific heat is negative. We, therefore, conclude that branch II represents an unstable phase of the black hole.

The above picture is similar to that of the van der Waals gas. In particular, the Gibbs free energy of van der Waals gas, for an isotherm, behaves in a similar manner as we vary pressure. A thermodynamic equilibrium state is reached by minimising the Gibbs free energy. Likewise, in our case, equilibrium state would correspond to branch I of the free energy all the way up to temperature T_2 and then branch III from temperature T_2 and above. The free energy curve then remains concave as expected for a thermodynamical system. We, however, note that since there is a discontinuity of dF/dT at $T = T_2$, one has a first order phase transition at T_2. Two black hole phases would differ from each other at this point by a discontinuous change in their entropies. We will call these as the first Hawking-Page (HP1) transition for reasons that will be obvious later.

This phase structure can be nicely described by constructing a Landau function

around the critical point. By identifying the dimensionless quantity $\bar{r}$ as an order parameter, we can construct a function $\Phi(T, \bar{r})$ as

$$\Phi(T, \bar{r}) = \frac{\omega_3 l^2}{\kappa_5}(3\bar{r}^4 - 4\pi l T \bar{r}^3 + 3\bar{r}^2 - 24\pi\bar{\alpha} l T \bar{r} + 3\bar{\alpha}). \tag{3.17}$$

At the saddle point of this function, that is when $\frac{\partial\Phi}{\partial\bar{r}} = 0$, we get back the expression of the temperature given in (3.16). If we then substitute back the expression of temperature in to (3.17), $\Phi(\bar{r})$ reduces to the free energy given in (3.12). As can be seen from figure 3.4, for temperature $T < T_2$, $\Phi(T, \bar{r})$ has only one global minimum. This corresponds to the small black hole phase. However, at $T = T_2$, appearance of two degenerate minima suggests a coexistence of small and big black hole phases. Finally for temperature beyond T_2, only the big black holes phase remains (as this phase minimizes the Landau function). Clearly, there is a discrete change in the order parameter $\bar{r}$ at $T = T_2$. This is what we expect for a first order phase transition.

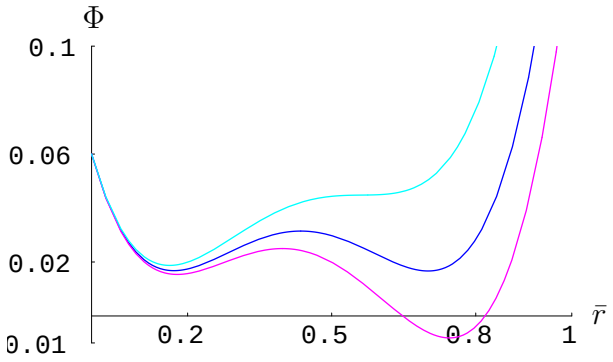

Figure 3.4: Landau function Φ as a function of order parameter $\bar{r}$ for different temperatures. We have taken $\bar{\alpha} = 1/50$. The blue curve is for temperature T_2, pink curve for temperature $T > T_2$ and the green one for temperature $T < T_2$.

3.3.2 Phase structure for $\bar{\alpha} > \bar{\alpha}_c$:

For $\bar{\alpha} > \bar{\alpha}_c$, the free energy curve is shown by the green line in figure 3.3. Unlike the previous case, free energy and its derivatives do not show any discontinuity. Therefore,

there is no HP1 transition. Only a single black hole phase is found to exist at any temperature.

3.3.3 Global phase structure of GB black holes:

As discussed earlier, for black holes with $\bar{\alpha} = 0$, there is a crossover from AdS to AdS black holes at a critical temperature $\frac{3}{2\pi l}$. What happens to this transition as we turn on $\bar{\alpha}$? In this situation, we note that we still have two geometries to consider. First one is again a thermal AdS with metric being the Euclidean continuation of (3.2). The function $V(r)$ is given in (3.5). We identify this thermal AdS space, having $\bar{\alpha}$ dependent effective cosmological constant, with zero free energy. Now, from figure 3.3. we see that above a critical temperature, the free energy of the GB black hole becomes negative, making it more stable compared to the effective AdS geometry. We identify this as a HP2 point. This crossover temperature can be computed as a power series in $\bar{\alpha}$ and is given by

$$T_c = \frac{3}{2\pi l} - \frac{33\bar{\alpha}}{4\pi l} + \mathcal{O}(\bar{\alpha}^2). \tag{3.18}$$

We notice here that the GB correction reduces the transition temperature. Similar phenomenon was noticed earlier in many AdS-gravity theories with higher curvature terms [15, 16, 17, 18]. The global phase structure is shown in figure 3.5.

To this end, we would like to point out that the above picture of GB black holes is quite similar to that of the five dimensional charged AdS black holes [27, 28]. The stability properties of the charged black holes depend on whether we are considering fixed potential ensemble or fixed charge ensemble. For the case of fixed charge ensemble, various phases of black holes resemble that of the red line in figure 3.3. As in our case, small black holes and large black holes are separated by a first order phase transition point. However, a major difference is that for the charged black holes, in fixed charge ensemble, thermal AdS is not a solution. Consequently, these holes are globally stable. This is unlike GB black holes, where there is a HP2 transition. Below

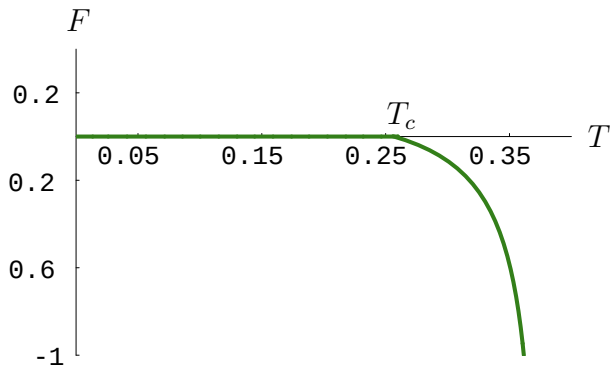

Figure 3.5: Global phase structure of GB black holes. For temperature $T < T_c$, AdS lowers the free energy, on the other hand for $T > T_c$ the black hole phase is preferred. This plot is for $\bar{\alpha} = 1/30$.

HP2 temperature, they are unstable.

3.4 Matrix Model :

In the previous sections we have analysed the phase structure of the gravitational theory in the presence of a higher derivative correction. We would now like to construct an effective Lagrangian for the gauge theory on the boundary. Like previous chapter, the effective theory on the boundary can be described by a unitary matrix model. Coefficients of this model depend on the "t Hooft coupling λ (that is related to $\alpha^{'}$ by, $\alpha^{'}\sqrt{2\lambda} = l^2$ from the AdS/CFT correspondence) and temperature T.

The phase structure in the bulk theory that we have discussed in Section 3.3 contains various distinct qualitative features depending on the value of the correction parameter $\alpha^{'}$. For nonzero $\alpha^{'}$, the phase diagram is modified in the regime where r_+ is small compared to $\sqrt{\alpha^{'}}$ (see figure 3.6). However as long as r_+ (the solutions corresponding to the black holes at a particular temperature) are greater than α', the phase diagram is qualitatively the same as that of the bulk theory without higher derivative corrections. There are two possibilities.

- We can ignore this small black hole solution in the supergravity approximation,

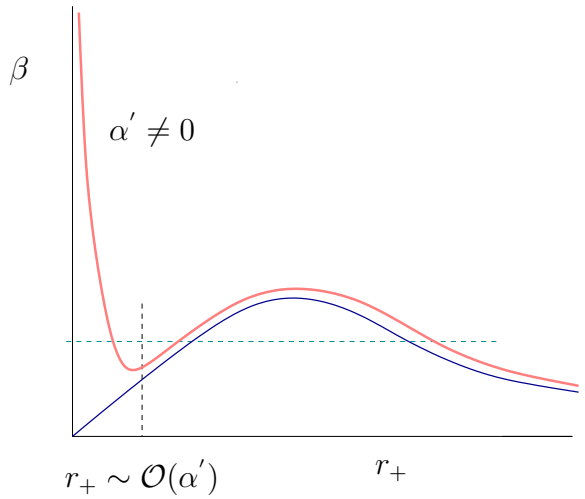

Figure 3.6: A schematic diagram of β vs r_+. Blue line is for $\alpha' = 0$ and red line is for $\alpha' \neq 0$

so that we only concentrate on solutions $r_+ > \sqrt{\alpha'}$. In this domain, it makes sense to compare the bulk physics with that of the boundary (a, b) matrix model discussed in the earlier chapter.

- If we include the small black hole solution in the supergravity approximation, then in order to reproduce the bulk phases, the boundary matrix model needs to be modified. In the next section we will propose a modified matrix model potential that captures the bulk physics including the solution r_+ which is less than $\sqrt{\alpha'}$.

Following the first possibility, this part of the section is devoted to a numerical study of the (a, b) model incorporating the corrections due to the finite "t Hooft coupling λ. In this analysis we consider $N \to \infty$. We first work in the limit $\lambda \to \infty$ and then by taking λ large but finite. The main aim is to compute a and b as of λ (to the first order in $1/\sqrt{\lambda}$) at fixed temperature T. This will be done by comparing the matrix model potential with the action on the gravity side with α' corrections as in

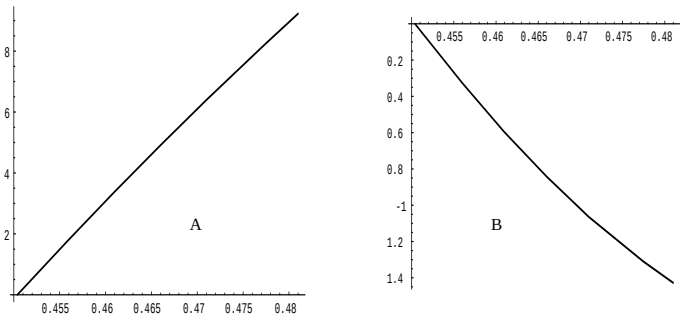

Figure 3.7: Plots of (A) $\partial a(T)/\partial(1/\sqrt{\lambda})$ and (B) $\partial b(T)/\partial(1/\sqrt{\lambda})$

subsection 2.6.3.

Having known the variations of $a(T,0)$ and $b(T,0)$ with respect to the temperature we now incorporate the α' corrections to $I_{1,2}$ of equation (2.50) to get the first order dependence on $1/\sqrt{\lambda}$. We have

$$\begin{aligned} a(T,1/\sqrt{\lambda}) &= a(T,0) + \frac{1}{\sqrt{\lambda}}\frac{\partial a(T)}{\partial(1/\sqrt{\lambda})}\mid_{1/\sqrt{\lambda}=0} + \mathcal{O}(1/\lambda^{3/2}), \\ b(T,1/\sqrt{\lambda}) &= b(T,0) + \frac{1}{\sqrt{\lambda}}\frac{\partial b(T)}{\partial(1/\sqrt{\lambda})}\mid_{1/\sqrt{\lambda}=0} + \mathcal{O}(1/\lambda^{3/2}). \end{aligned} \tag{3.19}$$

The first order variations of equation (2.50) with respect to $1/\sqrt{\lambda}$ gives,

$$2\frac{\partial a(T)}{\partial(1/\sqrt{\lambda})}\rho_{1,2}^2 + 2\frac{\partial b(T)}{\partial(1/\sqrt{\lambda})}\rho_{1,2}^4 = -\sqrt{\lambda}\delta I_{1,2}(T). \tag{3.20}$$

In the above equations, $\delta I_{1,2}(T)$ are given by,

$$\begin{aligned} \delta I_{1,2}(T) &= \alpha^{'}\beta(\delta F_{1,2}) \\ &= -\frac{\beta}{\sqrt{2\lambda}}(3r_{1,2}^4 + 24r_{1,2}^2 + 9). \end{aligned} \tag{3.21}$$

Where F is given by eqn(3.12). From these we get the values of $\frac{\partial a(T)}{\partial(1/\sqrt{\lambda})}$ and $\frac{\partial b(T)}{\partial(1/\sqrt{\lambda})}$ shown in figure (3.7).

At this point some comments about the sign of b are in order. In the limit when the 't Hooft coupling λ goes to infinity numerical computations show that b indeed is

positive. However as we move from $\lambda \to \infty$ to finite λ (that is obtained by including α' corrections in the bulk) we see that at any particular temperature $\partial b(T)/\partial(1/\sqrt{(}\lambda))$ is negative. Though this numerical calculation shows that b decreases from a positive value as we move down towards weak coupling, it is not clear whether the sign of b will turn out to be negative or positive at weak coupling. In case it turns out to be positive, we presume that the results for the gravitational side should correspond qualitatively to those of the weakly coupled gauge theory.

The above analysis shows that the behaviour of the coefficients as functions of temperature and λ are indeed the ones that we expect from the phases of the bulk theory as long as we concentrate on the black hole solutions with $r_+ > \sqrt{\alpha'}$. The expansions are carried out about $\lambda \to \infty$ as it was argued in [19] that the effective theory that is computed in the weak coupling falls in the same universality class as the one in the strong coupling limit. The addition of higher derivative term in the bulk does give information about $1/\sqrt{\lambda}$ corrections, however this (a, b) model is unable to capture the phases including the small black hole solution. In the following section we will analyse this issue, in detail, by proposing another model which qualitatively reproduces various bulk phases of section 3.3.

3.5 A modified Matrix model

In this section we propose a modified (toy) matrix model which incorporates some of the additional qualitative features on the gravity side arising due to the GB term. We find, the minimal action that would reproduce these features needs to be quartic in ρ^2 and can be given by

$$S(\rho^2) = 2N^2[A_4\rho^8 - A_3\rho^6 + A_2\rho^4 + (\frac{1-2A_1}{2})\rho^2] \quad , \tag{3.22}$$

where A_i's are the parameters, which depend on the temperature as well as on the coupling constant. In the limit where the A_4 and A_3 vanish we get the (a, b) model [19].

The equations of motion ensuing from the action in (3.22) are given as follows. We write

$$F(\rho) = \frac{\partial S(\rho^2)}{\partial \rho^2} = N^2[8A_4\rho^6 - 6A_3\rho^4 + 4A_2\rho^2 + (1-2A_1)]. \tag{3.23}$$

Then the equations in two different regions are

$$\begin{aligned} \rho F(\rho) &= \rho \quad , \qquad 0 \le \rho \le \tfrac{1}{2}, \\ &= \tfrac{1}{4(1-\rho)} \quad , \quad \tfrac{1}{2} \le \rho \le 1. \end{aligned} \tag{3.24}$$

The potentials that follows from the above action is given by

$$\begin{aligned} V(\rho) &= -A_4\rho^8 + A_3\rho^6 - A_2\rho^4 + A_1\rho^2 \quad , \qquad 0 \le \rho \le \frac{1}{2} \quad , \\ &= -A_4\rho^8 + A_3\rho^6 - A_2\rho^4 + (A_1 - \frac{1}{2})\rho^2 - \frac{1}{4}\log[2(1-\rho)] + \frac{1}{8} \quad , \quad \frac{1}{2} \le \rho \le 1 \end{aligned} \tag{3.25}$$

Let us analyze the solutions of equations of motion given by (4.29). The fact that there are four parameters instead of two has made the analysis technically more involved than (a, b) model[19]. For various ranges of parameters the model shows different qualitative behaviour. As we will see we need to impose necessary restrictions on the parameters so that the model reproduces the features that we found on the gravity side. Before analyzing the solutions one comment is in order. In the following we will find the analog of small stable black hole appearing as a minimum of the potential but it always comes with an additional maximum of the potential. We do not have on the bulk side a solution corresponding to this maximum. We interpret this solution as a possible decay mode of the small stable black hole which may be due to some stringy mechanism.

The behaviours of the solutions are encoded in the polynomial $F(\rho)$ given in (4.30). We begin with the coefficient of the lowest order term A_1. From (3.22) we see in order to make $\rho = 0$ tachyon-free we need $0 < F(0) \le 1$ *i.e.* $0 \le A_1 < 1/2$. Once that is imposed we consider the next coefficient A_2. As we see on the bulk side our action

should admit (in one phase) 3 solutions that correspond to a small black hole, an intermediate black hole and a big black hole. A necessary condition for the existence of three solutions is $A_2 > 0$. Though we get this constraint from a different argument it agrees with [19]. Thus our model at a vanishing limit of higher coefficients reduces to (a, b) model.

Restrictions on the higher coefficients are slightly more cumbersome and depends on the positions of the turning points of the polynomial F. In that context it is useful to consider the quadratic polynomial in ρ^2: $f(\rho^2) = (1/\rho)\frac{\partial}{\partial\rho}F(\rho)$. This is given by $f(x) = 48A_4x^2 - 24A_3x + 8A_2$. The zeroes of f determine the non-trivial turning points of F. In terms of this polynomial f the two different ranges of $\bar{\alpha}$ correspond to the following constraints:

• $\bar{\alpha} > 1/36$: For $f(1) = 48A_4 - 24A_3 + 8A_2 < 0$ there is one turning point at some $0 < \rho_- < 1$. With parameters in this range we can have either two solutions (one maximum and one minimum of potential) or no solution. There is no way we can obtain three solutions in this phase. Moreover, from the restriction on the parameters it is clear that the range of parameters is not continuously connected with the corresponding range where (a, b)-model is valid (*i.e.* $A_4 = A_3 = 0$). We identify this phase with the range of $\bar{\alpha}$ which corresponds to $\bar{\alpha} > 1/36$ on the gravity side. However, that is not sufficient to ensure that there is always one minimum that correspond to the single black hole on the bulk side. For that we need to impose a further restriction on the coefficients such that, the turning point satisfies $\rho_- < 1/2$ and $F(\rho_-) > 0$. Then we always get a maximum for $\rho < 1/2$ (that is in the region with no cut) and a minimum of the potential. As the parameter varies the position of this minimum changes from the $\rho < 1/2$ region to the $\rho > 1/2$ region. So this phase corresponds to the restrictions: $f(1) = 48A_4 - 24A_3 + 8A_2 < 0$, $\rho_- < 1/2$ and $F(\rho_-) > 0$.

• $\bar{\alpha} < 1/36$: Again we look for turning points in the range $0 < \rho \leq 1$. For $f(1) = 48A_4 - 24A_3 + 8A_2 > 0$ either we get two turning points which we call ρ_-

and ρ_+ ($\rho_- < \rho_+$) or none of them. That gives rise to 3 possibilities: the number of solutions could be 4 (consists of two maxima and two minima), or 2 (consists of one maximum and one minimum) or 0. This phase is continuously connected with that of the (a, b) model and we identify this phase with the range of $\bar{\alpha}$ given by $\bar{\alpha} < 1/36$ on the gravity side. The more detailed structure of the solutions depends on the positions of the turning points ρ_- and ρ_+ and the values of the polynomial $F(\rho)$ at the turning points. Let us first consider $F(\rho_-) > 0$ with $0 < \rho_- < 1/2$. There are two possibilities: (i) If $F(1/2) < 0$ we have two solutions, one maximum and other minimum in $\rho < 1/2$ range. The minimum corresponds to the stable small black hole. We may or may not have two more solutions in the range $\rho > 1/2$. If we have two solutions they would correspond to intermediate and big black hole. (ii) If $F(1/2) > 0$ we have one solution (maximum) in $\rho < 1/2$ and the other (minimum) in $\rho > 1/2$. This minimum corresponds to the big black hole. The remaining possibilities are (iii) $\rho_- < 1/2$, $F(\rho_-) < 0$ and (iv) $\rho_- > 1/2$, $F(1/2) < 0$. In both of these cases there is no solution in the range $0 < \rho < 1/2$. Finally if there is no turning point and $F(1/2) < 0$ there will be no solution in the range $0 < \rho < 1/2$. Since the analysis on the bulk side then requires that there is a solution for $1/2 < \rho < 1$ we need to impose the following constraint, namely, there should exist some value of ρ, $\rho_- < \rho_0 < 1$ such that $4\rho_0(1 - \rho_0)F(\rho_0) > 1$. That will give one maximum and one minimum in the range $1/2 < \rho < 1$ that corresponds to the small and the big black hole.

Thus we see for both the phases we need additional restrictions which shows there are regions of parameters that does not agree with the features of gravity phase. This suggests the fact that in the strongly coupled gauge theory there are restrictions on various parameters. It may be interesting to calculate these parameters from field theory set up (for weakly coupled gauge theory) and compare the values with the restrictions obtained above.

In order to discuss the variation of potential with parameters it is useful to give

a graphical description. We have four parameters, so for the sake of graphical description we restrict number of parameters to 2. We consider only the phases that corresponds to the $\bar{\alpha} < 1/36$. We take fixed values of A_1 and A_4 and study the features with the variation of two other parameters. We have chosen the values to be $A_1 = .025$ and $A_4 = 2.083$. We have given plot of the potential against ρ in figure 3.8 and 3.9. In order to make the extrema explicit we choose different scales for the potential for two different ranges of ρ, namely, $0 \leq \rho \leq 1/2$ and $1/2 \leq \rho \leq 1$. The values of A_2 and A_3 are decreasing from the curve in bottom to that in top in figure 3.8 and from the curve on top to that in bottom in figure 3.9. There is always one minimum at $\rho = 0$ where the potential vanishes. As we will see in figure 3.10 we need to choose values of A_2 and A_3 restricted within a particular region outside which the features that we get from the bulk will be absent. In the following, we give $V(\rho)$ vs. ρ plots for different values of A_2 and A_3:

- $(A_2, A_3) = (.45, 2)$: Here we get two solutions: one maximum and one local minimum in the range $\rho \leq 1/2$ (*i.e* where there is no cut) and no solution at $\rho \geq 1/2$. We identify the minimum with the small stable black hole. This corresponds to low temperature behaviour of GB black hole where we get only one small black hole solution.

- $(A_2, A_3) = (.4, 2)$: Here we get four solutions: In addition to the above maximum and minimum in the range $\rho \leq 1/2$ we get one more local maximum and one more local minimum appearing in the range $1/2 \leq \rho \leq 1$. These latter maximum and minimum can be identified with the intermediate black hole and the big black hole. We identify this with the nucleation of the big black hole and intermediate unstable black hole in the gravity picture.

- $(A_2, A_3) = (.385, 1.9375)$: For further decrease of the parameters, the heights of the local minimum in the range $0 \geq \rho \geq 1/2$ (fig. 3.8) increases and the height of the local minimum in the range $1/2 \geq \rho \geq 1$ decreases (fig. 3.9) . At this

value of the parameters the heights of the two minima become equal. We can identify this point with a transition from small black hole to big black hole on the gravity side which is termed as HP1 transition.

- $(A_2, A_3) = (.38485, 1.93688)$: (Due to close proximity this plot appears on the top of the earlier plot and not distinguishable in the present scale.) The height of the minimum in the range $\rho \geq 1/2$ becomes zero and thus equal to the potential at $\rho = 0$. On the gravity side this corresponds to energy of big black hole reaching zero and becoming equal to that of thermal AdS triggering HP2 transition.

- $(A_2, A_3) = (.25, 1.5)$: Here we get two solutions because in the region $\rho \leq 1/2$ the local minimum and local maximum is on the verge of disappearing. However, the two solutions in the range $\rho \geq 1/2$ will remain with the height of the minimum in $\rho \geq 1/2$ keeps on decreasing. This corresponds to the point beyond which the small black hole on the gravity side disappears.

- $(A_2, A_3) = (.248, 1.25)$: As we decrease A_2 and A_3 further, the solutions in the range $\rho \leq 1/2$ cease to exist (fig.3.8). The minimum in the range $\rho \geq 1/2$ (fig. 3.9) becomes more and more deeper. This is in keeping with the fact that, at high temperature on the gravity side the only stable configuration remains is the big black hole.

As we see from the above analysis the coefficients decrease with temperature, unlike the behaviour of the coefficients in the (a, b)-model. This can be interpreted as the temperature gradient of the coefficients at the first order of inverse 't Hooft coupling has a negative sign relative to that at the zeroth order. At this range, where appreciable $1/\lambda$ correction is taken into account, the contribution at first order dominates over that at zeroth order.

Here we give a graphical presentation of the behaviour of the solutions using a parametric plot of different critical points in the A_2-A_3 plane in figure 3.10 keeping

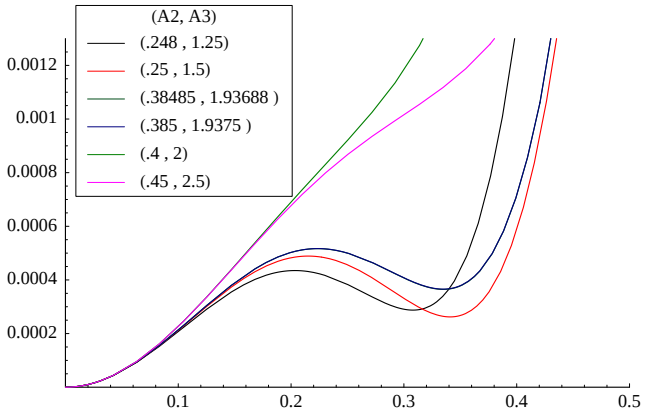

Figure 3.8: Potential as function of ρ for the range $0 \leq \rho \leq 1/2$ for increasing values of A_2 and A_3. The different values of (A_2, A_3) are given above. The plots associated with (.38485, 1.93688)and (.385, 1.9375) are not distinct in this scale.

A_1 and A_4 fixed as above. As we vary the parameters we encounter a curve IV in the A_2-A_3 plane, above which the saddle point associated with the small black hole has energy negative. From the analysis of black holes on the gravity side, it follows that the small black hole energy is always greater than thermal AdS ensuring the stability of the latter. So, in what follows, we restrict ourselves to the region below curve IV.

In the region bounded by IV, III and I, there are three saddle points. One is $\rho = 0$ which corresponds to the thermal AdS. There are two more saddle points: a local maximum at $\rho = \rho_1$ and a local minimum at $\rho = \rho_2$. The latter corresponds to the small black hole that we obtain on the gravity side. There is no solution analogous to ρ_1 in the gravity side. In the region bounded by II, III, IV and I, there appears two more saddle points. One of them $\rho = \rho_3$ is a local maximum and the other one $\rho = \rho_4$ is a local minimum. They correspond to the intermediate, and the stable big black hole respectively. In the region on the left hand side of curve I, the saddle points $\rho = \rho_1, \rho_2$ cease to exist. In the region above the curve IV, as we have already mentioned, the potential of the saddle point $\rho = \rho_1$ becomes negative showing the energy of the associated small black hole on the gravity side becomes less than that of thermal AdS.

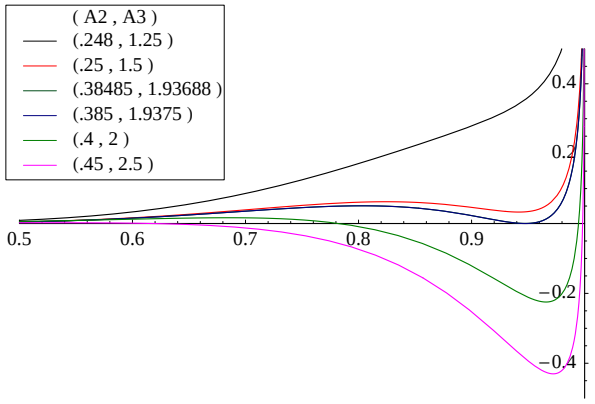

Figure 3.9: Potential as function of ρ for the range $1/2 \leq \rho \leq 1$ for increasing values of A_2 and A_3. The values of (A_2, A_3) used in the plots are given above. The plots associated with (.38485 , 1.93688) and (.385 , 1.9375) are not distinct in this scale.

Similarly, the thermal history (for this choice of parameter) can be obtained from figure 3.10 as follows. As we mentioned earlier, A_2 and A_3 will decrease with temperature along the curve C. As we follow the curve C from right to left, we find the $\rho = 0, \rho_1, \rho_2$ are the solutions on the right of curve III. As we cross curve III, we encounter two additional saddle points $\rho = \rho_3, \rho_4$. Crossing the curve II corresponds to the Hawking-Page transition. As we cross curve I, the saddle point corresponds to the small black hole disappears.

Like the general case, here also as we see in the region bounded by the curve I, along with a local minimum (at $\rho = \rho_1$) we always obtain a local maximum (at $\rho = \rho_2$). We interpret this maximum, as we said earlier, as a bounce solution through which the small stable black hole decays. It will be interesting to understand this instability on the gravity side.

3.6 Discussion

In this chapter, we have discussed phase transition of asymptotically AdS black hole solutions in presence of Gauss-Bonnet term. As long as $\bar{\alpha}$, strength of the coupling to

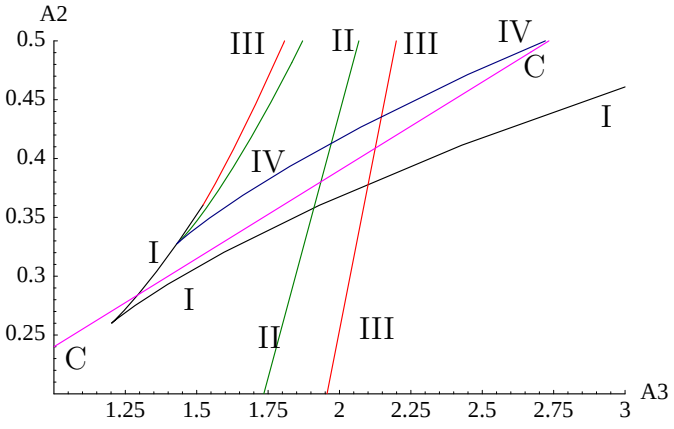

Figure 3.10: Parametric plots of different critical points in the A_2-A_3 plane. We choose $A_1 = 0.25$ and $A_4 = 2.083$. In the region which is below or on the left side of curve I the saddle points $\rho_\pm$ cease to exist. In the region above curve IV the potential of ρ_+ vanishes. Curve II corresponds to HP transition and on curve III the saddle points ρ_1 , ρ_2 merge.

GB term remains above certain critical value $\bar{\alpha}_c$, one gets a single black hole phase at any temperature. However, as the coupling comes down below the critical value two additional black holes appear. We called them small and intermediate black holes. The intermediate black hole is found to have negative specific heat. It turns out that this small stable black hole is a local minimum below a critical temperature. Beyond this temperature small black hole disappears. We have studied the associated phase diagram and find that the phase structure resembles that of van der Wall's gas. In addition to the the standard Hawking-Page transition, we have identified one more phase transition where the two branches of the phase diagram meet. We find the specific heat diverges at this new critical point.

Five dimensional theory of gravity usually corresponds to some gauge theory on the boundary and the analysis on the gravity side has natural implications about the gauge theory. In absence of Gauss-Bonnet term, the gravity theory on Euclidean AdS (along with S^5) is known to be dual to be pure $\mathcal{N} = 4$ SYM on a three sphere at

finite temperature and the phase diagram associated with the gravity theory captures thermal history of $\mathcal{N} = 4$ SYM on S^3. In a similar spirit, we expect, dual of this five dimensional gravity theory in presence of Gauss-Bonnet term is some deformation of the above gauge theory and the phase diagram captures its thermal history. In [19], qualitative features of $\mathcal{N} = 4$ SYM on S^3 was studied from the perspective of a matrix model. This model is phenomenological in nature and is charecterised by two parameters (a, b). On generic ground, one expects these parameters to be λ and T dependent. Appealing to the universal nature of this model near the critical points, we find out λ dependence of (a, b). This is done by mapping the bulk α' correction to the boundary. This method can easily be used to find similar $1/\lambda$ dependence of matrix model coefficients in the case of other higher derivative corrections of the gravity action, such as, R^4 term in IIB theory.

We have also proposed a modified matrix model that captures the qualitative features of the phase diagram of the bulk theory. Unlike (a, b) matrix model this model is non-universal and the phase diagram is reproduced only in a selected region of the parameter space. In addition the temperature dependence of the coefficients turn out to be different from usual linearly increasing function. We also find that there is an extra maximum, that always comes with the minimum corresponding to small black hole and which has no analog in the bulk side. This could be related to some state in string theory. At this point it may be mentioned that appearance of string state in boundary theory occurred in [19, 20]. This corresponds to the Gross-Witten transition [29, 30] and can be identified as a crossover from supergravity black hole solution to string state [31]. Thus we keep this extra maximum in the region $0 \leq \rho \leq 1/2$. In the bulk side, this stringy phase may act as a bounce via which the small black hole can decay to AdS solution.

Bibliography

[1] S. W. Hawking and D. N. Page, *Thermodynamics of black holes in anti-de Sitter space*, Commun. Math. Phys. **87**, 577 (1983).

[2] S. Kalyana Rama and B. Sathiapalan, *The Hagedorn transition, deconfinement and the AdS/CFT correspondence,* Mod. Phys. Lett. A **13**, 3137 (1998) [arXiv:hep-th/9810069].

[3] B. Sundborg, *The Hagedorn transition, deconfinement and N = 4 SYM theory,* Nucl. Phys. B **573**, 349 (2000) [arXiv:hep-th/9908001].

[4] O. Aharony, J. Marsano, S. Minwalla, K. Papadodimas and M. Van Raamsdonk, *The Hagedorn/Deconfinement Phase Transition in Weakly Coupled Large N Gauge Theories*, Adv. Theor. Math. Phys. 8 (2004) 603 [arXiv:hep-th/0310285].

[5] H. Liu, *Fine structure of Hagedorn transition*, arXiv:hep-th/0408001.

[6] O. Aharony, J. Marsano, S. Minwalla, K. Papadodimas and M. Van Raamsdonk, *A first order deconfinement transition in large N Yang-Mills theory on a small* S^3, Phys. Rev. D **71**, 125018 (2005) [arXiv:hep-th/0502149].

[7] M. Brigante, G. Festuccia and H. Liu, *Hagedorn divergences and tachyon potential,* arXiv:hep-th/0701205.

[8] J. M. Maldacena, *The large N limit of superconformal field theories and supergravity*, Adv. Theor. Math. Phys. **2**, 231 (1998) [Int. J. Theor. Phys. **38**, 1113 (1999)] [arXiv:hep-th/9711200].

[9] S. S. Gubser, I. R. Klebanov and A. M. Polyakov, *Gauge theory correlators from non-critical string theory*, Phys. Lett. B **428**, 105 (1998) [arXiv:hep-th/9802109].

[10] E. Witten, *Anti-de Sitter space and holography*, Adv. Theor. Math. Phys. **2**, 253 (1998) [arXiv:hep-th/9802150].

[11] E. Witten, *Anti-de Sitter space, thermal phase transition, and confinement in gauge theories*, Adv. Theor. Math. Phys. **2**, 505 (1998) [arXiv:hep-th/9803131].

[12] J. L. Petersen, *Introduction to the Maldacena conjecture on AdS/CFT*, Int. J. Mod. Phys. A **14**, 3597 (1999) [arXiv:hep-th/9902131].

[13] O. Aharony, S. S. Gubser, J. M. Maldacena, H. Ooguri and Y. Oz, *Large N field theories, string theory and gravity*, Phys. Rept. **323**, 183 (2000) [arXiv:hep-th/9905111].

[14] D. G. Boulware and S. Deser, *String Generated Gravity Models*, Phys. Rev. Lett. **55**, 2656 (1985).

[15] S. S. Gubser, I. R. Klebanov and A. A. Tseytlin, *Coupling constant dependence in the thermodynamics of $N = 4$ supersymmetric Yang-Mills theory*, Nucl. Phys. B **534**, 202 (1998) [arXiv:hep-th/9805156].

[16] Y. h. Gao and M. Li, *Large N strong/weak coupling phase transition and the correspondence principle*, Nucl. Phys. B **551**, 229 (1999) [arXiv:hep-th/9810053].

[17] K. Landsteiner, *String corrections to the Hawking-page phase transition*, Mod. Phys. Lett. A **14**, 379 (1999) [arXiv:hep-th/9901143].

[18] M. M. Caldarelli and D. Klemm, *M-theory and stringy corrections to anti-de Sitter black holes and conformal field theories*, Nucl. Phys. B **555**, 157 (1999) [arXiv:hep-th/9903078].

[19] L. Alvarez-Gaume, C. Gomez, H. Liu and S. Wadia, *Finite temperature effective action, AdS_5 black holes, and 1/N expansion*, Phys. Rev. D **71**, 124023 (2005) [arXiv:hep-th/0502227].

[20] L. Alvarez-Gaume, P. Basu, M. Marino and S. R. Wadia, *Blackhole / string transition for the small Schwarzschild blackhole of $AdS_5 \times S^5$ and critical unitary matrix models*, Eur. Phys. J. C **48**, 647 (2006) [arXiv:hep-th/0605041].

[21] R. C. Myers, *Superstring gravity and black holes*, Nucl. Phys. B **289** (1987) 701.

[22] S. Nojiri and S. D. Odintsov, *Anti-de Sitter black hole thermodynamics in higher derivative gravity and new confining-deconfining phases in dual CFT*, Phys. Lett. B **521**, 87 (2001) [Erratum-ibid. B **542**, 301 (2002)] [arXiv:hep-th/0109122].

[23] R. G. Cai, *Gauss-Bonnet black holes in AdS spaces*, Phys. Rev. D **65**, 084014 (2002) [arXiv:hep-th/0109133].

[24] M. Cvetic, S. Nojiri and S. D. Odintsov, *Black hole thermodynamics and negative entropy in deSitter and anti-deSitter Einstein-Gauss-Bonnet gravity*, Nucl. Phys. B **628**, 295 (2002) [arXiv:hep-th/0112045].

[25] Y. M. Cho and I. P. Neupane, *Anti-de Sitter black holes, thermal phase transition and holography in higher curvature gravity*, Phys. Rev. D **66**, 024044 (2002) [arXiv:hep-th/0202140].

[26] T. Torii and H. Maeda, *Spacetime structure of static solutions in Gauss-Bonnet gravity: Neutral case*, Phys. Rev. D **71**, 124002 (2005) [arXiv:hep-th/0504127].

[27] A. Chamblin, R. Emparan, C. V. Johnson and R. C. Myers, *Charged AdS black holes and catastrophic holography*, Phys. Rev. D **60**, 064018 (1999) [arXiv:hep-th/9902170].

[28] A. Chamblin, R. Emparan, C. V. Johnson and R. C. Myers, *Holography, thermodynamics and fluctuations of charged AdS black holes*, Phys. Rev. D **60**, 104026 (1999) [arXiv:hep-th/9904197].

[29] D. J. Gross and E. Witten, *Possible Third Order Phase Transition In The Large N Lattice Gauge Theory,* Phys. Rev. D **21**, 446 (1980).

[30] S. R. Wadia, *N = Infinity Phase Transition In A Class Of Exactly Soluble Model Lattice Gauge Theories,* Phys. Lett. B **93**, 403 (1980).

[31] G. T. Horowitz and J. Polchinski, *A correspondence principle for black holes and strings,* Phys. Rev. D **55**, 6189 (1997) [arXiv:hep-th/9612146].

Chapter 4

Higher Derivative Gravity and Dual Matrix Model: R-charged Black Holes

4.1 Introduction

In continuation with our previous chapter, we study the effects of Gauss-Bonnet (GB) corrections to charged black hole in the AdS/CFT set up. Our aim is to identify some of the universal features of the boundary matrix models at strong coupling. The charged sector of the GB action contains a Maxwell term besides the GB corrections. Maxwell term typically comes in type IIB theory on $AdS_5 \times S^5$ from angular momentum along S^5 direction, or in other words, from the $SO(6)$ gauge symmetry arising from the group of isometries of S^5. We focus our attention to those black hole configurations which have equal $U(1)$ charges for all the three commuting $U(1)$ subgroups of $SO(6)$. These black holes and their phase structures were considered in [1, 2] (see also [3]). We study the changes of phase structures due to GB corrections in canonical and grand canonical ensembles. On the gauge theory side, in order to describe the charged sector, we use the same model as in previous chapter

except we allow the coefficients of the model to depend on appropriate parameters of the ensemble as well along with the temperature (T) and the t'Hooft coupling (λ). In this direction we first focus our attention on the phase structures of this black hole in canonical and grand canonical ensembles.

Grand canonical Ensemble (Fixed Potential):
In the grand canonical ensemble, the black hole is allowed to emit and absorb charged particles keeping the potential fixed till the thermal equilibrium is reached, which, in this case, is governed by a fixed chemical potential. Here the phase diagram is characterized by the chemical potential Φ and the GB coupling which we call $\bar{\alpha}$ in this chapter.

($\mathbf{\Phi \neq 0}, \bar{\alpha} = \mathbf{0}$) : On the gravity side, the phase diagrams have been analyzed in [1, 2]. If the potential Φ is below a critical value, various phases are similar to that of AdS-Schwarzschild black hole while for Φ large enough, the black hole free energy becomes negative compared to that of the thermal AdS at any fixed temperature. On the gauge theory side, at zero and small λ, the phase structure was analysed in [4, 5], while for large λ, a phenomenologically motivated matrix model can be constructed and we will have occasion to elaborate on it at a later stage of this chapter.

($\mathbf{\Phi \neq 0}, \bar{\alpha} \neq \mathbf{0}$) : This case is studied in section 4.2.1 where we find the critical value of Φ depends on α. For small Φ, there are three different black hole phases; one of them being unstable. Identifying the rest two as a small and a big black hole, we find that there is a first order phase transition from the small to the big black hole. However, once thermal AdS is included in the phase diagram, we find both the small and big black hole phases are metastable at low temperature and big black hole becomes stable only at high temperature. In order to clearly illustrate the various phases in this range of Φ we construct a Landau function with black hole horizon radius as the order parameter. When Φ is above the critical value, phase diagram shows a single black hole phase which is stable beyond certain temperature while a crossover from black hole phase to thermal AdS occurs for temperature lower than

that. If we increase Φ even further, the black hole phase is always found to be stable. All these phases can be summarized in a $(\Phi^2 - \bar{\alpha})$ diagram; see figure 4.1. We also note that, in all the above cases, wherever there is Hawking-Page transition from AdS to the black hole phase, the transition temperature is found to decrease with $\bar{\alpha}$.

We study the grand canonical ensemble of the dual theory in section 4.3.1 and 4.3.2. Here the parameters of the matrix model depend on the chemical potential (μ). We find for the chemical potential less than the critical value the analysis is similar to that of previous chapter. As earlier, the matrix model has an extra saddle point that has no analogue in supergravity. We interpret this saddle point with some phase in string theory. Beyond the critical potential we encounter different possible situations depending on the position (expectation value of the Polyakov loop) of the extra saddle point.

Canonical ensemble (Fixed Charge):
In the canonical ensemble, the black hole is allowed to emit and absorb radiation, keeping the charge fixed till the thermal equilibrium is reached and the phase diagrams are characterized by the charge of the black hole, q and the GB coupling $\bar{\alpha}$.

$(\mathbf{q \neq 0}, \bar{\alpha} = \mathbf{0})$: The phase structure is discussed in [1, 2] in great detail. There exists a critical charge q_c above which, at all temperature, only one black hole phase exists. Below q_c, there can be at most three black hole phases. We call them small, intermediate and large. While the intermediate one is unstable, the small and big black holes are stable. It was also noted that thermal AdS is not an admissible phase. When we increase the temperature, there is a crossover from a small black hole to a large black hole phase via a first order phase transition.

$(\mathbf{q \neq 0}, \bar{\alpha} \neq \mathbf{0})$: This part of the analysis is given in section 4.2.2, where, we find the phase structure depends on two parameters q and $\bar{\alpha}$. In particular, in $(q^2 - \bar{\alpha})$ plane, we identify two distinct regions (see fig. 4.5) where region I consists of three black hole phases, while in region II, only one black hole phase exists. Thermal AdS continues to be non-admissible phase. As before, there is a transition from small to

big black hole at a critical temperature. This temperature decreases as we increase $\bar{\alpha}$.

Study of the canonical ensemble of the dual theory is discussed in section 4.3.3. Since the explicit dependence of the coefficients of the matrix model on the chemical potential is very hard to determine at strong coupling, we assume the the zero coupling result is valid there or at least the universality class of the theory does not change once we tune up the gauge coupling. We find that this dependence is consistent with one of the possible scenarios. For this scenario, we write down the matrix model for the fixed charge and find that this model correctly reproduces the phases of the black holes with fixed charge.

The chapter is structured as follows. We begin with the thermodynamics of charged sector in presence of GB coupling in section 4.2. Subsections 4.2.1 and 4.2.2 are devoted to discussion of canonical and grand canonical ensembles. The dual theory is discussed in section 4.3. The grand canonical ensemble of the dual theory is considered in subsection 4.3.1 and 4.3.2 while the canonical ensemble is discussed in subsection 4.3.3.

4.2 Gauss-Bonnet black hole with electric charge

We start with $n+1$-dimensional ($n \geq 4$) action

$$I = \int d^{n+1}x\sqrt{-g_{n+1}}\Big[\frac{R}{\kappa_{n+1}} - 2\Lambda + \alpha(R^2 - 4R_{ab}R^{ab} + R_{abcd}R^{abcd}) - \frac{F^2}{\kappa_{n+1}}\Big]. \quad (4.1)$$

This action possesses black hole solutions which we call charged GB black holes [3]. These solutions have the form

$$ds^2 = -V(r)dt^2 + \frac{dr^2}{V(r)} + r^2 d\Omega^2_{n-1}, \quad (4.2)$$

where $V(r)$ is given by

$$V(r) = 1 + \frac{r^2}{2\hat{\alpha}} - \frac{r^2}{2\hat{\alpha}}\Big[1 - \frac{4\hat{\alpha}}{l^2} + \frac{4\hat{\alpha}m}{r^n} - \frac{4\hat{\alpha}q^2}{r^{2(n-1)}}\Big]^{\frac{1}{2}}. \quad (4.3)$$

The parameter q gives the charge

$$Q = \frac{2\sqrt{2(n-1)(n-2)}\omega_{n-1}q}{\kappa_{n+1}}, \tag{4.4}$$

of the electric gauge potential

$$A_t = -\sqrt{\frac{n-1}{2(n-2)}}\frac{q}{r^{n-2}} + \Phi, \tag{4.5}$$

where Φ is a constant which we will fix below. Denoting r_+ as the largest real positive root of $V(r)$, we find that the metric (4.3) describes a black hole with non-singular horizon if

$$\Big(\frac{n}{n-2}\Big)r_+^{2n-2} + l^2 r_+^{2n-4} \geq q^2 l^2. \tag{4.6}$$

Finally, we shall choose the gauge potential A_t to vanish at the horizon. This fixes Φ to be

$$\Phi = \sqrt{\frac{n-1}{2(n-2)}}\frac{q}{{r_+}^{n-2}}. \tag{4.7}$$

This quantity is the electrostatic potential between the horizon and infinity. Asymptotically, the metric (4.3) goes to AdS space, as in this limit,

$$V(r) = 1 + \Big[\frac{1}{2\hat{\alpha}} - \frac{1}{2\hat{\alpha}}\Big(1 - \frac{4\hat{\alpha}}{l^2}\Big)^{\frac{1}{2}}\Big]r^2. \tag{4.8}$$

Hence we notice that the metric is real if,

$$\hat{\alpha} \leq \frac{l^2}{4}. \tag{4.9}$$

We shall restrict ourselves to $\hat{\alpha}$ which satisfy the above bound. In this chapter, we will primarily consider black holes in five dimensions ($n = 4$). However, it is easy to extend the results of this section to higher dimensions.

The thermodynamic properties of the black hole will depend on whether we consider the canonical ensemble (fixed charge Q) or grand canonical ensemble (fixed potential Φ). The equilibrium temperature T can identified from the period β of the Euclidean time of the metric (4.3), which in five dimensions is given by

$$\beta = \frac{2\pi r_+(r_+^2 + 2\hat{\alpha})}{r_+^2 + 2r_+^4/l^2 - q^2/r_+^2}. \tag{4.10}$$

As it will be useful for us to write thermodynamic quantities, as before, in terms of dimensionless quantities, we define

$$\bar{r} = \frac{r}{l}, \bar{\alpha} = \frac{\hat{\alpha}}{l^2}, \bar{q} = \frac{q}{l^2}, \bar{m} = \frac{m}{l^2}. \tag{4.11}$$

In terms of these quantities, (4.10) can be expressed as

$$\beta = \frac{2\pi l\bar{r}(\bar{r}^2 + 2\bar{\alpha})}{\bar{r}^2 + 2\bar{r}^4 - \bar{q}^2/\bar{r}^2}. \tag{4.12}$$

4.2.1 Grand canonical ensemble

In the grand canonical ensemble, with fixed potential Φ, the free energy can be computed from the Euclidean continuation of the action (4.1). We obtain the action (subtracting the AdS background) as

$$I_{\rm gc} = -\frac{\omega_3 l^2\beta}{\kappa_5(\bar{r}^2 + 2\bar{\alpha})}\Big[\bar{r}^6 + (18\bar{\alpha} - 1 + 4\Phi^2/3)\bar{r}^4 + 3\bar{\alpha}(1 - 8\Phi^2/3)\bar{r}^2 - 6\bar{\alpha}^2\Big], \tag{4.13}$$

where β is inverse of T expressed in terms of potential

$$\beta = \frac{2\pi l(\bar{r}^2 + 2\bar{\alpha})}{\bar{r}(1 - 4\Phi^2/3 + 2\bar{r}^2)}. \tag{4.14}$$

It will be important for us to find out the number of turning points of $\beta(\bar{r})$ as we vary $\bar{\alpha}$ and Φ. First of all, the nature of $\beta(\bar{r})$ depends crucially on the value of Φ^2. For $\Phi^2 > 3/4$, $\beta(\bar{r})$ blows up at $\bar{r}^2 = (4\Phi^2/3 - 1)/2$. Consequently, the temperature is zero. Following [1, 2], we would like to identify this with an extremal hole. For $\bar{r}$ less than this value, $\beta(\bar{r})$ becomes negative. It can easily be checked that as long as $\Phi^2 > 3/4$, regardless of the value of $\bar{\alpha}$, there is no turning point of $\beta(\bar{r})$. If, on the other hand, $\Phi^2 = 3/4$, β diverges at $\bar{r} = 0$ and goes to zero for large $\bar{r}$. Now, to have turning points, $\partial\beta/\partial\bar{r} = 0$. This gives

$$\bar{r}^2_{1,2} = \frac{1}{12}\Big(3 - 36\bar{\alpha} - 4\Phi^2 \pm \sqrt{(-3 + 12\bar{\alpha} + 4\Phi^2)(-3 + 108\bar{\alpha} + 4\Phi^2)}\Big). \tag{4.15}$$

From here, it follows that in order to have real roots, $\bar{\alpha}$ should *not* lie within the window

$$\frac{1}{36}\Big(1 - \frac{4\Phi^2}{3}\Big) \leq \bar{\alpha} \leq \frac{1}{4}\Big(1 - \frac{4\Phi^2}{3}\Big). \tag{4.16}$$

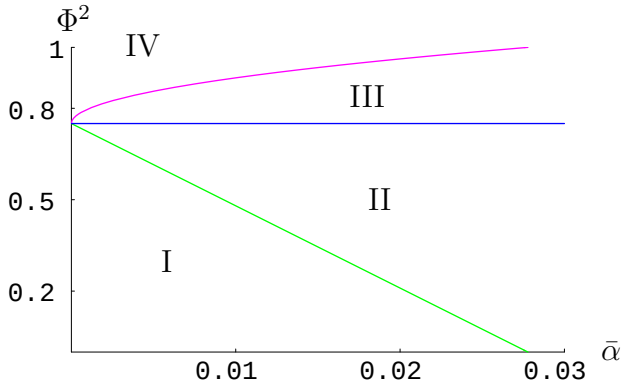

Figure 4.1: The curves in the ($\bar{\alpha}$-Φ^2) plane separating various regions with different behaviours of black holes.

However, it is easy to check that for $\bar{\alpha} \geq \frac{1}{4}(1 - \frac{4\Phi^2}{3})$, $\bar{r}^2_{1,2}$ are negative while $\bar{\alpha} \leq \frac{1}{36}(1 - \frac{4\Phi^2}{3})$, $\bar{r}^2_{1,2}$ are positive. Hence, we have the following picture. For $\Phi < \sqrt{3}/2$, β has two turning points only if

$$\bar{\alpha} \leq \frac{1}{36}(1 - \frac{4\Phi^2}{3}). \tag{4.17}$$

The above features of $\beta(\bar{r})$ can be nicely summarized is a $(\Phi^2 - \bar{\alpha})$ diagram. This is shown in figure 4.1. The region satisfying (4.17) is the region I in the figure. So, here $\beta(\bar{r})$ has two turning points. However, note that for $\Phi^2 < 4/3$ and $\alpha = 0$, $\beta(\bar{r})$ has only one turning point at non-zero $\bar{r}$. In the rest of the regions namely II, III and IV, there are no turning points of $\beta(\bar{r})$. However, as in I, in region II, $\beta(\bar{r})$ diverges at $\bar{r} = 0$ while in regions III and IV, $\beta(\bar{r})$ blows up at finite non-zero values of $\bar{r}$. There are other differences in these four regions (particularly when the free energies of the black holes are considered). This is what we discuss in the next paragraph. Various representative plots of the β versus $\bar{r}$ for all these regions are shown in figure 4.2.

Free Energy: The free energy can be obtained from (4.13) as $W = I_{\rm gc}/\beta$. For different values of the parameters, W has been plotted as a function of temperature

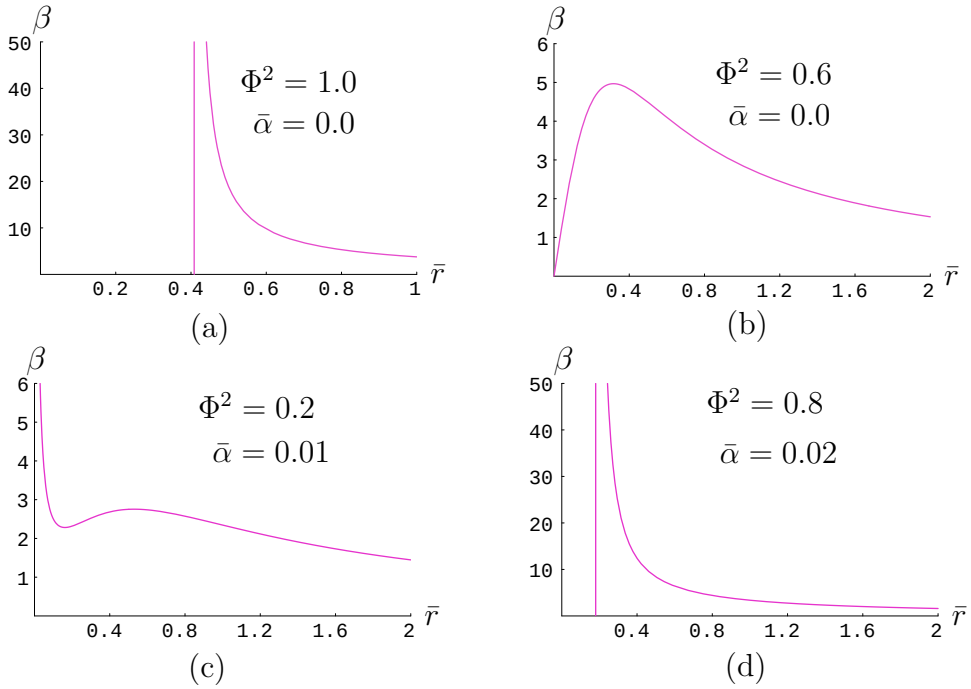

Figure 4.2: Plots of β *vs* $\bar{r}$ for various values of $(\Phi^2, \bar{\alpha})$.

in figure 4.3. In this figure, (a) corresponds to the parameter values where we have only one stable black hole solution. This is also the situation in the case of (d). However, there is a distinct difference in their phase structures as is evident from the plots. While the black hole phase has lower free energy than thermal AdS in (a) for all temperatures, there is a Hawking-Page transition at T_c in (d). This difference can easily be located in $(\Phi^2 - \bar{\alpha})$ diagram in figure 4.1. In the region IV of this figure, black hole at $T = 0$ has less energy than the thermal AdS and hence is stable. However, in regions II and III, a hole at $T = 0$ is in a metastable phase while AdS is the stable one. Hence this hole would decay to AdS by radiating away its energy. The line separating III and IV represents hole with zero free energy at $T = 0$. The equation of this line as a function of $\bar{\alpha}$ and Φ^2 is obtained by setting $W(\bar{r}, \bar{\alpha}, \Phi^2) = 0$, where $\bar{r^2} = 1/2(1 - 4\Phi^2/3)$. Note that this also means that on this line the Hawking-Page

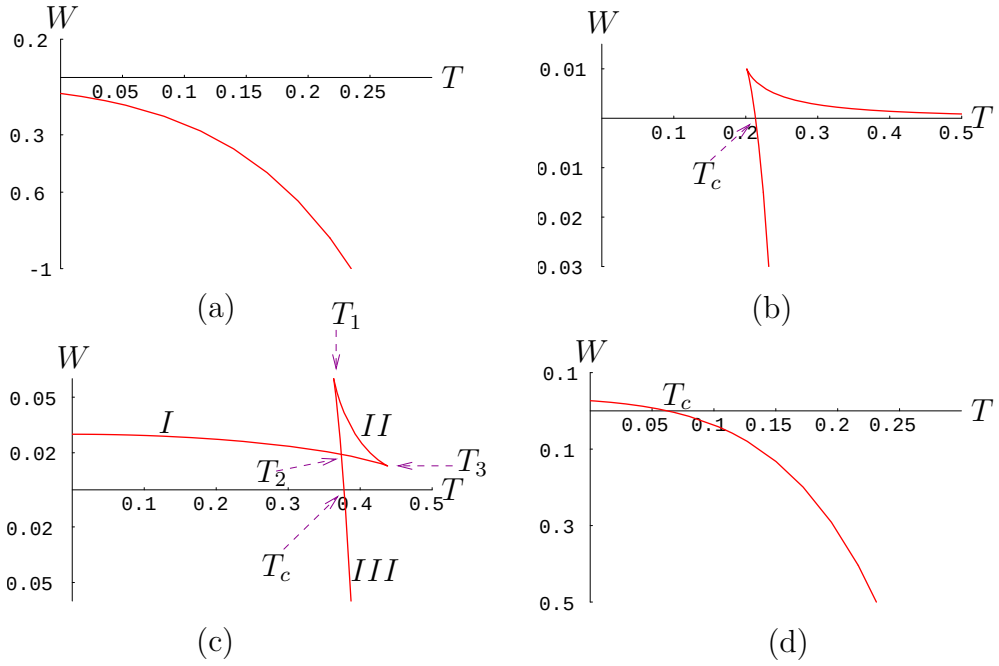

Figure 4.3: Free energy W as a function of T. (a), (b), (c), (d) correspond to values of Φ^2 and $\bar{\alpha}$ of figure(4.2)

temperature vanishes.

Now returning back to figure 4.3(b), we see that at low temperatures there is no black hole phase. Two black hole phases appear as we increase the temperature. The small one turns out to be unstable and the large one undergoes a Hawking Page transition at T_c. Note that figure 4.3(c) is similar to the one we found in our previous chapter (i.e for $\Phi^2 = 0, \bar{\alpha} \neq 0$). As in earlier chapter, we have therefore the following scenario. At low temperature, free energy has only one branch (branch I). However, as temperature is increased, two new branches (branch II and III) appear. Branch II meets branch I at a certain temperature (T_3) and they both disappear. On the other hand, branch III continues to decrease, cuts branch I at a particular temperature (T_2) and becomes negative at temperature T_c. These three branches represent small,

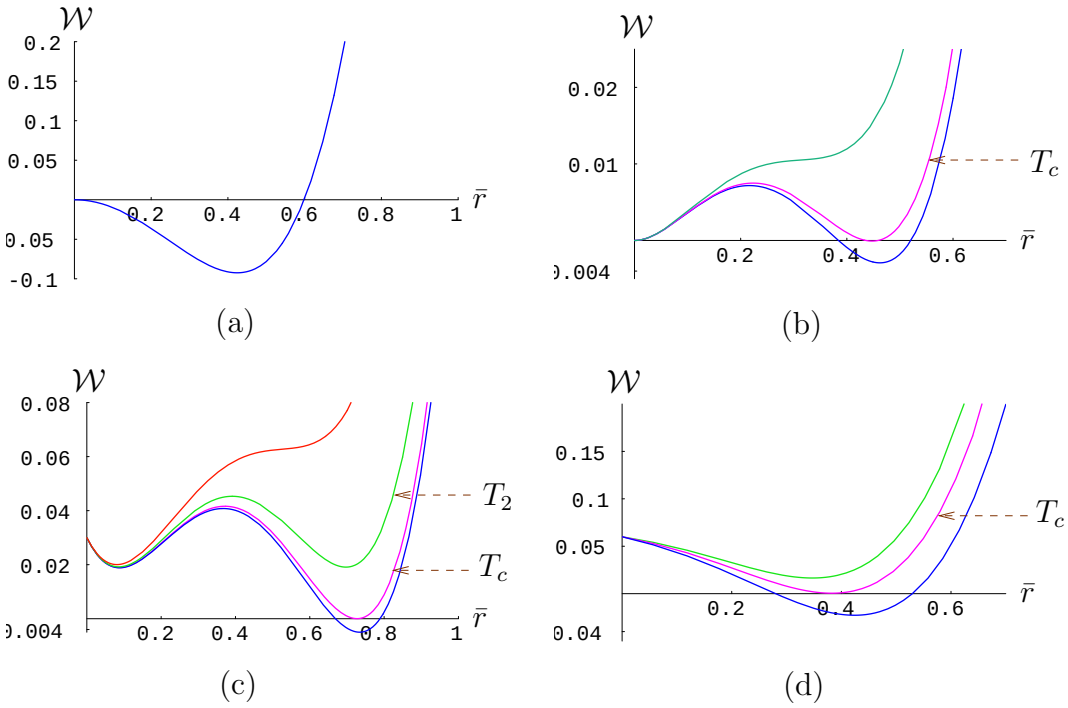

Figure 4.4: Landau function $\mathcal{W}$ *vs.* $\bar{r}$ for different temperatures. (a), (b), (c), (d) correspond to values of Φ^2 and $\bar{\alpha}$ of figure(4.2)

intermediate and large black hole. Out of these three, the intermediate black hole is unstable with negative specific heat, while the rest are classically stable. As in previous chapter, we get two first order phase transitions (HP1, HP2). HP1 is a transition between small and large black hole at temperature T_2 and the other (HP2) is the usual transition between AdS to large black hole as T_c.

It is easy to construct a Landau function which represents the behaviour of the free energy around the critical points. Identifying $\bar{r}$ as the order parameter, this function can be written as

$$\mathcal{W}(\bar{r},T)=\frac{\omega_3 l^2}{\kappa_5}\Big[3\bar{r}^4-4\pi lT\bar{r}^3+(3-4\Phi^2)\bar{r}^2-24\pi\bar{\alpha}lT\bar{r}+3\bar{\alpha}\Big]. \tag{4.18}$$

Notice that this expression reduces to the one in [6] when we set $\bar{\alpha}$ to zero and to the

one in previous chapter as we set Φ to zero. It can be checked that at the saddle point of this function, we get the temperature (given by the inverse of the expression in (4.14)). Substituting back the temperature in $\mathcal{W}$, we get the free energy W. We have plotted the Landau function in figure 4.4. Consider (c) in figure 4.4 in particular. This is for $\Phi^2 = 0.2, \bar{\alpha} = 0.01$. Clearly, for $T < T_2$, the global minimum occurs for small $\bar{r}$, representing a stable small black hole phase. At $T = T_2$, small and big black hole co-exist. At even higher temperature, big black hole represents the stable phase. However, all these phases are meta-stable below $T < T_c$ if we include thermal AdS (representing the horizontal line with $\mathcal{W} = 0$). Big holes then are only stable beyond T_c. Note, that for (a) in figure 4.4, black hole is always the stable phase while for (b), there is a crossover from thermal AdS to black hole at T_c. Finally, figure (d) is similar to (a) except that the $\bar{r} = 0$ hole has more energy than the thermal AdS. To this end, we note that since $W = E - TS - \Phi Q$, we get the energy, entropy and charge as

$$\begin{aligned} E &= \Big(\frac{\partial I_{\rm gc}}{\partial \beta}\Big)_{\Phi} - \frac{\Phi}{\beta}\Big(\frac{\partial I_{\rm gc}}{\partial \Phi}\Big)_{\beta} = M \\ S &= \beta\Big(\frac{\partial I_{\rm gc}}{\partial \beta}\Big)_{\Phi} - I_{\rm gc} = \frac{4\pi l^3 \omega_3 \bar{r}(\bar{r}^2 + 6\bar{\alpha})}{\kappa_5} \\ Q &= -\frac{1}{\beta}\Big(\frac{\partial I_{\rm gc}}{\partial \Phi}\Big)_{\beta}, \end{aligned} \tag{4.19}$$

where expressions for Q, M in terms of q, m respectively were defined earlier. It can be checked that the first law of thermodynamics $dE = TdS + \Phi dQ$ is satisfied.

4.2.2 Canonical ensemble

We now consider the system in canonical ensemble where the charge q is kept fixed. We first note from the expression of the temperature (4.10) that T is non-negative if

$$\bar{r}^2 + 2\bar{r}^4 - \frac{\bar{q}^2}{\bar{r}^2} \geq 0. \tag{4.20}$$

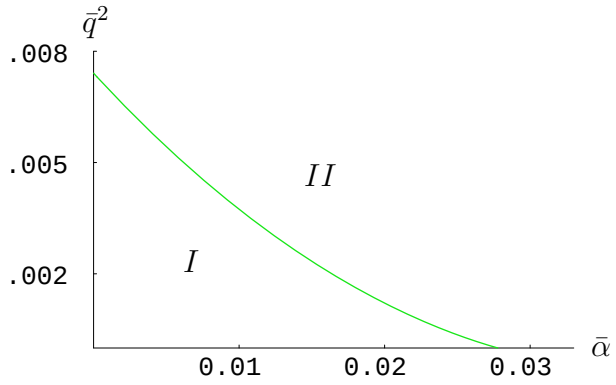

Figure 4.5: The curve in $\bar{\alpha} - \bar{q}^2$ plane separating regions with various number of solutions.

When the equality is saturated, the temperature is zero and we call this an extremal black hole. Denoting mass and the scaled horizon radius as $\bar{m}_e$ and $\bar{r}_e$ respectively, we see that the following relation is satisfied:

$$\bar{m}_e = \bar{\alpha} + \frac{\bar{r}_e^2}{2} + \frac{3\bar{q}^2}{2\bar{r}_e^2}. \tag{4.21}$$

Like in the previous case of fixed potential, we now identify the relevant regions in the ($\bar{\alpha}$-$\bar{q}^2$) plane. The curve separating the regions for various number of positive solutions for $\bar{r}$ is given by the following parametric equations in $\bar{r}$:

$$\begin{aligned} \bar{q}^2 &= \frac{1}{15}\left(6\bar{r}^6 - \bar{r}^4\right), \\ \bar{\alpha} &= \frac{5}{3}\left(\frac{\bar{r}^2 - 3\bar{r}^4}{18\bar{r}^2 + 2}\right). \end{aligned} \tag{4.22}$$

The curve is shown in figure 4.5. It can easily be checked that for any point in region II, there is one real positive root for $\bar{r}$ at any temperature. Below this, that is in region I, there is a maximum of three. Furthermore, unlike the fixed potential case, the vertical $\bar{q}^2$-axis i.e. for $\bar{\alpha} = 0$ we also have a maximum of three real positive solutions as long as $\bar{q}^2 < \bar{q}_c^2 (= 1/135)$. We also notice that thermal AdS exists only when $\bar{q}^2 = 0$. The corresponding β-$\bar{r}$ plots for these regions are shown in figure 4.6.

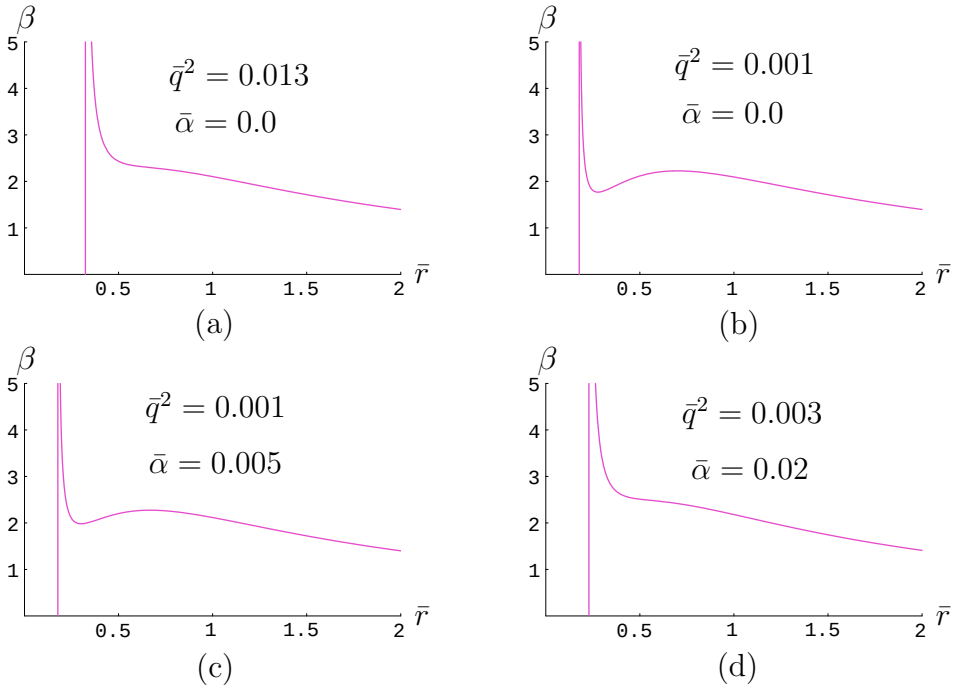

Figure 4.6: Plots of β *vs* $\bar{r}$ for various values of $(\bar{q}^2, \bar{\alpha})$.

Free Energy: We now compute the action (4.1) in the fixed charge ensemble. After properly adding a boundary charge and subtracting the contribution to the extremal background, we get

$$I_{\rm c} = \frac{\omega_3 l^2 \beta}{\kappa_5}\Big[\bar{r}^2 - \bar{r}^4 + \frac{5\bar{q}^2}{\bar{r}^2} + \frac{8\bar{\alpha}(\bar{q}^2 - \bar{r}^4 - 2\bar{r}^6)}{\bar{r}^2(\bar{r}^2 + 2\bar{\alpha})} - \frac{3}{2}\bar{r}_e^2 - \frac{9\bar{q}^2}{2\bar{r}_e^2}\Big], \tag{4.23}$$

where β is

$$\beta = \frac{2\pi l(\bar{r}^2 + 2\bar{\alpha})\bar{r}}{\bar{r}^2 + 2\bar{r}^4 - \bar{q}^2/\bar{r}^2}. \tag{4.24}$$

The free energy can therefore be obtained as $F = I_{\rm c}/\beta$. Behaviours of free energy for different values of $(q^2, \bar{\alpha})$ are shown in figure 4.7. We first of all note that, in fixed charge ensemble, black holes with negative free energies are always the stable compared to thermal AdS. Secondly, in (a) and (d), we see that given any temperature, there is a single black hole phase, while in (b) and (c), there can at most be three

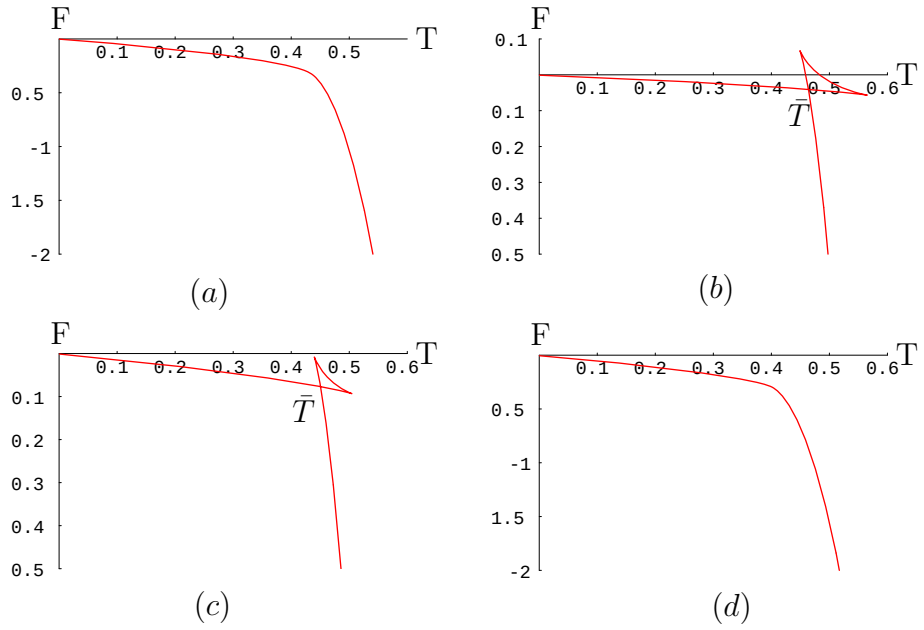

Figure 4.7: The free energy in canonical ensemble as a function of temperature. (a), (b), (c), (d) represent plots for values of $\bar{q}^2$ and $\bar{\alpha}$ of figure (5).

phases. We call them small, big and intermediate black hole phases. We find that at a certain temperature, which we call $\bar{T}$ later, there is a first order phase transition from small to big black hole phase. On the other hand, the intermediate black hole is an unstable phase with negative specific heat. It can be shown by comparing (b) and (c), that $\bar{T}$ decreases as $\bar{\alpha}$ increases.

Finally, the Landau function can be constructed as before. It is given by

$$\mathcal{F}(\bar{r},T)=\frac{\omega_3 l^2}{\kappa_5}\Big[3\bar{r}^4-4\pi lT\bar{r}^3+3\bar{r}^2-24\pi l\bar{\alpha}T\bar{r}+\frac{3\bar{q}^2}{\bar{r}^2}-\frac{9\bar{q}^2}{2\bar{r}_e^2}-\frac{3\bar{r}_e^2}{2}\Big]. \tag{4.25}$$

It can be checked that, at the saddle point, it reproduces correct temperature T and the free energy F. A plot of this function for different temperatures is shown in figure 4.8. As can be seen in (a), for high $\bar{q}$, there is a single black hole phase for all temperatures. As we reduce $\bar{q}$ beyond certain value, two new black hole phases

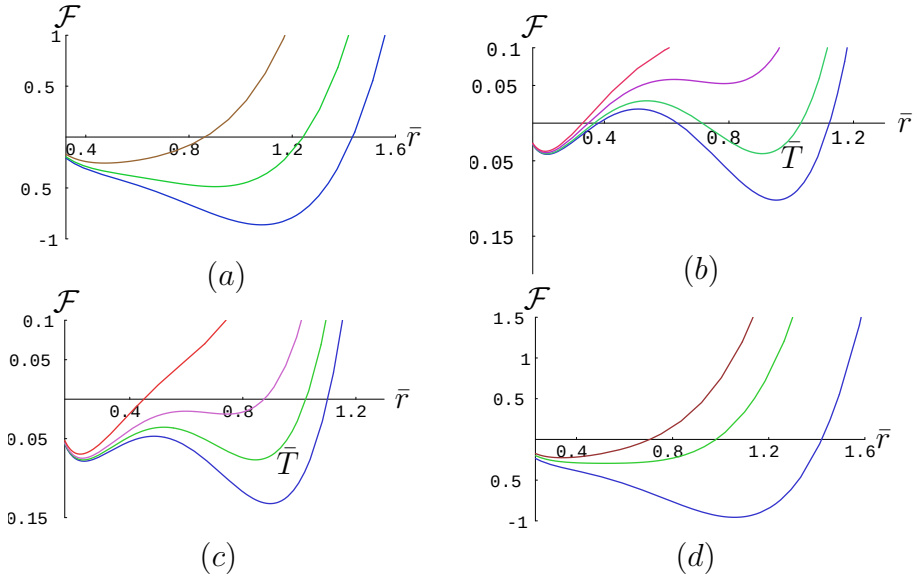

Figure 4.8: The Landau Function $\mathcal{F}$ as a function of $\bar{r}$ for different temperatures. The critical temperature at which there is a transition between the small black hole to the large black hole is shown by $\bar{T}$ in the figures. Finally, (a), (b), (c), (d) represent plots for values of $\bar{q}^2$ and $\bar{\alpha}$ of figure 4.6.

appear in (b) for a certain range of temperature. Above and below this range there is only one black hole solution. When the temperature is within this range, for $T < \bar{T}$, the small black hole is favoured. Otherwise, big black hole is the stable one. There are degenerate minima at $T = \bar{T}$ representing phase co-existence.

Now as we turn on $\bar{\alpha}$, we get (c) for low values of $\bar{q}, \bar{\alpha}$. This is similar to (b) except that the critical temperature $\bar{T}$ reduces with $\bar{\alpha}$. Again, for large $\bar{\alpha}$, we get (d) which is qualitatively similar to that of (a).

Finally, since $F = E - TS$, we have

$$E = \Big(\frac{\partial I_c}{\partial \beta}\Big)_Q = M - M_e$$
$$S = \beta\Big(\frac{\partial I_c}{\partial \beta}\Big)_Q - I_c = \frac{4\pi l^3 \omega_3 \bar{r}(\bar{r}^2 + 6\bar{\alpha})}{\kappa_5}$$

$$\Phi = \frac{1}{\beta}\big(\frac{\partial I_{\rm c}}{\partial Q}\big)_\beta = \sqrt{\frac{3}{4}}\big(\frac{\bar{q}}{\bar{r}^2} - \frac{\bar{q}}{\bar{r}_e^2}\big). \tag{4.26}$$

It can be checked that they satisfy the first law of thermodynamics $dE = TdS + (\Phi - \Phi_e)dQ$.

In the next section, we study the matrix model representing the bulk at finite temperature.

4.3 Dual Matrix Model

The dual matrix model, as we will see, has the same structure as before, except that the parameters depend on the chemical potential μ besides λ and T. In the next two subsections we discuss this model in grand canonical and canonical ensemble respectively.

4.3.1 Matrix model with fixed chemical potential

Once we turn on a non-zero chemical potential the coefficients of the matrix models will depend on the chemical potential. At zero coupling, *i.e* at $\lambda = 0$, this dependence is easy to determine. As we mentioned in the introduction of this chapter, since three equal $U(1)$ charges come from the the rotational symmetry of $SO(6)$, the vector part of the partition function of equation (2.34) will not have any contribution from chemical potential. However the scalar and fermionic parts will contribute. To include this contribution, we consider scalars and fermions have ± 1 and $\pm\frac{1}{2}$ charges respectively with respect to $U(1) \subset SO(6)$. The partition functions in these two parts modify as

$$\begin{aligned} z_S(x^n, \mu) &= \Big[exp(+\mu) + exp(-\mu)\Big] z_S(x^n)/2 = \cosh(\mu) z_S(x^n), \\ z_F(x^n, \mu) &= \Big[exp(+\mu/2) + exp(-\mu/2)\Big] z_F(x^n)/2 = \cosh(\mu/2) z_F(x^n). \end{aligned} \tag{4.27}$$

Then the total partition function in this case is given by (2.34) with

$$z(x^n, \mu) = z_V(x^n) + z_S(x^n)\cosh(\mu) + (-1)^{n+1} z_F(x^n)\cosh(\mu/2). \tag{4.28}$$

This matrix model was studied in [4] and it happens to be similar to the case with $\mu = 0$, where there is first order deconfinement transition at temperature T_H. Here T_H is given by $z(x) = 1$. There is a discontinuous change in ρ from zero to a nonzero value. Above T_H, the deconfined phase is preferred and has free energy $\mathcal{O}(N^2)$. Below T_H, the preferred confined phase has free energy $\mathcal{O}(1)$.

When a small λ is turned on, to the quadratic order in λ one gets a term of the form $(\mathrm{Tr}(U)\mathrm{Tr}(U^{-1}))^2$. One may thus be inclined to propose a matrix model corresponding to the black holes with chemical potential as was done earlier with the (a, b) model for the black holes zero chemical potential. However, the dependence of the coefficients, (a, b) on the chemical potential, though obvious in the $\lambda = 0$ case, is not easy to determine when $\lambda \neq 0$. As was mentioned, the lowest correction is $\mathcal{O}(\lambda^2)$ that involves a three loop computation[1]. On the other hand, an alternative approach is to write down a model in the strong coupling regime by comparing with gravity. Though we do not hope to determine the exact dependence of the parameters on the chemical potential, the restrictions on them so that the matrix model reproduces the qualitative features of gravity can be inferred.

Let us begin with the case without $\alpha^{'}$ corrections first and then include the effect of $\alpha^{'}$ corrections in the next subsection 4.3.2. We will consider the equation (2.48), where now apart from λ and T, a and b are also functions of the chemical potential μ.

When comparing with gravity, $a(\lambda, T, \mu)$ and $b(\lambda, T, \mu)$ will be assumed to be positive for all values of μ. We have seen in section (4.2.1) that there exists a critical value of the potential (μ_c) above which there is only one solution. Below this there are a maximum of two solutions. The phase structure below the critical potential is same as that of the uncharged case. This is reproduced by the (a, b) model [9] when $a < 1$ and $b > 0$ as described in second chapter of this thesis.

From equation (4.14), we see that the radius of the small black hole at and above

[1]To our knowledge this computation is not available in the literature.

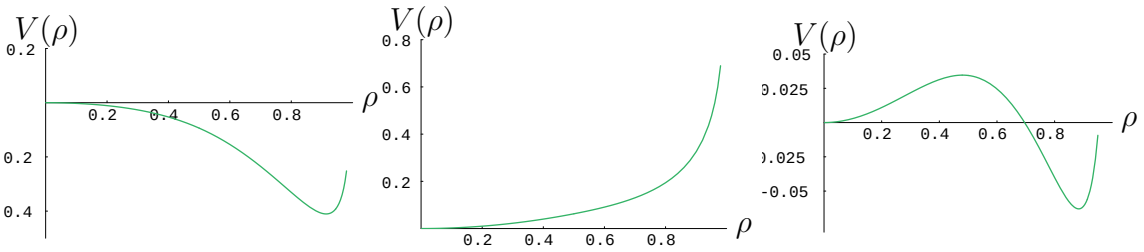

$T > 0$ (A) $a(\mu, T) > 1$ $T = 0$ $T > 0$ (B) $a(\mu, T) < 1$

Figure 4.9: Plots of the matrix model potential *vs.* ρ above μ_c showing the two possible situations at finite temperature. At $T = 0$ the extremal black hole decays into AdS, shown as a saddle point at $\rho = 0$.

the critical potential, becomes zero and negative respectively. The black hole with positive radius approaches an extremal limit at $T = 0$. We know that thermal AdS exists for all temperatures and at $T = 0$ the gauge theory is in the confined phase. We thus have two solutions in gravity corresponding to the confined phase. However the extremal black hole being nonsupersymmetric will ultimately decay into AdS at zero temperature [1, 2]. We do not expect to capture the dynamics of this decay with the static potential given by the (a, b) model. In fact the zero temperature configuration with only the AdS is not continuously connected to the finite temperature (a, b) model as we will see below.

At finite temperature, we always need to introduce an unstable saddle point (a maximum). This follows from the observation that the smooth potential given by the (a, b) model which gives two minima (corresponding to thermal AdS and the large black hole in gravity) always includes a maximum in between. For $\mu > \mu_c$ this maximum corresponding to the unstable black hole ceases to show up in gravity above. In the matrix model, we interpret this phenomenon as follows. As μ increases beyond μ_c this unstable saddle point in the matrix model enters the $\rho < 1/2$ region from $\rho > 1/2$ region. Thus the region beyond μ_c corresponds to the values of a and b when

the unstable small black hole of the (a, b) model has already undergone the third order Gross-Witten transition [7, 8]. This imposes a constraint on the values of a and b. Another constraint comes from the fact that the energy of the large black hole in this region is lower than thermal AdS for all temperatures. At any finite temperature, the theory is thus always in the deconfined phase. Both of these constraints are satisfied if we set $b > 2(1 - a)$. However, in light of these remarks, it is not possible to tell whether the unstable saddle point has energy less or more than that of AdS or whether it is at $\rho = 0$ or away from it. Thus it gives rise to two possible scenarios depending on whether the unstable saddle point is at $\rho = 0$ or in the region $0 < \rho < 1/2$ as shown in figure 4.9. In the following we discuss these two scenarios separately .

(A) Unstable maximum is at $\rho = 0$ ($a(\mu \geq \mu_c, T) \geq 1$): In this case we define the critical potential μ_c by $a(\mu_c, T) = 1$. Here the unstable saddle point at $\rho = 0$ does not correspond to thermal AdS but to the unstable configuration not visible in gravity as mentioned above. Thermal AdS does not feature in the plot. It has energy higher than the black hole. The condition $b > 2(1 - a)$ is automatically satisfied as b is assumed to be positive.

(B) Unstable maximum is at $0 < \rho < 1/2$ ($a(\mu \geq \mu_c, T) < 1$): In this case the saddle point at $\rho = 0$ is thermal AdS. The unstable saddle point has energy higher than AdS. Since the black hole has energy less than AdS, a and b correspond to values above the Hawking-Page transition. Also the saddle point for the maximum is at $\rho < 1/2$. The critical potential in this case is given by, $b(\lambda, T, \mu_c) = 2\left[1 - a(\lambda, T, \mu_c)\right]$ or by the curve in the parameter space of a and b that gives the Hawking-Page transition, depending on whichever satisfies both the above conditions.

Finally we draw a diagram in the $(a - b)$ parameter space to show the various regions which depend on the number of saddle points. This is shown in figure 4.10. For

$\mu > \mu_c$ we have the following situation: At $T = 0$ the only solution which is thermal AdS, is given by the region below line I. At any finite temperature the parameters jump to values in regions (A) or (B).

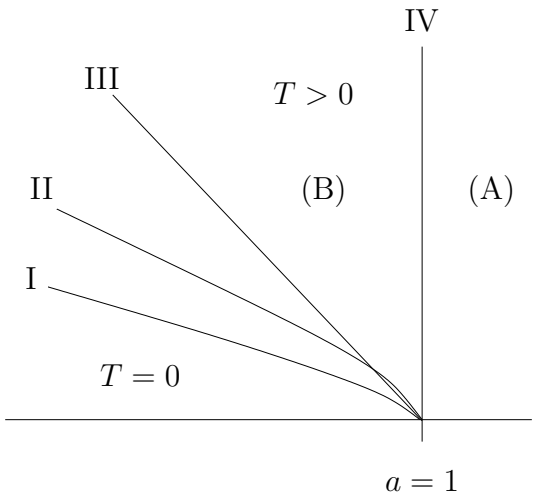

Figure 4.10: The $a - b$ parameter space for $\mu > \mu_c$. The zero temperature region is below I and the finite temperature region is beyond III or II. Below I there is only one saddle point at $\rho = 0$ corresponding to thermal AdS. On II the Hawking Page transition occurs. III is the Gross-Witten transition line. IV is the line, $a = 1$

4.3.2 Including $\alpha^{'}$ corrections : Fixed potential

As mentioned before, now we include $\alpha^{'}$ corrections along with nonzero chemical potential, the coefficients in the action (3.22) depend also on α'. The equations of motion are of the same form as given in the $\mu = 0$ case:

$$\begin{aligned} \rho F(\rho) &= \rho \quad , \qquad 0 \leq \rho \leq \frac{1}{2}, \\ &= \frac{1}{4(1-\rho)} \quad , \quad \frac{1}{2} \leq \rho \leq 1, \end{aligned} \tag{4.29}$$

where we have defined

$$F(\rho) = \frac{\partial S(\rho^2)}{\partial \rho^2} = N^2[8A_4\rho^6 - 6A_3\rho^4 + 4A_2\rho^2 + (1 - 2A_1)]. \tag{4.30}$$

The potentials that follows from the above action are given by

$$\begin{aligned} V(\rho) &= -A_4\rho^8 + A_3\rho^6 - A_2\rho^4 + A_1\rho^2 \quad , \qquad 0 \le \rho \le \frac{1}{2} \\ &= -A_4\rho^8 + A_3\rho^6 - A_2\rho^4 + (A_1 - 1/2)\rho^2 - \frac{1}{4}\log[2(1-\rho)] + \frac{1}{8} \quad , \quad \frac{1}{2} \le \rho \le 1. \end{aligned} \tag{4.31}$$

As seen from (4.29) $\rho = 0$ is always a solution. The action (3.22) evaluated at $\rho = 0$ vanishes. For zero chemical potential and $\bar{\alpha}$ this solution corresponds to the thermal AdS on the bulk side [9].

In the analysis of phase structure we saw as the chemical potential Φ and temperature T vary we arrive different regions having different thermodynamic features. Similarly in the matrix model as chemical potential and temperature vary the coefficients of the matrix model action vary as well. Thus if we consider a four dimensional space corresponding to the four coefficients of (3.22) it is sectioned into various regions which are analogous to the regions in the phase diagram. This is essentially same as what we did graphically in figure 4.10 for two coefficients. Analogously, here we will identify different regions in four dimensional space of the coefficients with various ranges of temperature and chemical potential.

Let us begin with the various regions in the (Φ^2-$\bar{\alpha}$) plane depending on the number and nature of the solutions, as discussed in subsection 4.2.1 (see fig. 4.1). In particular, there is a line in the (Φ^2-$\bar{\alpha}$)-plane that separates region with three solutions and that with one solution. Let us consider constraints imposed on the coefficients A_i that corresponds to these regions or in other words, regions above and below the critical potential μ_c at fixed λ. For that purpose it is useful to consider the quadratic polynomial in ρ^2: $f(\rho^2) = (1/\rho)\frac{\partial}{\partial\rho}F(\rho)$. This is given by $f(x) = 48A_4x^2 - 24A_3x + 8A_2$. The zeroes of f determine the non-trivial turning points of F. We will see below that the parameters at $T = 0$ are continuously connected to the finite temperature ones

for $\mu < \mu_c$ but they are not so for $\mu > \mu_c$ as we saw in absence of α' correction.

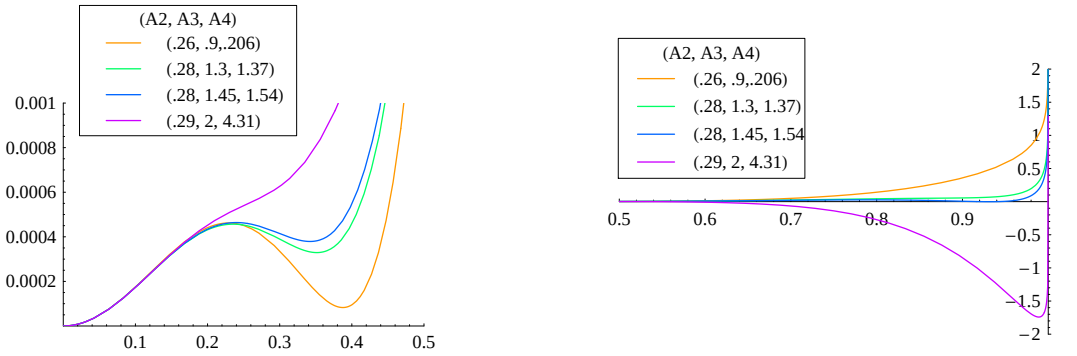

Figure 4.11: For $\mu < \mu_c$, Potential as function of ρ for the ranges $0 \leq \rho \leq 1/2$ and $1/2 \leq \rho \leq 1$. The values of (A_2, A_3, A_4) used in the plots are given above. $A_1 = 0.02$.

Sub-critical Potential ($\mu < \mu_c$)**:** This corresponds to the region I in figure 4.1. In this range the behaviour is very similar to the case of zero chemical potential. As is evident from the plot in figure 4.2(c) obtained on the gravity side we have two characteristic temperatures, among others. One is $T = T_{N2}$ where the stable big black hole and unstable intermediate black hole nucleates. Another is $T = T_{N1} > T_{N2}$ where the intermediate unstable black hole combines with stable small black hole and beyond that temperature they cease to exist as solutions. This leads to three qualitatively different ranges of temperature and in the following we discuss them separately.

$T_{N2} < T < T_{N1}$**:** Here on the gravity side we have three black holes and so we expect at least three solutions of the saddle point equation (4.29) obtained from the Matrix model. The small black hole has a size of the order of α'. In addition, as we have already seen in the analysis of $\mu = 0$ case, we have an (unstable) solution which is a maximum of the potential. Since this solution does not appear in the gravity that is beyond an analysis of order α'. So we expect these two solutions occur generically in the range $0 \leq \rho \leq \frac{1}{2}$. The other two solutions, which are analogues to unstable

intermediate black hole and stable big black hole, and having bulk analogue, are expected them to appear generically in the range $\frac{1}{2} \leq \rho \leq 1$. Therefore we get four solutions for this region. So this region corresponds to the range of the coefficients A_i for which (4.29) has four solutions within the domain of ρ. From (4.29) we see this requires $f(\rho^2) = 0$ has two positive solutions $0 \leq \rho_-^2 \leq \rho_+^2 \leq 1$ where ρ_- is a maximum and ρ_+ is a minimum of $F(\rho)$. That $f(\rho^2) = 0$ has two solutions requires

$$\triangle = 3A_3^2 - 8A_2A_4 > 0, \qquad A_4.A_2 > 0, \tag{4.32}$$

where the second condition is to ensure that both the solutions $\rho_\pm^2$ are positive. That $\rho_\pm$ are minimum and maximum of F respectively implies $F''(\rho_-) < 0$, $F''(\rho_+) > 0$ from which we obtain

$$\rho_\pm^2 = \frac{A_3}{4A_4} \pm \sqrt{(\frac{A_3}{4A_4})^2 - \frac{A_2}{6A_4}}, \quad A_2 > 0. \tag{4.33}$$

Other conditions that we need to impose so that (4.29) admits four solutions are $F(\rho_-) > 1$ and $F(\rho_+) < 1$, which when written in terms of A_i's become

$$\frac{A_2 \cdot A_3}{3A_4} > 2A_1 + 16A_4\Big[(\frac{A_3}{4A_4})^2 - \frac{A_2}{6A_4}\Big]\rho_-^2 \quad , \tag{4.34}$$

$$\frac{A_2 \cdot A_3}{3A_4} < 2A_1 + 16A_4\Big[(\frac{A_3}{4A_4})^2 - \frac{A_2}{6A_4}\Big]\rho_+^2 \quad . \tag{4.35}$$

The above conditions (4.32,4.33,4.34, 4.35) ensure that there exist a minimum (ρ_{min}) corresponding to the small black hole and a maximum (ρ_{max}) that does not have a gravity analogue. These solutions are in general different from $\rho_\pm$ and since F is a cubic polynomial in ρ^2 the expressions are complicated. In addition, on the gravity side we saw that stable small black hole have positive energy. So we expect the solution of the saddle point equation that correspond to this stable small black hole should have positive energy. So we need at the minimum

$$V_1(\rho_{min}) > 0 \quad . \tag{4.36}$$

whose explicit form is not very illuminating.

In addition as we said from gravity analysis we expect two solutions should appear, generically, in the first half of the domain of ρ while two other in the second half. We consider two halves of the domain of ρ separately. Let us begin with the range $0 \leq \rho \leq \frac{1}{2}$. That we have two solutions of the saddle point equation (4.29) in this range imposes two further conditions:

$$\rho_- < \frac{1}{2}, \quad F(\frac{1}{2}) < 1. \tag{4.37}$$

(In this form it is easier to obtain the restriction on the parameters. Otherwise we could write $0 < \rho_{min}, \rho_{max} < \frac{1}{2}$ which are more direct but the expressions are cumbersome.) These conditions, when written in terms of the parameters, reduce to the following two equations:

$$\frac{A_3}{4A_4} - \sqrt{(\frac{A_3}{4A_4})^2 - \frac{A_2}{6A_4}} \;<\; \frac{1}{4} \quad , \tag{4.38}$$

$$2A_1 + \frac{3A_3}{8} \;>\; A_2 + \frac{A_4}{8}. \tag{4.39}$$

These conditions (4.32,4.33,4.34,4.35,4.36) are real inequalities in four parameters. Each of them will give rise to one (or more) codimension 1 wall(s) in the four dimensional parameter space described by A_1, A_2, A_3, A_4. Since this involves four parameters it is difficult to have a graphical representation of it. As we see each of the inequalities corresponds to wall(s) which we cross when we go beyond this range of temperature and chemical potential. However, crossing the wall corresponding to (4.36) will take us to some unphysical region as that implies the stable small black hole has energy less than that of AdS which implies on the gauge theory side absence of confinement in low temperature. The equations (4.38,4.39) also give rise to codimension one walls but a more elaborate analysis is required to understand the correct significance of them.

We expect the other two solutions to appear in the other half namely $\frac{1}{2} \leq \rho \leq 1$. On this part the situation is pretty much similar to that of (a, b)-model. This requires

we have one solution $\frac{1}{2} \leq \rho_1 \leq 1$ such that it satisfies

$$F(\rho_1) = \frac{1}{4\rho_1(1-\rho_1)} \quad , \qquad F'(\rho_1) > \frac{1}{4}(-\frac{1}{\rho_1^2} + \frac{1}{(1-\rho_1)^2}), \tag{4.40}$$

where this ρ_1 will appear as the analogue of the unstable intermediate black hole solution that we got on the gravity side. Actually, this condition is sufficient to ensure that there is the analogue of stable big black hole too. This condition (4.40) along with (4.32,4.33,4.34,4.35) completes the list of necessary and sufficient condition to have four solutions of the saddle point equations. As temperature increases, ρ_1 will decrease. At the Gross-Witten temperature [7, 8] $T = T_g$ this reaches the lower boundary of this region $\rho = \frac{1}{2}$. At $T = T_g$ the restriction on the parameters can be written as

$$2A_1 + \frac{3A_3}{8} = A_2 + \frac{A_4}{8} \quad , \quad 3A_4 + 8A_2 > 6A_3. \tag{4.41}$$

This corresponds to a third order phase transition.

$T \leq T_{N2}$: In this range of temperature the conditions that we obtain on the first half of the domain of ρ remains the same. On the second half of the domain the two solutions will merge at $T = T_{N2}$. This implies in the four parameter space we are on the wall that corresponds to (4.40). The following equations corresponds to T_{N2}:

$$F(\rho) = \frac{1}{4\rho(1-\rho)} \quad , \quad F'(\rho_1) = \frac{1}{4}(-\frac{1}{\rho_1^2} + \frac{1}{(1-\rho_1)^2}). \tag{4.42}$$

As temperature decreases the value of $F(\rho)$ will monotonically decrease and there will be no solution in the second half.

$T \geq T_{N1}$: Here we have no solution in the first half of domain of ρ at $T > T_{N1}$. But that can happen in two possible ways and we discuss them in the following. One possibility is the two extrema of $V_1(\rho)$ merge at $T = T_{N1}$ which implies we cross the wall corresponds to (4.34). In terms of the parameters this means at $T = T_{N1}$

$$\frac{A_2 A_3}{3A_4} = 2A_1 + 16A_4\big[(\frac{A_3}{4A_4})^2 - \frac{A_2}{6A_4}\big]\rho_-^2. \tag{4.43}$$

This is a consistent possibility that can occur in the matrix model. Another significance of this equation is this corresponds to the bound beyond which we get the features of (a, b)-model and so this region sits in the same universality class of that of (a, b)-model.

The second possibility is crossing the wall corresponding to (4.35), where the minimum of V_1 meets the maximum of V_2. However, In terms of the coefficients, then, at T_{N1} we have

$$\frac{A_2 A_3}{3A_4} = 2A_1 + 16A_4\Big[(\frac{A_3}{4A_4})^2 - \frac{A_2}{6A_4}\Big]\rho_+^2. \tag{4.44}$$

This possibility seems more plausible as it matches with what we saw on the gravity side. There at $T = T_{N1}$ the unstable intermediate black hole merges with the stable small black hole. At this point we should comment on the relative values of T_{N1} and T_g. If $T_{N1} < T_g$ this merging occurs before the system reaches it Gross-Witten point and therefore there will be no Gross-Witten transition. On the other hand for $T_{N1} > T_g$ the intermediate solution has already undergone the GW transition and becomes a black hole of the order of α'. The other possibility is if $T_{N1} = T_g$ where the small black hole merges with the intermediate black hole exactly at the Gross-Witten point or the two walls corresponding to (4.35) and (4.38) merge.

Super-critical Potential ($\mu > \mu_c$)**:** This region corresponds to the parameter space above region I in figure 4.1 and therefore should have a single minimum of the potential. In the matrix model like the $\mu < \mu_c$ region here also we have an additional unstable maximum of the potential that does not have any bulk analogue and so it is beyond the gravity analysis of the α' order. Once again we restrict this in the region, $\rho < 1/2$ so that this corresponds to some stringy phase as suggested in [9]. Therefore, similar to the analysis for $\alpha' = 0$ (and unlike the $\mu < \mu_c$ case) we consider two possible scenarios depending on whether the unstable maximum lies at $\rho = 0$ or it lies away from $\rho = 0$. In the following we discuss the two scenarios separately.

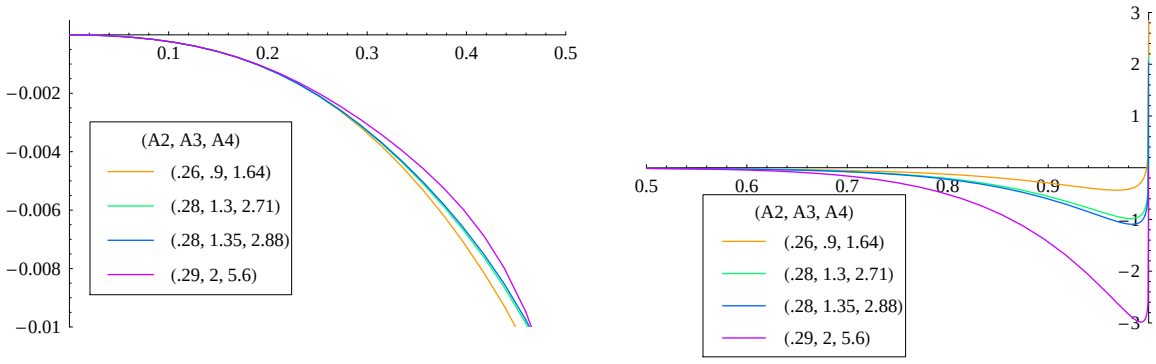

Figure 4.12: For $\mu > \mu_c, A_1 < 0, \triangle < 0$: Potential as function of ρ for the range $0 \leq \rho \leq 1/2$ and $1/2 \leq \rho \leq 1$ .The values of (A_2, A_3, A_4) used in the plots are given above. $A_1 = -0.02$.

(A) Unstable maximum is at $\rho = 0$ ($A_1 < 0$): If we have ($A_1 < 0$) the unstable maximum will always be at $\rho = 0$. In addition, in the matrix model we expect to have one and only one stable minimum for $\rho > 0$ (The energy of this black hole could be greater or less than that of thermal AdS depending on the values of μ and λ (see figure 4.3). The condition $A_1 < 0$ alone does not ensure this and we need to impose additional constraints on A_2, A_3 and A_4. We note that there are two ways in which one can ensure that there is only one stable black hole solution. We discuss them separately in the following:

One possibility is, at $\mu = \mu_c$ the three solutions merge into one at some value of $\rho = \rho_+ > 0$. A similar merging occurs on the gravity side when the chemical potential reaches its critical value. Since the corresponding solution is manifested in the gravity limit we expect that $\rho_+ > 1/2$. Then, at $\mu = \mu_c$, apart from the condition $A_1 = 0$, A_2, A_3 and A_4 satisfy,

$$V'(\rho_+) = 0 \;\; ; \;\; V''(\rho_+) = 0 \;\; ; \;\; V'''(\rho_+) = 0 \;\; \text{for} \;\; \frac{1}{2} \leq \rho_+ \leq 1. \tag{4.45}$$

Thus we obtain the parametric solutions of $A_2(\rho_+)$, $A_3(\rho_+)$ and $A_4(\rho_+)$ from (4.45) which corresponds to the line separating the number of solutions in gravity in figure 4.1. We do not write these parametric equations here as they are not compact enough. For, $\rho_+ = 0.8$ we have, $A_1 = 0$, $A_2 = 0.583$, $A_3 = 1.481$, $A_4 = 1.293$.

Examining the equation of motion (4.29), one can find an indirect way to obtain a (slightly more general) constraint in compact form. This ensures there is exactly one solution at some point $\rho > 0$ in addition to the one at $\rho = 0$. However, that the three solutions merge at this point is not guaranteed. If we relax the first inequality of (4.32) by making the discriminant $\triangle$ negative so that there is no turning point of F then we are left with only a single solution. This can be thought of as identifying the wall corresponds to the first condition of (4.32) with $\mu = \mu_c$. The merging of the three solutions at this point appears as a special case of it and so that condition is more ramified. We have plotted the associated potentials in figure 4.12.

The other possibility that one can consider to obtain a single minimum is setting $A_4(\mu = \mu_c) = 0$ and $A_4(\mu > \mu_c) < 0$. This amounts to relaxing the second inequality of (4.32) so that one of the turning point becomes imaginary. This corresponds to identifying $\mu = \mu_c$ with the second condition of (4.32). For this choice, as μ increases beyond its critical value, one of the turning point comes down to $\rho = 0$ and then disappears. This possibility is not continuously connected with the above mentioned constraint, which gives rise to merging of three solutions. However, this possibility can give a simple form for the fixed charge case. We have plotted the related potentials in figure 4.13.

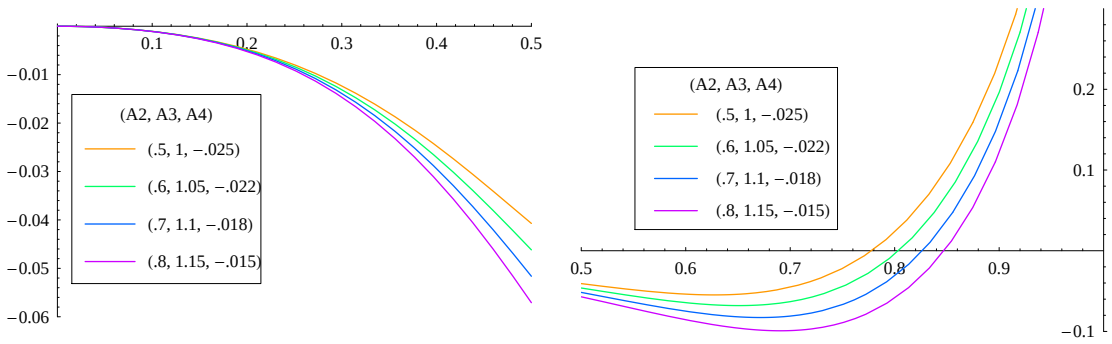

Figure 4.13: For $\mu > \mu_c, A_1 < 0, A_4 < 0$: Potential as function of ρ for the range $0 \leq \rho \leq 1/2$. The values of (A_2, A_3, A_4) used in the plots are given above. $A_1 = -0.1$.

(B) Unstable maximum lies at $0 < \rho < 1/2$ ($A_1 > 0$): In this scenario for $\mu > \mu_c$ the unstable maximum is in the range $0 < \rho < 1/2$. The usual saddle point $\rho = 0$ is also there but this time it corresponds to the thermal AdS. In addition, there exists only one minimum. (The energy of this minimum is either greater or less than that of AdS at low temperatures. If the energy is greater than that of AdS energy, at high temperature, the black hole undergoes Hawking Page transition.) In order to make sure that this is the one and the only one minimum, once again we identify μ_c to be the limit where three saddle points merge. However unlike the previous case where the small maximum was at $\rho = 0$, here it lies in $0 < \rho < 1/2$. This configuration satisfies,

$$V'(\rho_+) = 0 \;\; ; \;\; V''(\rho_+) = 0 \;\; ; \;\; V'''(\rho_+) = 0 \;\; \text{for} \;\; \frac{1}{2} \leq \rho_+ \leq 1.$$
$$\text{and} \quad V'(\rho_-) = 0 \;\; \text{for} \;\; 0 \leq \rho_- \leq \frac{1}{2}. \tag{4.46}$$

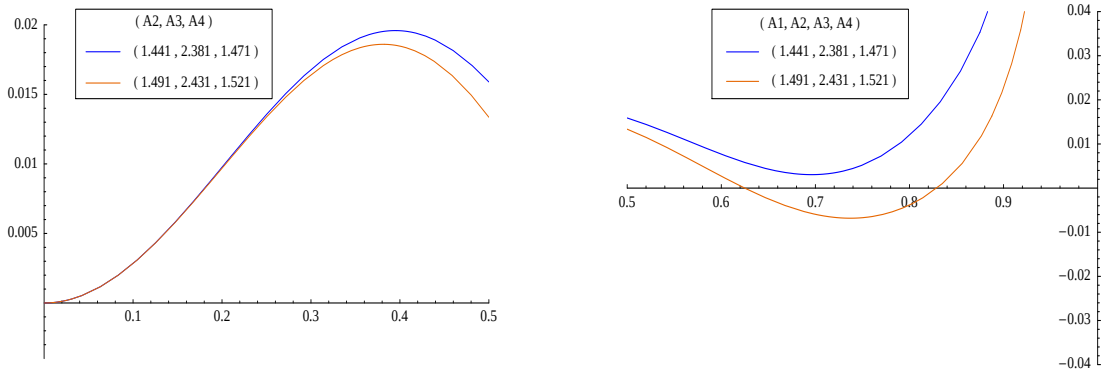

Figure 4.14: For $\mu > \mu_c$ and $A_1 > 0$: Potential as function of ρ for the range $0 \leq \rho \leq 1/2$ and $1/2 \leq \rho \leq 1$. The values of (A_2, A_3, A_4) used in the plots are given above. $A_1 = 0.298$.

Apart from being functions of ρ_+ the A_i's are now also functions of ρ_-. With $\rho_- = 0.5$ and $\rho_+ = 0.8$ we get, $A_1 = 0.418$, $A_2 = 1.561$, $A_3 = 2.501$ and $A_4 = 1.691$. In this case the energy of the merging point (ρ_+) is positive. This gives rise to a stable minimum with positive energy as we move beyond μ_c. We now vary the parameters with increasing temperature and see that the minimum crosses zero corresponding to

the Hawking-Page transition in the bulk. The plots for $\mu > \mu_c$ are shown in figure 4.14.

One can similarly derive the parameters for which the energy of the merging point (ρ_+) is less than zero. This is given by, $\rho_- = 0.4$ and $\rho_+ = 0.72$ which gives $A_1 = 0.006$, $A_2 = 0.06$, $A_3 = 0.291$ and $A_4 = 0.535$. Note that for $\rho_- = 0$ we get ($A_1 = 0$), which is the possibility (A). As we move away from the critical potential, this gives rise to a minimum with energy less than AdS. With further variation of the parameters this saddle point goes deeper as shown in figure 4.15. This can be mapped to the variation of the minimum with temperature as it happens for the black hole in gravity.

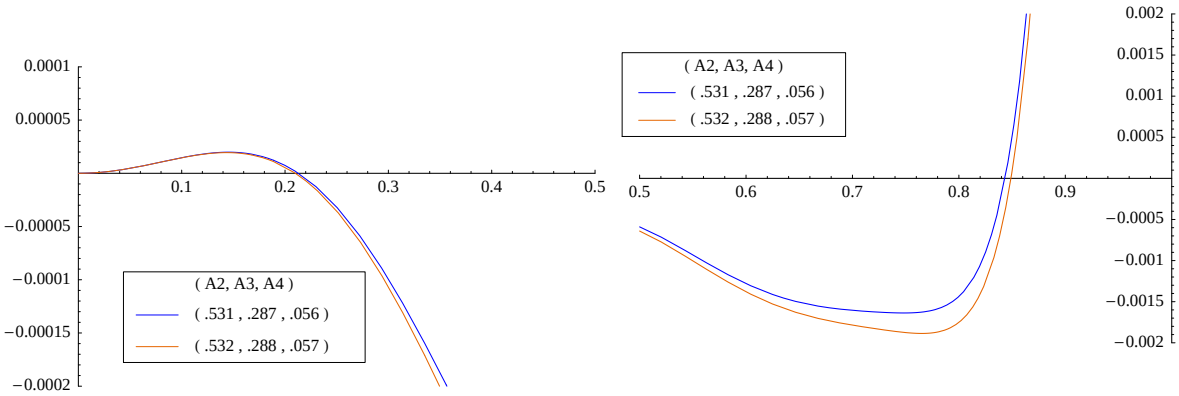

Figure 4.15: For $\phi > \phi_c, A_1 > 0$: Potential as function of ρ for the range $0 \leq \rho \leq 1/2$ and $1/2 \leq \rho \leq 1$. The values of (A_2, A_3, A_4) used in the plots are given above. $A_1 = 0.002$.

In the above discussion we consider, on the matrix model side, the various possibilities, which can reproduce the bulk behaviour that we obtained in the analysis on the gravity side. The different possibilities gives rise to different ranges of the parameters, of which some are mutually exclusive. With this amount of input it is not possible to decide which one is the correct behaviour. We need the explicit dependence of A_i's on μ in the strong coupling regime. Perhaps a weak coupling calculation of the associated terms in the model can serve as a clue.

4.3.3 Including $\alpha^{'}$ corrections : Fixed charge

We have seen in the last section that, when restricted to various values of the parameters A_i, the matrix model (3.22) reproduces the features of gravity below and above the critical potential, μ_c. In general thus A_i will depend on the chemical potential. In the fixed charged case, since chemical potential can take any value, the matrix model for the canonical ensemble is obtained by integrating over the chemical potential. For this, the explicit knowledge of the dependence of A_i are necessary in this strong coupling regime, which we do not have. Out of the cases studied in the earlier section, there is one that allows us to construct a toy model for the fixed charge consistently. This is given by the second possibility of (A), when both A_1 and A_4 become negative above the critical potential. This implies that we can consistently assume A_1 and A_4 are dependent on chemical potential and others are independent of μ.

In the following, we will assume the result from the zero coupling regime to be valid in the strong coupling. In the free theory, the partion function is given by [4, 10]

$$Z(x,Q) = \int d\mu e^{(-i\mu Q)} \int [dU] e^{(\sum \frac{z_n[x,i\mu]}{n} \mathrm{Tr}(U^n)\mathrm{Tr}(U^{-n})}. \tag{4.47}$$

The second integration looks like the partition function of the grand canonical system with chemical potential $i\mu$. Equation(4.28) shows the exact dependence of A_1 on μ in the free theory. In this case, including only the charged scalars, A_1 is given by, $[1-2A_1(\lambda,T,\mu)] = [c(\lambda,T)+d(\lambda,T)\cos(\mu)]$, where c and d are $z_V(x^n)$ and $z_S(x^n)$ respectively. Since we are only interested in the qualitative features of this model, for simplicity we will take, $A_4 = a_4(\lambda,T)\cos(\mu)$ with A_2 and A_3 functions only of λ and T. The action with this dependence on the potential is,

$$S(\rho^2) = 2N^2 \left[a_4 \cos(\mu)\rho^8 - A_3\rho^6 + A_2\rho^4 + \left(\frac{c+d\cos(\mu)}{2}\right)\rho^2 \right]. \tag{4.48}$$

In terms of unitary matrix U, we recast the action in the form as

$$\begin{aligned} S(U) &= 2\Big[\frac{a_4}{N^6}\cos(\mu)\left(\mathrm{Tr}(U)\mathrm{Tr}(U)^\dagger\right)^4 - \frac{A_3}{N^4}\left(\mathrm{Tr}(U)\mathrm{Tr}(U)^\dagger\right)^3 + \frac{A_2}{N^2}\left(\mathrm{Tr}(U)\mathrm{Tr}(U)^\dagger\right)^2 \\ &+ \left(\frac{c+d\cos(\mu)}{2}\right)\mathrm{Tr}(U)\mathrm{Tr}(U)^\dagger\Big]. \end{aligned} \tag{4.49}$$

Hence following [10], the partition function is

$$Z(Q,T,\lambda) = \int d\mu e^{(-i\mu Q)} \int [dU] e^{S(U)}. \tag{4.50}$$

The partition function for the canonical ensemble is obtained by integrating over the chemical potential. This in terms of ρ is

$$Z(Q,T,\lambda) = \int d\rho \exp\{-N^2 V(\rho)\}, \tag{4.51}$$

where, the potential is,

$$\begin{aligned} V(\rho) &= -\frac{1}{2N^2} S_{eff}(\rho^2) + \frac{1}{2}\rho^2 \quad , \qquad 0 \le \rho \le \frac{1}{2}, \\ &= -\frac{1}{2N^2} S_{eff}(\rho^2) - \frac{1}{4}\log[2(1-\rho)] + \frac{1}{8} \quad , \quad \frac{1}{2} \le \rho \le 1, \end{aligned} \tag{4.52}$$

with,

$$S_{eff}(\rho^2) = N^2\left[c\rho^2 + 2A_2\rho^4 - 2A_3\rho^6\right] + \log\left[I_Q\left(N^2(2a_4\rho^8 + d\rho^2)\right)\right]. \tag{4.53}$$

Here $I_Q(x)$ is a Bessel Function. We are interested in the the large N limit. This is obtained by keeping in mind that $Q^2 \sim \mathcal{O}(N^2)$ so that $Q^2 = N^2 q$ where $q \sim \mathcal{O}(1)$. The resulting effective action in the large N limit is thus,

$$\begin{aligned} S_{eff}(\rho^2) &= N^2\left[c\rho^2 + 2A_2\rho^4 - 2A_3\rho^6\right] + \\ &+ N^2 q\left[\left(1 + \frac{\rho^4(d+2a_4\rho^6)^2}{q^2}\right)^{\frac{1}{2}} + \log\left[\frac{\frac{\rho^2(d+2a_4\rho^6)}{q}}{1+\{1+\frac{\rho^4(d+2a_4\rho^6)^2}{q^2}\}^{\frac{1}{2}}}\right]\right] \\ &+ \mathcal{O}\left(\frac{1}{N^2}\right). \end{aligned} \tag{4.54}$$

Defining, $F(\rho) = \partial S(\rho^2)/\partial\rho^2$, the equation of motion is given by (4.29).

The phase structure is qualitatively the same as when there are no α' corrections. Unlike the fixed potential thermal AdS is not a solution. It is easily seen from (4.54) that $\rho = 0$ is not a solution of the equation of motion. We have seen in section 4.2.2, that there exists a critical charge for a fixed $\bar{\alpha}$ beyond which there is only one solution.

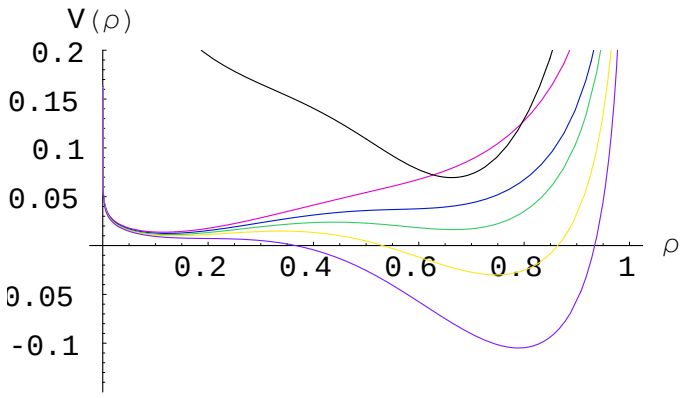

Figure 4.16: Coloured curves: Potential for various temperatures corresponding to the variations of A_1, A_2, A_3, a, c and a_4 for $q < q_c$ Black curve: Potential for $q > q_c$.

Below this critical charge there are a maximum of three solutions. See equation (4.22) and figure 4.5. In the matrix model, this critical charge (q_c) is given by the merging of the three saddle points of (4.52).

Figure 4.16 shows the thermal history for the canonical ensemble. The coloured curves are for $q < q_c$ for some fixed λ. This corresponds to region I in figure 4.5. At low temperatures, there is a single minimum in the range $0 < \rho < 1/2$ (curves in pink). This corresponds to the small black hole. Two new saddle points appear at $T = T_1$ with the new minimum in the range $1/2 < \rho < 1$ (shown in blue) . These correspond to the intermediate (unstable) and large black holes. The small black hole has lower energy upto $\bar{T}$ (the green curve), beyond which the large black hole phase is favoured (yellow). Thus there is a phase transition at $\bar{T}$ corresponding to the one in the bulk. The small and the intermediate black holes disappear at T_3 and at high temperature, the large black hole (the phase with the saddle point in the range $1/2 < \rho < 1$) remains (shown in purple).

The black curve in figure 4.16 shows the single saddle point when $q > q_c$. This corresponds to the single large black hole that exists above the critical charge for fixed $\bar{\alpha}$, in the region II of figure 4.5.

4.4 Discussion

In this chapter we studied GB gravity with R-charge and also the corresponding boundary theory. We first studied the gravity theory for both grand canonical and canonical ensembles. We focused on the gauge theory on the boundary.

In the grand canonical ensemble, without GB correction, the phase diagram is characterized by the chemical potential Φ. For large Φ, there is only one black hole solution which is always stable with respect to thermal AdS. However for small Φ, there exist two solutions. The smaller one is unstable due to negative specific heat and the large one is stable with positive specific heat. It goes through Hawking-Page transition from AdS to the black hole phase at Hawking temperature T_c. Once we incorporate GB correction in the theory, the phase diagram is characterized by the chemical potential Φ and the GB coupling $\alpha^{'}$. Depending on the thermodynamic behaviour of the black holes, $(\Phi - \alpha)$ plane is divided into four regions. In the first region, where Φ is below the critical value Φ_c (which depends on $\alpha^{'}$), there are three different black hole solutions; we call them small, intermediate and big black hole. Small one is unstable and the other two are stable. At low temperature only small black hole exists and at temperature T_2 there is a first order phase transition between small and big black hole. However, with the inclusion of thermal AdS in the phase diagram, it is found that both the small and the big black hole phases are metastable at low temperature and the big black hole becomes stable only at high temperature. In the second region, where Φ is less than a critical value, there is only one black hole solution and the extremal black hole with positive free energy appears at $r = 0$. Black hole goes for HP transition at temperature T_c. In other two (III & IV) regions where Φ is greater than the critical value, there is also one black hole solution, but extremal black hole has a finite radius. For region III, extremal black hole has positive free energy, while in region IV, it has negative free energy. In order to clearly illustrate various phases, we construct a Landau function with black hole horizon radius as the order parameter. It is worth noting that in every case where there is Hawking-Page

transition, the transition temperature is found to decrease with $\alpha^{'}$. From here we conclude that as we perturbatively increase the gravitational strength, the critical temperature reduces its value.

Now, coming back to the canonical ensemble, from thermodynamic point of view, there is no qualitative difference between theories with and without GB coupling. The phase diagrams are characterized by the charge of the black hole and the GB coupling. Depending on the values of charge q and GB coupling $\alpha^{'}$, there are two distinct regions. In region I, where q is less than the critical value q_c (which depends on coupling $\alpha^{'}$), consists of three black hole phases, while in region II, where q is greater than q_c, only one black hole phase exists. Thermal AdS continues to be a non-admissible phase. As before, there is a transition from small to big black hole at a critical temperature. This temperature decreases as we increase $\alpha^{'}$. Here also we construct a Landau function which represents various phases around the critical points.

Assuming AdS/CFT correspondence, we studied corresponding phase transitions on the dual gauge theory at the boundary. This is done by constructing a phenomenologically motivated two (a, b) or four (A_1, A_2, A_3, A_4) parameter matrix model for both (canonical and grand canonical) ensembles. For the grand canonical case, we first studied without $\alpha^{'}$ correction. In this case, we need only a two-parameter model to capture all the features of the gravity theory. The parameters here are functions of λ, T and chemical potential μ, but the explicit dependence of the parameters on them is very hard to determine. For $\mu < \mu_c$, it is possible to get the whole phase diagram of the gravity side by considering them to be positive. However, for $\mu > \mu_c$, there is an extra maximum that always comes with the minimum. This has no analogue in the bulk theory. We interpret this extra maximum with some stringy phase. Thus we always keep this point in the region $0 \leq \rho \leq 1/2$ by imposing restrictions on the parameters. In particular, to get maximum at $\rho = 0$, a has to be negative. Otherwise

a and b are always positive for all values of μ. Thus, we expect b is positive for all values of μ and a is related to μ in such a way that it becomes negative when the above condition is satisfied. At zero coupling, this dependence can easily be calculated. Once we incorporate $\alpha^{'}$ correction in this theory, we need a four-parameter model to capture all the features of the gravity theory. In this case we also have an extra maximum, independent of whether μ is greater or less than μ_c. This does not show up in the gravity side and, once again, we restrict this to the region, $0 \leq \rho \leq 1/2$. Here also to get maximum at $\rho = 0$ for $\mu > \mu_c$, either A_1 or both A_1 and A_4 have to be negative. Otherwise A_1, A_2, A_3 and A_4 are always positive for all values of μ. We again expect A_2, A_3 are always positive for any μ and $A_1$and A_4 are related to μ as before.

Finally, in the canonical ensemble, we have studied the same four-parameter model with $\alpha^{'}$ correction. Since in this case, μ can take any value, we have to sum over all the values. For that, we need to know the explicit dependence of the parameters on the chemical potential. At zero coupling, it is easy to determine the dependence of A_1 on μ. However, as we already mentioned, the explicit dependence of the parameters on μ is very hard to determine at strong coupling. As a toy exercise, by assuming that the zero coupling result continues to hold in the strong coupling limit, we take only A_1 and A_4 to be explicitly dependent on μ and others are independent. This is consistent with one of the cases in the grand canonical ensemble. In this scenario, we write down the matrix model for the fixed charge. Amusingly, we find that this model correctly reproduces all phases of the black holes with fixed charge.

Bibliography

[1] A. Chamblin, R. Emparan, C.V. Johnson and R.C. Myers, *Charged AdS Black Holes and Catastrophic Holography,* Phys. Rev. D60, 064018 (1999) [arXiv:hep-th/9902170].

[2] A. Chamblin, R. Emparan, C.V. Johnson and R.C. Myers, *Holography, Thermodynamics and Fluctuations of Charged AdS Black Holes*, Phys. Rev. D60, 104026 (1999) [arXiv:hep-th/9904197].

[3] T. Torii and H. Maeda, *Spacetime structure of static solutions in Gauss-Bonnet gravity: charged case*, Phys. Rev. D72 (2005) 064007 [arXiv:hep-th/0504141].

[4] D. Yamada and L.G. Yaffe, *Phase Diagram of N=4 Super-Yang-Mills Theory with R-Symmetry Chemical Potentials*, JHEP 0609:027,2006 [arXiv:hep-th/0602074].

[5] T. Torii and H. Maeda, *Spacetime structure of static solutions in Gauss-Bonnet gravity: Neutral case,* Phys. Rev. D **71**, 124002 (2005) [arXiv:hep-th/0504127].

[6] A. Biswas and S. Mukherji, *On the Hawking-Page transition and the Cardy-Verlinde formula,* Phys. Lett. B **578**, 425 (2004) [arXiv:hep-th/0310238].

[7] D. J. Gross and E. Witten, *Possible Third Order Phase Transition In The Large N Lattice Gauge Theory,* Phys. Rev. D **21**, 446 (1980).

[8] S. R. Wadia, *N = Infinity Phase Transition In A Class Of Exactly Soluble Model Lattice Gauge Theories,* Phys. Lett. B **93**, 403 (1980).

[9] L. Alvarez-Gaume, C. Gomez, H. Liu and S. Wadia, *Finite temperature effective action, AdS_5 black holes, and $1/N$ expansion*, Phys. Rev. D71 (2005) 124023 [arXiv:hep-th/0502227].

[10] P. Basu and S.R. Wadia, *R-charged AdS_5 black holes and large N unitary matrix models*, Phys.Rev. D73 (2006) 045022 [arXiv:hep-th/0506203].

Chapter 5

Summary

According to the AdS/CFT correspondence, type IIB string theory on $AdS_5 \times S^5$ is dual to the four-dimensional $\mathcal{N} = 4, SU(N)$ gauge theory on the boundary. In the weak coupling and large curvature limit, the string theory can be approximated by the supergravity description. However, because of the dual nature of the AdS/CFT correspondence, this corresponds to strongly coupled regime of gauge theory. The study of gauge theory in this regime is very difficult due to lack of systematic formulation. In this thesis, we systematically exploit this correspondence in order to gain understanding about the strongly coupled regime of gauge theory by studying the weakly coupled gravity theory. In particular, we have obtained a phenomenological description of the thermodynamic behaviour which can be encoded in a matrix model. Such a construction is by no means unique but our main interests are restricted to the behaviour near the critical point where qualitative behaviours are believed to be universal in the sense that, it does not depend on precise details of the theory. Therefore, the effective model presented here belongs to the same universality class as that of the gauge theory. In addition, wherever possible we have pushed the correspondence further to make semi-quantitative analysis and obtain the behaviour of effective action under variation of different thermodynamic quantities.

In chapter 2, we discussed the thermodynamics of five dimensional bulk theory in the supergravity limit and reviewed the formalism to construct an effective Lagrangian for the strongly coupled dual. The bulk has two configurations with same asymptotic geometry. One of them is the thermal AdS and the other is the black hole. Though thermal AdS can exist for arbitrary temperature, the black hole nucleates only above a particular temperature T_{min}. Above this temperature T_{min}, there are two black hole solutions. Depending on their horizon sizes, we call them big and small. Bigger one is the stable one, and has a positive specific heat. From the free energy calculation one can see even in the presence of the black holes, thermal AdS remains the preferred phase for $T < T_c$. While for $T > T_c$, it is the big black hole phase that takes over. This phase transition at $T = T_c$ is a first order transition and is known as Hawking-Page (HP) transition. The small black hole remains unstable at all temperature due to its negative specific heat and acts as a bounce for the decay of big black hole at $T > T_c$. Witten identified this phase transition with the large N confinement/deconfinement transition of the boundary gauge theory in the strong coupling regime. In the boundary theory, which is a gauge theory on an S^3, one can show all the degrees of freedom got massive except a Wilson loop operator. One can integrate out the rest and write down an effective Lagrangian which has the Wilson loop operator as its degree of freedom. For low enough temperature it can be approximated by a simple matrix model known as (a, b) matrix model as it has two parameters a and b[1]. For certain ranges of these two parameters, the matrix model captures complete thermodynamic behaviour of the bulk theory. These parameters depend on the 't Hooft coupling λ and the temperature T. Both turn out to be monotonically increasing functions of temperature for fixed λ.

In chapter 3, we incorporate Gauss-Bonnet (GB) correction to the gravity action and study various phases of the bulk geometry with AdS asymptotics. These phase

[1]This is done by assuming that the weak coupling results are valid in the strong coupling regime mainly for 't Hooft coupling $\lambda \to \infty$

structures depend crucially on GB coupling $\alpha^{'}$. Except within a certain range of this coupling, there is only one black hole phase, otherwise there exist three black hole phases. We call them small, intermediate or unstable, and big black hole phases. It turns out that there are two first order phase transitions. One of them is from small black hole to the big one at a temperature much lower than that of inverse AdS curvature scale. The other one is similar to that of the usual HP transition where a crossover occurs from thermal AdS to the big black hole phase. We then study the dual gauge theory at the boundary by the same two-parameter matrix model. We find the λ dependence of these parameters. By introducing higher derivative terms in the bulk, we study corrections of order $1/\lambda$ in the gauge theory. This essentially allows us to find the λ dependence of (a, b) for large but finite λ. We find that a is an increasing function of λ while b decreases with λ.

Furthermore, we find that the simple (a, b) model fails to capture all the phases (small, intermediate and large black hole phases) in the bulk. To incorporate all the bulk phases, we constructed a toy model which requires introduction of higher dimensional operators in the matrix model. This model has four parameters which depend on the temperature as well as the gauge coupling. Besides reproducing all the qualitative features of the bulk, this model also gives an extra saddle point. We interpret this saddle point as a phase in string theory which has no analogue in the supergravity. This stringy phase arises at the Gross-Witten transition point. This Gross-Witten transition may be identified as a crossover from supergravity black hole solution to string state in the bulk side. In the bulk side, this stringy phase may also serve as a bounce for the decay of the small black hole to the thermal AdS.

Finally in chapter 4, we include the effects of electric charge with the above theory. On the gravity side these charges come from the rotation of the internal S^5. We first focus our attention on the phase structures of this bulk theory in both canonical and grand canonical ensembles. In the grand canonical ensemble, the phase structure

crucially depends on $\alpha^{'}$ as well as chemical potential Φ. For a certain range of the chemical potential Φ and $\alpha^{'}$, there exist three black hole phase and have two HP transitions. Outside this range, only one black hole phase survives and unlike simple GB theory, we get a HP transition. For the canonical ensemble the number of black hole phases are similar to the GB theory but here thermal AdS is not an allowed geometry. Therefore, there exist only one first order phase transition between small and big black hole (in the certain range of $\alpha^{'}$ and fixed charge q). We then construct a matrix model for the gauge theory dual. This model is similar to the one discussed in the previous paragraph. However the four coefficients are now not only function of λ, and T, but also depend on the chemical potential. In the grand canonical ensemble, like GB theory, matrix model has an extra saddle point that has no analogue in the gravity side and we interpret this as a bounce. In the canonical ensemble, since chemical potential can take any value, one has to sum over all the values. To do that it is necessary to know the exact dependence of parameters on potential. This is very hard to determine in the strong coupling limit. For simplicity, we write down the model where only two parameters are explicitly dependent on chemical potential and other two are constant. This is consistent with one of the possible scenarios of the grand canonical case. Amusingly we find that the model correctly reproduces the corresponding bulk behaviour.